Dissertation

Modulation of cardiac function by low-density lipoprotein modified via HOCl, a potent myeloperoxidase-derived oxidant

submitted by

Chintan Navinchandra KOYANI

for the Academic Degree of

Doctor of Philosophy (PhD)

at the

Medical University of Graz,

Institute of Molecular Biology and Biochemistry

under the Supervision of

Ao. Univ. Prof. Dr. Ernst MALLE

2015

Declaration

I hereby declare that this thesis and the work included in it are my own original work and that I have fully acknowledged names of all individuals and organizations that have contributed to the research of this thesis. Due acknowledgement has been made in the text to all other materials used. Throughout this project and in all related publications I have followed the guidelines of “Good Scientific Practice”.

Graz, December 2015

Chintan Navinchandra KOYANI

Acknowledgements

I would like to thank Prof. Ernst Malle for giving me the opportunity to carry out my PhD thesis in his lab. I heartily thank him for his guidance throughout my PhD and providing continuous support, whenever needed, and financial support for the prolongation of PhD project.

I thank the Austrian Science Fund (FWF), the DK-MCD PhD program and the Medical University of Graz for the financial support and for giving the opportunity to conduct part of my work at the Medical University of Leipzig, Germany.

I would like to thank my PhD committee members, Prof. Brigitte Pelzmann, Prof. Frank Heinzel and Prof. Klaus Groschner, for their enormous support, suggestions and critical comments for this project.

Humble thanks to Prof. Brigitte Pelzmann for providing opportunity to perform patch clamp experiments, critical reading and improving my thesis. I would like to thank the team of Prof. Brigitte Pelzmann including Dr. Susanne Scheruebel, Dr. Klaus Zorn-Pauly and Petra Lang, for helping in performing patch clamp experiments, scientific discussions, analyses and interpretation of data.

I kindly thank to Dr. Dirk von Lewinski and Dr. Ewald Kolesnik for their collaboration and support for experiments with human atrial trabeculae.

I am thankful to Prof. Gerald Hoefler and Silvia Schauer for their assistance and collaboration for immunohistochemistry.

I would like to thank: Dr. Heinrich Maechler for providing right atrial appendages; Christopher Trummer and Laura Frank for helping for cell culture experiments, Western blotting and qPCR; members of the Institute of Molecular Biology and Biochemistry as well as the Institute of Biophysics for friendly environment and off-work activities.

A special thanks to my friends including Anita, Piyush, Peter, Susi, Simin, Niroj, Shailaja, Manjula, Pritesh, Sri Veena, Nadja and Cristiana, for their personal and professional support.

At last but not least, I heartily thank my parents, family and relatives for encouragement and mental support.

Table of Contents

Abbreviations

ACE	angiotensin converting enzyme
AP	action potential
APD	action potential duration
apoB-100	apolipoprotein B-100
AT	angiotensin
AVR	aortic valve replacement
BMI	body mass index
BSA	bovine serum albumin
CABG	coronary artery bypass grafting
CAD	coronary artery diseases
CaMKII	Ca^{2+}/calmodulin-dependent protein kinase II
CaT	calcium transient
CaV1.2	L-type calcium channel
CaV3.2	T-type calcium channel
Cs-pip	caesium pipette solution
CsT	caesium Tyrode
CVDs	cardiovascular diseases
DADs	delayed-afterdepolarization
DMSO	dimethyl sulfoxide
EADs	early-afterdepolarization
EC	excitation-contraction
EF	ejection fraction
GAPDH	glyceraldehyde-3-phosphate dehydrogenase
GPV	guinea pig ventricular
H_2O_2	hydrogen peroxide
HF	heart failure
HOCl/OCl^-	hypochlorous acid/hypochlorite
HOCl-LDL	hypochlorous acid-modified low-density lipoprotein
$I_{Ca,L}$	L-type Ca^{2+} current
I_f	funny current
I_{K1}	inward-rectifier potassium current

I_{Kr}	rapid potassium current
I_{Ks}	slow potassium current
I_{Kur}	ultra-rapid potassium current
I_{Na}	Na^+ current
I_{NaL}	late Na^+ current
I_{NS}	non-selective cation current
I_{ss}	steady state current
I_{to}	transient outward current
I-V	current-voltage
Kir	inward rectifier potassium channel
LAD	left anterior descending
LDL	low-density lipoprotein
LDL-R	LDL-receptor
LOX-1	lectin-like oxidized LDL receptor-1
LV	left ventricle
MI	myocardial infarction
MPO	myeloperoxidase
$MPO^{-/-}$	myeloperoxidase knock out
MPO-LDL	LDL modified by the MPO-H_2O_2-chloride system
MSRA	methionine sulfoxide reductase A
MSRB	methionine sulfoxide reductase B
Na-pip	sodium pipette solution
NaT	sodium Tyrode
NaV1.5	sodium channel
NCX1	Na^+/Ca^{2+} exchanger
nLDL	native LDL
N-pip	normal pipette solution
NT	normal Tyrode
oxCaMKII	oxidized-Ca^{2+}/calmodulin-dependent protein kinase II
PBS	phosphate-buffered saline
pCaMKII	phosphor-CaMKII
PCSK9	proprotein convertase subtilisin/kexin type 9
PLB	phospholamban
qPCR	real time quantitative PCR

RAA	right atrial appendage
ROS	reactive oxygen species
RT50	relaxation time 50%
RyR2	ryanodine receptor
SDS	sodium dodecyl sulfate
SEM	standard error of mean
SERCA2a	sarcoplasmic reticulum Ca^{2+}-ATPase pump
siRNA	small interfering RNA
SR-A1	scavenger receptors class A1
SR-B1	scavenger receptors class B1
TBST	Tris-buffered saline containing Tween 20
$V_{1/2act}$	membrane potential of half maximum activation
$V_{1/2inact}$	membrane potential of half maximum inactivation
VLDL	very low-density lipoprotein
V_{rest}	resting membrane potential
WHO	World Health Organization
WT	wild type

Abstract in German

Massive Einwanderung von Neutrophilen und erhöhte Konzentrationen des hauptsächlich von Neutrophilen sekretierten Protein Myeloperoxidase (MPO) im Myokard fungieren als klinische Marker für zukünftige kardiovaskuläre Ereignisse. Weiters korrelieren erhöhte Plasma MPO Spiegel direkt mit der Mortalität von Patienten mit koronarer Herzkrankheit, Herzinsuffizienz und Myokardinfarkt. Das Enzym MPO generiert hypochlorige Säure (HOCl) aus H_2O_2 und Chlorid Ionen. HOCl ist ein starkes Oxidationsmittel das mit einer Vielzahl biologischer Moleküle, einschließlich Lipoproteinen, reagiert. HOCl-modifizierte Low-Density-Lipoproteine (HOCl-LDL) wurden bereits in humanen atherosklerotischen Läsionen nachgewiesen. Kardiomyocyten sind in der Lage, Apolipoprotein B-100-hältige Lipoproteine, also LDL-Partikel, zu sekretieren, die möglicherweise unter akuten bzw. chronischen Bedingungen mit MPO von Neutrophilen bzw. MPO-generiertem HOCl im Myokard reagieren können.

Die in der vorliegenden Arbeit mittels Immunhistochemie erhobenen Daten beweisen massive Akkumulation von Neutrophilen und MPO sowie massive Anreicherung von HOCl-modifizierte Epitopen im humanen Myokard. Die Färbung von HOCl-modifizierten Epitopen ist vorrangig in Bereichen zu finden, wo massive Färbung von apoB-100 (das Haupt Apolipoprotein von LDL) auftritt. Diese Befunde deuten darauf hin, dass bei kardiovaskulären Erkrankungen eine oxidative Modifikation von LDL durch MPO-generiertes HOCl auftritt. Daher war das Hauptziel der weiteren Studie, die Auswirkungen von HOCl-LDL auf die Funktion von Kardiomyozyten zu untersuchen.

HOCl-LDL führte zu einer Verlängerung der Aktionspotentialdauer, einer Depolarisation des Membranruhepotentials und einer verringerten Aufstrichsgeschwindigkeit des Aktionspotentials aufgrund eines reduzierten I_{K1} und eines vergrößerten I_{NaL}. Weiters nahm die Stromdichte von I_{ss} und I_{NS} zu. In weiterer Folge veränderte HOCl-LDL den Kalziumhaushalt, was sich in einer Reduktion des $I_{Ca,L}$, des Kalziumtransienten, des Kalziumgehaltes im sarcoplasmatischen Retikulum und der Zellkontraktion ausdrückte. In HOCl-LDL behandelten Zellen kam es zu einer rascheren Anstiegsphase und zu einer

verlangsamten Rückbildung des Kalziumtransienten. Zusammenfassend kann festgehalten werden, dass die durch HOCl-LDL bedingten zellulären elektrophysiologischen Veränderungen zum Auftreten von arrhythmischen Ereignissen und einer gestörten Kontraktion in humanen Trabekeln aus dem rechten Herzohr führen.

Molekularbiologische Untersuchungen zeigten, dass HOCl-LDL zu einer rezeptor-vermittelten (LOX-1 und CD36) Oxidation der Ca^{2+}/Calmodulin-abhängigen Protein Kinase II (CaMKII) führt. Eine erhöhte Superoxid-Anion-Produktion trug ebenfalls zu einer CaMKII-Oxidation bei. Sowohl die Blockade der CaMKII-Aktivität (KN93), als auch des I_{NaL} (Ranolazine) schützen vor HOCL-LDL induzierten arrhythmischen Ereignissen und gestörten Muskelkontraktionen.

Abstract in English

Neutrophil infiltration and elevated levels of neutrophil-derived myeloperoxidase (MPO) in the myocardium are clinical markers for prediction of future cardiovascular events. Elevated plasma MPO levels were further correlated with mortality in patients with coronary artery disease, heart failure and myocardial infarction. Activated MPO generates hypochlorous acid (HOCl) from H_2O_2 and Cl^-. HOCl is a potent oxidant that reacts with numerous biological molecules including lipoproteins. Most importantly, HOCl-modified low-density lipoproteins (HOCl-LDL) are found in human atherosclerotic lesions. Moreover, cardiomyocytes secret apoB-100 containing lipoproteins that in turn may react with MPO-generated HOCl in the myocardium.

The present immunohistochemistry data reveal the presence of neutrophils, MPO and HOCl-modified epitopes in the infarcted myocardium. Interestingly, the pattern of immunostain of HOCl-modified epitopes and apoB-100 (the major apolipoprotein of LDL) in the serial sections strengthens the hypothesis of LDL modification by HOCl in vivo during cardiovascular diseases. Therefore, the major aim of the present study was to evaluate the impact of HOCl-LDL on cardiac tissue and myocyte function.

HOCl-LDL altered electrophysiological characteristics of cardiomyocytes. Prolonged action potential duration, depolarized resting membrane potential and reduced maximal upstroke velocity became apparent as a result of reduced I_{K1} and increased I_{NaL} density. Moreover, increased I_{ss} and I_{NS} were observed at outward positive and inward negative membrane potentials. HOCl-LDL altered calcium homeostasis, namely reduced $I_{Ca,L}$, calcium transient, sarcoplasmic reticulum Ca^{2+} content and cell shortening. Moreover, increased time to peak and reduced RT50 were observed in HOCl-LDL-treated myocytes. Altogether, the observed changes at the cellular level contributed to arrhythmic episodes and contractile dysfunction of human right atrial trabeculae in response to HOCl-LDL.

Molecular biology experiments reveal that HOCl-LDL treatment oxidized Ca^{2+}/calmodulin-dependent protein kinase II (CaMKII) via LOX-1 and CD36 receptor-mediated signalling. Moreover, elevated superoxide anion production contributed to oxidation of CaMKII. KN93, a blocker of CaMKII activity, and Ranolazine, an inhibitor of I_{NaL}, protected cardiac tissue and myocytes against HOCl-LDL-induced arrhythmia and contractile dysfunction.

1. Introduction

1.1 Cardiovascular diseases (CVDs)

CVDs are the most prevalent chronic diseases worldwide. Even though much is known about the etiology of various CVDs, the death count due to these diseases stays even higher than all cancer together (Figure I). According to the World Health Organization (WHO), about 17.3 million people die annually because of CVDs (WHO, 2015). Moreover, despite of advancement in diagnosis and treatment of CVDs, the occurrences of these diseases is still increasing year by year. CVDs including atherosclerosis and hypertension can lead to coronary artery diseases (CAD), myocardial infarction (MI) and eventually heart failure (HF).

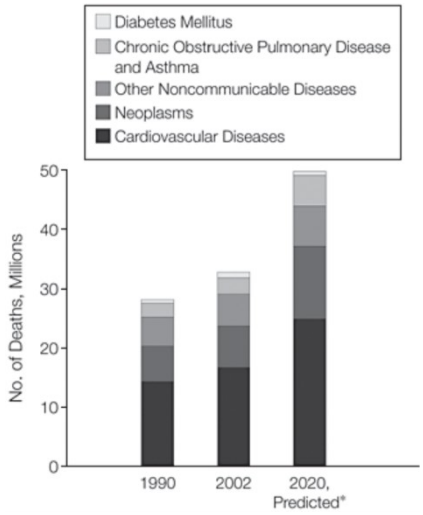

Figure I. Worldwide mortality due to chronic diseases (Yach et al., 2004).

Cardiovascular risks are widely associated with diabetes (Huang et al., 2014; Ipadeola and Adeleye, 2015), obesity (Yatsuya et al., 2014), kidney diseases (Sun et al., 2014), dyslipidemia (Zhang and Lu, 2015), sepsis (De Backer and Scolletta, 2013), inflammation (Golia et al., 2014) and others. Since many decades elevated blood levels of lipoproteins are clinically used to predict cardiovascular risks (Wood and Joint European Societies Task, 2001).

1.2 Low-density lipoprotein (LDL) and CVDs

LDL contains 75-78% lipids, 20-22% proteins and 3-5% carbohydrates. The lipid moiety includes cholesterol ester, phospholipids, unesterified (free) cholesterol and triglycerides. ApoB-100, the major apolipoprotein of LDL, has a molecular mass of about 450 kDa. LDL is the major carrier of cholesterol in the circulation. The uptake of LDL is mediated via LDL-receptor (LDL-R) that is present on the membrane of most cells. Upon binding of apoB-100 to LDL-R, lipoprotein particles are internalized via receptor-mediated endocytosis. The liver secrets very low-density lipoproteins (VLDL) that get converted into LDL and then transports cholesterol to the peripheral tissues. Though LDL is generated mainly by liver, also heart is reported to secrete apoB-100-containing lipoproteins (Boren et al., 1998; Nielsen et al., 1998).

Basically, elevated levels of circulating LDL predict high risk of CVDs. LDL is the major source of lipids (primarily cholesterol) that contribute to the development and progression of atherosclerosis. The native LDL (nLDL) is non-atherogenic within physiological levels (50-70 mg/dl) (O'Keefe et al., 2004), while high levels of LDL may possess pro-atherogenic activity. Moreover, nLDL can evade endothelial layer of circulatory vessels and migrate into the intima and there it can be oxidized by enzymes or radicals. Oxidized LDL activates adjacent endothelial cells to produce chemotactic proteins that attract monocytes, granulocytes and lymphocytes at the site of lesion. Macrophages take up oxidized LDL and turn into foam cells, which reside in the vessel wall. Necrosis of foam cells results in accumulation of extracellular lipids and cell debris. These processes lead to an increase in lesion size and ultimately narrowing of the artery lumen. Oxidized LDL does not interact with LDL-R but has high affinity for scavenger receptors such as scavenger receptors class A1 (SR-A1), SR-B1, CD36 and Lectin-like oxidized LDL receptor-1 (LOX-1) (Steinberg et al., 1989). SR-A1/B1 and CD36 are highly expressed in macrophages, while LOX-1 is abundantly expressed on endothelial cells. Alternatively, cardiomyocytes are reported to express CD36 (Greenwalt et al., 1995) and LOX-1 (Riahi et al., 2015). Moreover, SR-A1 is reported to play crucial roles in various CVDs (Ben et al., 2015; Hu et al., 2011).

Beyond any doubt high LDL levels are considered as a marker for cardiovascular risk since decades. LDL reduction by statins can effectively reduce CVDs risk and progression of MI and stroke in both primary and secondary prevention (Baigent et al., 2005). Another LDL-lowering therapeutic approach by Proprotein convertase subtilisin/kexin type 9 (PCSK9, an enzyme that binds to LDL-R) inhibition has also been found to reduce cardiovascular risk (Tavori et al., 2015). Therefore, LDL is considered as a primary lipid-related risk factor (LDL-cholesterol) for CVDs and lipid-lowering therapy was implemented in order to suppress progression of CVDs in patients with high LDL (in particular LDL-cholesterol) levels. However, there are other lipids that emerged as cardiovascular risk markers and got attention from recent clinical studies. High circulatory levels of small dense-LDL particles, commonly seen in patients with metabolic syndrome and type-2 diabetes, are emerging as novel cardiovascular risk markers (Hirayama and Miida, 2012). Moreover, apoB-100 and oxidized-LDL levels are considered as highly sensitive biomarkers to predict cardiovascular events (Heneghan et al., 2013; Holvoet et al., 2001).

1.3 LDL-modification in vitro and in vivo

A variety of methods has been used to modify LDL in order to mimic in vivo diseased conditions. Under in vitro conditions, LDL can be oxidized by a variety of radicals and enzymatic oxidants. Elevated reactive oxygen species (ROS) levels at the site of atherosclerotic lesion may oxidize LDL particles in the vessel wall. Copper-oxidized LDL has widely been used in various studies though it is not an in vivo occurring oxidative modification of LDL, since copper ions are not circulating freely. Moreover, acetylated-LDL has also been used during several in vitro studies (Ringseis et al., 2008). Under in vivo conditions LDL is found to be modified by enzymes including, lipooxygenase, NADPH oxidase and myeloperoxidase.

1.4 Myeloperoxidase (MPO)

MPO is mainly present in neutrophils and monocytes accounting up to 5% and 1% of total cell protein, respectively (Bos et al., 1978; Schultz and Kaminker, 1962). Certain types of macrophages like microglia and Kupffer cells have also been reported to express MPO (Brown et al., 2001; Gray et al., 2008). Neutrophils, the major source of MPO, are the first defensive mechanism of the immune system and thus play a pivotal role in various inflammatory diseases. Neutrophil infiltration in the myocardium is widely observed under ischemia-reperfusion injury (Jordan et al., 1999; Schofield et al., 2013). A series of published articles emphasizes detrimental role of neutrophils on disease severity and mortality in patients with CAD (O Hartaigh et al., 2013), MI (Carbone et al., 2013) and HF after acute MI (Rashidi et al., 2008). Recently, the neutrophil/lymphocyte ratio has gained clinical attention to predict cardiovascular events (Bhat et al., 2013).

MPO consists of two dimers that are made up of a heavy chain (59-64 kDa) and a light chain (14 kDa), which are coupled with a heme molecule (Arnhold and Flemmig, 2010). Native state of MPO [Fe(III)] is inactive but in the presence of hydrogen peroxide (H_2O_2) it gets oxidized to [Fe(V)=O] state that is able to react with various anions/radicals including Cl^-, $NO_2^{\cdot}$ and $Tyr^{\cdot}$ (Malle et al., 2003). Under in vivo conditions in the presence of Cl^-, the MPO-H_2O_2 system generates hypochlorous acid (HOCl), which is a potent oxidant and possesses anti-microbial property. However, elevated levels of MPO and HOCl have been reported to damage surrounding tissues in various diseases. Apart from its anti-microbial activity, HOCl is reported to generate protein/lipid adducts, chlorotyrosine and chloramines that are found to be present in atherosclerotic lesion (Hazell et al., 1996; Hazen and Heinecke, 1997) (Figure II).

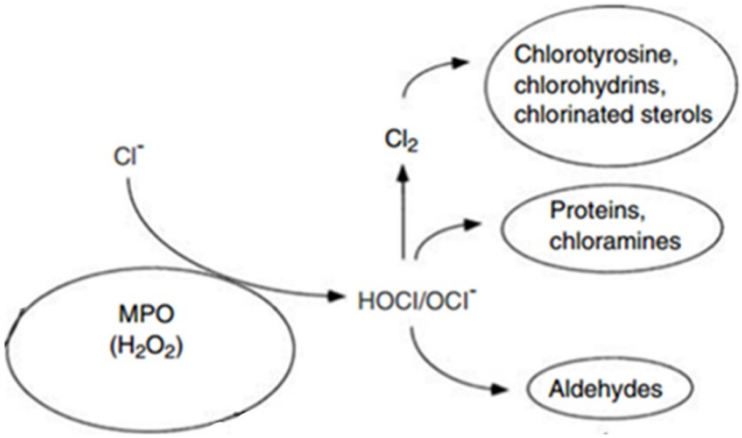

Figure II. Modification of various biological molecules by HOCl generated by MPO-H_2O_2 system (modified figure) (Malle et al., 2003). The MPO-H_2O_2 system generates HOCl that interacts with various biological molecules.

1.5 HOCl-modified LDL (HOCl-LDL)

The MPO-H_2O_2-halide system generates HOCl that promotes modification of LDL under in vitro as well as in vivo conditions (Arnold et al., 1989; Hazell and Stocker, 1993). The first footprint of active MPO in human lesion material was reported by Daugherty and co-workers (Daugherty et al., 1994). Next, HOCl-modified apoB-100 was identified by Hazell and co-workers in human atherosclerotic lesions (Hazell et al., 1996). Moreover, 3-chlorotyrosine was found to be elevated in the LDL fraction isolated from human lesion (Hazen and Heinecke, 1997).

Under in vitro conditions HOCl-LDL has been found to possess potential pro-atherogenic property that can stimulate formation of macrophage foam cells (Malle et al., 2006a). As shown in Figure III, MPO, secreted by neutrophils, damage endothelial junction that facilitates infiltration of monocytes, neutrophils and LDL in the intima. MPO oxidizes LDL that interacts with the scavenger receptors (e.g. CD36, Figure III) that are present on the surface of macrophages (Soehnlein, 2012).

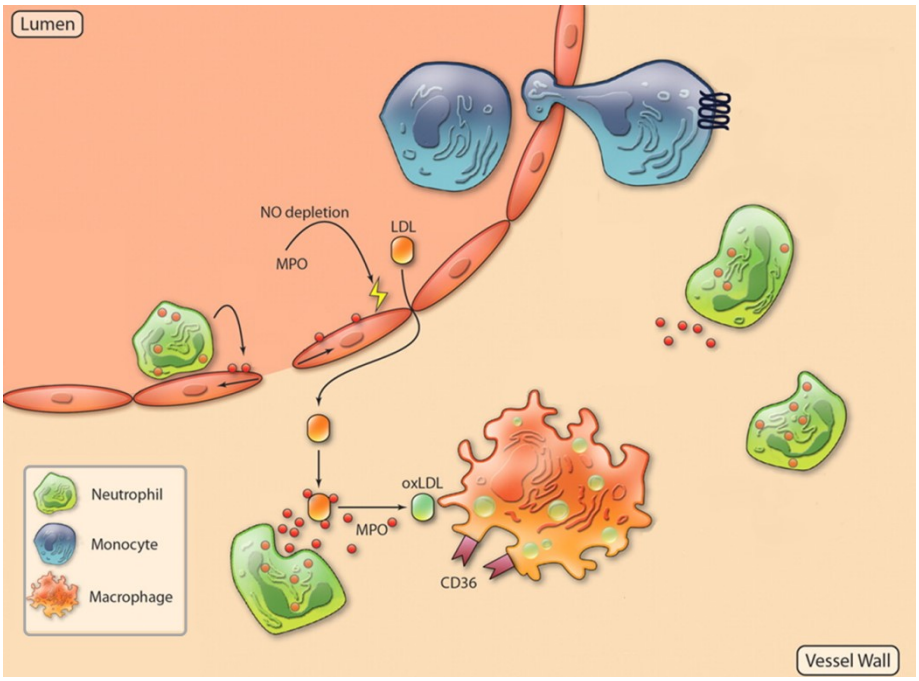

Figure III. **Oxidation of LDL by neutrophil-generated MPO in the intima (modified figure) (Soehnlein, 2012)**. MPO-mediated endothelial dysfunction facilitates migration of neutrophils, monocytes and LDL into the intima. LDL is oxidized by the MPO-H_2O_2-Cl^- system and taken up by macrophages via scavenger receptors.

Receptor-binding studies proved a high affinity of HOCl-LDL to SR-B1 and CD36 in THP-1 macrophages (Marsche et al., 2003). In addition, with the increase in modification (oxidant:lipoprotein molar ratio), HOCl-LDL loses its ability to bind to LDL-R (Malle et al., 2006a). Moreover, published data reveal that MPO is able to get attached to LDL particles under in vivo conditions (Carr et al., 2000; Sokolov et al., 2011) and favours its oxidative modification via generating HOCl. Nevertheless, differences have been observed while modifying LDL by HOCl added as a reagent or generated by the MPO-H_2O_2-Cl^- system (Delporte et al., 2014). Furthermore, modification of amino acid residues of apoB-100 in the LDL-buoyant fraction isolated from patients with high cardiovascular risk could be correlated with the extent of in vitro LDL modification by HOCl (Delporte et al., 2014). All these data confirm that LDL-modification by MPO/HOCl under in vivo condition is detrimental for cardiovascular system and may contribute to CVDs.

1.6 MPO and CVDs

Although major cardiovascular risk factors are identified in diseased patients, novel markers are still emerging. Out of known cardiovascular risk markers, MPO has gained clinical interest (Nicholls and Hazen, 2005). High MPO levels in the circulation have been found to be associated with higher risk of CVDs (Schindhelm et al., 2009) including atherosclerosis (Nambi, 2005), ischemic heart diseases (Loria et al., 2008), MI (Kaya et al., 2012) and HF (Tang et al., 2011). Moreover, high MPO levels have been correlated with higher mortality in patients with CAD (Scharnagl et al., 2014), acute ischemic stroke (Tay et al., 2015), HF (Michowitz et al., 2008) and ST-segment elevation MI (Stankovic et al., 2012).

MPO is reported to play a crucial role during development and progression of CVDs (Nicholls and Hazen, 2005) and MPO-generated oxidants have been found to modulate cardiac function at cellular and tissue levels. In hamster ventricular cardiomyocytes HOCl reduced L-type calcium current density in a concentration-dependent manner and shortened action potential duration (Hammerschmidt and Wahn, 1998). Treatment of human cardiomyocytes with MPO and H_2O_2 induced contractile dysfunction whereby MPO inhibitors could protect cardiomyocyte function (Kalasz et al., 2015). Moreover, in a mouse model of coronary artery ligation-induced MI, $MPO^{-/-}$ mice showed 35% less left ventricular (LV) dilation and 52% less impairment in LV function compared to wild-type (WT) mice (Vasilyev et al., 2005). Altogether, these data strengthen the hypothesis that MPO/HOCl-mediated modification of LDL might alter cardiomyocyte function in terms of electrophysiological characteristics and excitation-contraction coupling.

1.7 Excitation-contraction (EC) coupling

Intracellular Ca^{2+} acts as a central messenger that translates cardiac electrophysiological signals into contraction of the heart. The highly sophisticated process of EC coupling involves ion channels, pumps and transporters that are present on the plasma membrane and sarcoplasmic reticulum that contributes to Ca^{2+} movement in the cellular compartments in a well-controlled beat-to-beat process. Thereby, elevation of intracellular Ca^{2+} levels due to electrical stimulation of a cardiomyocyte triggers actin-myosin interaction and leads to contraction during systole. In detail, due to the depolarization of membrane potential during an action potential (AP) the voltage gated L-type Ca^{2+} channels (CaV1.2) facilitates entry of a small amount of Ca^{2+} into the cell. This Ca^{2+}-influx proceeds to the opening of cardiac ryanodine receptors (RyR2) that release sarcoplasmic reticulum Ca^{2+} into the cytoplasm. The highly increased cytosolic Ca^{2+} binds to troponin C, activates myofilaments and leads to contraction. Next, during the relaxation phase about 70% of cytosolic Ca^{2+} is pumped back to sarcoplasmic reticulum by cardiac sarcoplasmic reticulum Ca^{2+}-ATPase pump (SERCA2a). The remaining Ca^{2+} is removed out of the cell mainly by the Na^{+}/Ca^{2+} exchanger (NCX1) (Neef and Maier, 2013).

The function and regulation of channels, pumps and transporters involved in EC coupling are under control of mainly Ca^{2+}/calmodulin-dependent protein kinase II (CaMKII) (Maier et al., 2003) and protein kinase A (Antos et al., 2001). These enzymes can directly phosphorylate/activate CaV1.2 and RyR2, while the regulation of SERCA2a is controlled by phospholamban (PLB). In addition, CaMKII is reported to regulate Na^{+} (Wagner et al., 2006) and K^{+} (Wagner et al., 2009) channels.

1.8 Cardiac Electrophysiology

The AP is the basic electrical signal of excitable cells like cardiomyocytes and neurons, and it represents a transient, self-propagating and regenerative change in the membrane potential of a cell. In the heart the sum of all cellular cardiac activities is reflected in the ECG in which the P wave describes depolarisation of the atria, the QRS complex represents depolarisation of the ventricles and the T wave summarises repolarisation of the ventricles (i.e. the average duration of the ventricular AP corresponds to the QT interval). Cardiac AP is the outcome of the current flowing through over a dozen mainly voltage-gated ion channels (Figure IV).

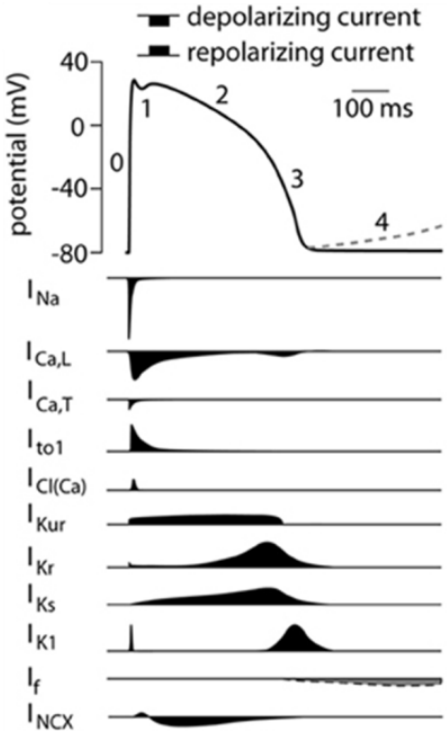

Figure IV. Schematic representation of AP of human ventricular myocyte with indicated current components and their contribution to the AP (modified figure) (Hoekstra et al., 2012).

At the resting phase the membrane potential of a ventricular cardiomyocyte is negative (about -85 mV) inside the cell. The resting membrane potential (Phase 4, Figure IV) is stabilized mainly by the inward-rectifier potassium current (I_{K1}) in atrial/ventricular myocytes (Miake et al., 2002) whereas in sino-atrial node cells

(Verkerk et al., 2007) the funny current (I_f) contributes to a diastolic depolarization (dotted line in Phase 4, Figure IV). Upon generation of an impulse in sino-atrial node cells and its propagation over the whole heart, membrane potential of atrial/ventricular myocytes depolarizes to the threshold potential of about -70 mV that activates Na^+ channels (NaV1.5) and resulting in a large inward Na^+ current (I_{Na}), which in turn very rapidly depolarizes membrane potential to about +50 mV very rapidly representing the upstroke phase of AP (Phase 0, Figure IV). This upstroke phase is a very transient phenomenon since normally Na^+ channels are inactivating very quickly after its activation thereby becoming nonconductive. The depolarization of membrane potential also activates a variety of repolarizing potassium channels. The transient outward current (I_{to}) causes a transient repolarization of the AP (Phase 1, Figure IV) that is quickly counterbalanced by the inward L-type Ca^{2+} current ($I_{Ca,L}$) conducted by the voltage-dependent CaV1.2 channels. $I_{Ca,L}$ is largely responsible for the plateau phase of AP (Phase 2, Figure IV). During this phase further K^+ currents (I_{Kur}, I_{Kr} and I_{Ks}) get activated that repolarize membrane potential to resting values. The last repolarization phase is contributed mainly to K^+-efflux conducted by I_{K1} and partially to Na^+/K^+ ATPase pump (Phase 3, Figure IV). The Na^+/Ca^{2+} exchange is considered as one of the most important cellular mechanisms for removing Ca^{2+} out of the cell (one Ca^{2+} ion is eliminated in exchange for three Na^+ ions by so called “forward mode” of I_{NCX}). Via extrusion of intracellular Ca^{2+}, being elevated during systole, I_{NCX} generates a net inward current (carried by Na^+) thereby contributing to the maintenance of the AP plateau.

1.9 Ca^{2+}/calmodulin-dependent protein kinase II (CaMKII)

CaMKII is a serine/threonine kinase that is under control of the Ca^{2+}/calmodulin complex. There are four isoforms of the enzyme, namely CaMKIIα, β, δ, and γ, out of which the heart expresses primarily the δ isoform. CaMKII is a multifunctional enzyme that contributes to ion channel regulation, Ca^{2+} homeostasis and electrophysiological function of cardiomyocytes. Furthermore, studies have confirmed the role of CaMKII in inflammation, apoptosis and CVDs including hypertrophy, arrhythmia, cardiac remodelling, MI and others (Erickson et al., 2011; Mollova et al., 2015).

CaMKII is composed of 12 subunits that contain three domains: a catalytic domain that performs kinase function, a regulatory domain that regulates activation and an association domain that controls holoenzyme assembly (Figure V). The catalytic and regulatory domains are associated with each other under resting conditions. During activation phase calcified-calmodulin binds to the regulatory domain of CaMKII that makes conformational shift of the catalytic domain for substrate binding. In the presence of ATP or oxidizing molecules CaMKII undergoes phosphorylation or oxidation at threonine (T^{287}) or methionine ($M^{281/282}$) residues, respectively. Phosphorylation/oxidation of the regulatory domain provides persistent activity to CaMKII even after Ca^{2+}/calmodulin dissociation (Erickson et al., 2008).

CaMKII is known to be activated by angiotensin, β-adrenergic stimulation and ROS (Erickson et al., 2011; Erickson et al., 2008). While autophosphorylation of CaMKII at T^{287} residue is Ca^{2+}-dependent, its oxidation at $M^{281/281}$ is found to be independent of Ca^{2+}/calmodulin complex (Erickson et al., 2008). Elevated ROS levels in myocardium have been reported to adversely affect heart function during various CVDs including MI and HF (Kinugawa et al., 2000; Maack et al., 2003; Sugamura and Keaney, 2011). Oxidized-CaMKII (oxCaMKII) plays pivotal roles in sinus node function (Swaminathan et al., 2011), diabetic cardiomyopathy (Luo et al., 2013) and arrhythmia (Foteinou et al., 2015).

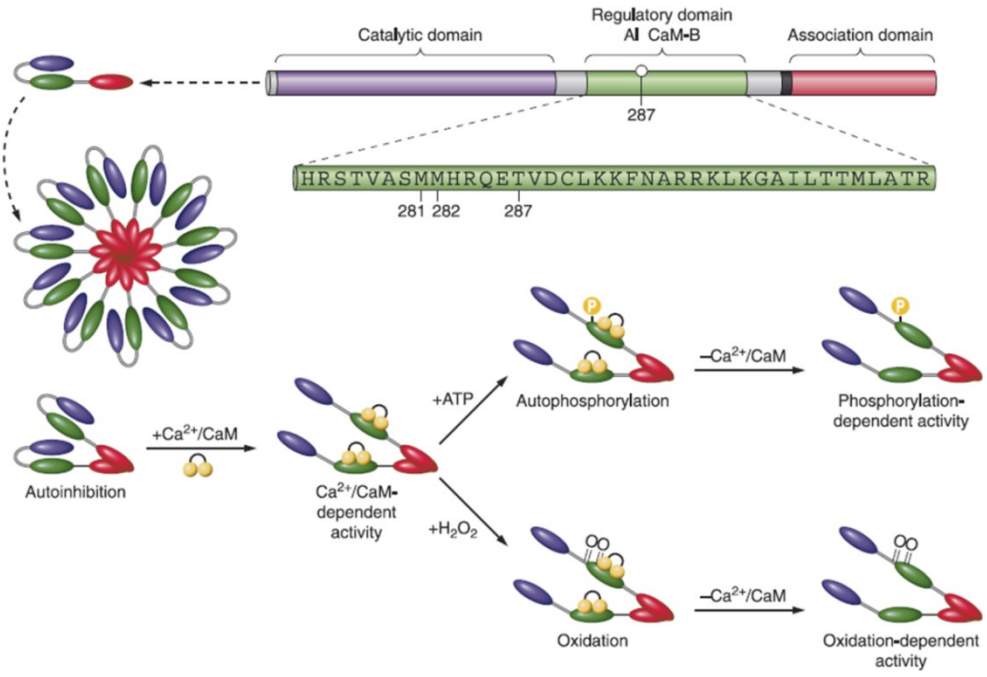

Figure V. CaMKII structural domains and their conformational changes during autophosphorylation and oxidation of the enzyme.

2. Materials and Methods

2.1 Cell culture

HL-1 cells (a murine atrial cardiomyocyte cell line) were cultured in fibronectin (0.5%, w/v)/gelatin (0.02%, w/v) (Sigma-Aldrich, MO, USA) coated flasks and supplied with Claycomb medium (Sigma-Aldrich) containing 10% (v/v) fetal bovine serum (Sigma-Aldrich), 0.1 mM norepinephrine (Sigma-Aldrich), 2 mM L-glutamine (Sigma-Aldrich), 100 IU/ml penicillin and 100 µg/ml streptomycin and maintained at 37°C under 5% CO_2. For all experiments cells were seeded in 6- or 12-well plates and grown to 70% confluence.

2.2 Isolation and purification of LDL

LDL was isolated from plasma of healthy volunteers as described (Malle et al., 1995b). After adding a point of a spatula of EDTA and sodium azide to the plasma, density was adjusted to 1.063 g/ml using KBr. After ultracentrifugation for 24 h at 48,000 rpm (10°C, 50.2 Ti rotor; Beckman Coulter Inc., Fullerton, CA, USA), LDL was collected from the upper layer and dialysed against isotonic saline solution (0.15 M NaCl) for 30 min. To remove very low-density lipoprotein (VLDL), a density of 1.027 g/ml was adjusted using NaCl followed by ultracentrifugation for 24 h at 45,000 rpm (10°C). Next, NaCl was used to adjust the density of 1.063 g/ml and the LDL fraction was covered with isotonic saline solution followed by ultracentrifugation for 24 h at 40,000 rpm (15°C). LDL was collected from the middle of the centrifuge tube, sterilized using Rotilabo®-syringe filter and stored at 4°C until use.

2.3 Modification of LDL by HOCl

NaOCl (Sigma-Aldrich) was diluted 1:400 in NaOH (0.1 M) and the concentration of NaOCl was calculated using the molar absorption co-efficient of 350 M^{-1} cm^{-1} at 292 nm (Morris, 1966). The amount of NaOCl to modify LDL was calculated according to the oxidant:lipoprotein molar ratio where the molecular mass of apoB-100 is 550 kDa. The pH of NaOCl was adjusted to 7.4 using HCl (0.1 M) prior to addition to LDL and kept for at least 1 h at 4°C (Hazell and Stocker, 1993). LDL (1-2 mg/ml in NT or modified-Tyrode, pH 7.4) was incubated with final NaOCl concentrations of 0.4 or 0.8 mM, which resulted in oxidant:lipoprotein molar ratio of 200:1 or 400:1, respectively (Malle et al., 1995a).

2.4 Modification of LDL by the MPO-H_2O_2-chloride system (MPO-LDL)

The MPO-H_2O_2-chloride system was used to generate HOCl enzymatically and in turn to modify LDL at 37°C (Malle et al., 2000). After incubation of LDL (1 mg/ml in PBS, pH 7.4) at 37°C for 10 min, 20 µM H_2O_2 was added in 5-min intervals for 20 times. Along with the first and then every third H_2O_2 addition step, MPO (1 µg/ml, Planta Natural Products, Vienna, Austria) was added for eight times. The reaction mixture was kept at 37°C for 3 h in total and further at 25°C overnight. Finally, the samples were kept at 4°C and used within 24 h.

2.5 Solutions

Following solutions were used for cardiomyocyte isolation and cell perfusion. Composition is given in mM.

1. Normal Tyrode (NT): NaCl 137, KCl 5.4, $CaCl_2$ 1.8, $MgCl_2$ 1.1, $NaHCO_3$ 2.2, NaH_2PO_4 0.4, HEPES/Na^+ 10, D(+)-glucose 5.6, pH 7.4 was adjusted with NaOH.
2. Caesium Tyrode (CsT): NaCl 137, CsCl 5.4, $CaCl_2$ 1.8, $MgCl_2$ 1.1, $NaHCO_3$ 2.2, NaH_2PO_4 0.4, HEPES/Na^+ 10, D(+)-glucose 5.6, pH 7.4 was adjusted with CsOH.
3. Sodium Tyrode (NaT): NaCl 130, tetraethylammonium chloride 10, CsCl 4, $MgCl_2$ 1, D(+)-glucose 10, HEPES 10, pH 7.4 was adjusted with NaOH.
4. Modified-Tyrode: NaCl 127, KCl 2.3, $CaCl_2$ 2.5, $MgSO_4$ 0.6, $NaHCO_3$ 25, KH_2PO_4 1.3, D(+)-glucose 11.2, insulin 5 IU/l, pH 7.4 was adjusted with NaOH.

Following solutions were used to fill patch-pipettes. Composition is given in mM.

1. Normal pipette solution (N-pip): KCl 110, ATP/K^+ 4.3, $MgCl_2$ 2, $CaCl_2$ 1, EGTA 11, HEPES/K^+ 10, pH 7.4 was adjusted with KOH (estimated free $[Ca^{2+}]<10^{-8}$ M).
2. Caesium pipette solution (Cs-pip): CsCl 110, ATP/Na^+ 4.3, $MgCl_2$ 2, $CaCl_2$ 1, EGTA 11, HEPES/Cs^+ 10, pH 7.4 was adjusted with CsOH (estimated free $[Ca^{2+}]<10^{-8}$ M).
3. Sodium pipette solution (Na-pip): CsCl 40, Cs-glutamate 80, NaCl 5, $MgCl_2$ 0.92, Mg-ATP 5, Li-GTP 0.3, HEPES 10, niflumic acid 0.03, nifedipine 0.02, strophanthidin 0.004, pH 7.4 was adjusted with CsOH (estimated free $[Ca^{2+}]<10^{-8}$ M).

2.6 Atrial trabeculae contractile response

Human right atrial appendages (RAAs) were obtained from 8 patients undergoing cardiac surgery. Information about patients, diseases and medicaments are given in Table 1. The use of human tissue was approved by the ethics committee of the Medical University of Graz (Austria) and all patients gave informed consent. Tissues were provided by the Department of Cardiology, Medical University of Graz (Austria) and transported in a cold modified-Tyrode solution containing 2,3-butanedione 2-monoxime (5 mM, Sigma-Aldrich) and low calcium (500 μM) to the laboratory. Trabeculae (muscle strips with a cross-sectional area of < 0.6 mm^2) were isolated with the help of a stereo microscope (VMT Olympus, Tokio, Japan) and mounted on miniature hooks connected to a force transducer (Scientific Instruments, Gilching, Germany). Electrical stimulation (1 Hz, voltage 25% over threshold) was induced by a stimulator (STM1, Scientific Instruments) and the trabeculae were perfused with modified-Tyrode solution during whole experiment (Wallner et al., 2015). Trabeculae were stretched stepwise to reach a level of optimum preload (baseline). After baseline recording trabeculae were incubated with KN93 (5 μM, Sigma-Aldrich) or Ranolazine (10 μM, Tocris, Vienna, Austria) (at 0 min time-point) for 15 min followed by addition of HOCl-LDL (200:1, 250 μg/ml) (at 15 min time-point). At 0, 15, 30, 45, 75 and 105 min stimulation (1 Hz) was stopped (0 Hz) for 1 min followed by 0.5 Hz stimulation (1 min) and another minute without stimulation (0 Hz) (Figure 3C). Except these time points trabeculae were stimulated at 1 Hz during whole experiments. Data were stored digitally (Labview) and analogously using a thermorecorder (Graphtec Linearcorder WR 3320). During non-stimulation (0 Hz) period numbers of spontaneous contractions/45 s were counted as arrhythmic episodes. Diastolic tension (%) was calculated from the ratio of diastolic to systolic force at 30 min time point.

Table 1. Information about patients, diseases and medicaments

Number of patients	8
Gender, n (male) (%)	8 (100%)
Age (years)	64.25 ± 3.43
BMI (kg/m²)	28.45 ± 1.4
CABG, n (%)	6 (75%)
AVR, n (%)	3 (37.5%)
Sinus-rhythm, n (%)	8 (100%)
Atrial fibrillation, n (%)	0 (0%)
Paroxysmal atrial fibrillation, n (%)	0 (0%)
Diabetes mellitus, n (%)	0 (0%)
Hypertension, n (%)	8 (100%)
%EF	51.63 ± 2.46
MEDICATION:	
Aspirin, n (%)	7 (87.5%)
Statins, n (%)	5 (62.5%)
AT II antagonists, n (%)	2 (24%)
ACE inhibitors, n (%)	4 (50%)
Beta blockers, n (%)	5 (62.5%)

ACE: Angiotensin Converting Enzyme; AT: Angiotensin; AVR: Aortic Valve Replacement; BMI: Body Mass Index; CABG: Coronary Artery Bypass Grafting; EF: Ejection Fraction.

2.7 Isolation of primary guinea pig ventricular (GPV) myocytes

GPV myocytes were isolated as described previously (Piper et al., 1982). Briefly, GP were euthanized, hearts were quickly excised, mounted on a Langendorff apparatus and afterwards the coronary system was perfused with a solution containing 100 IU/ml collagenase (Worthington CLS 2, Worthington Biochemical Corporation, New Jersey, USA) at 37°C. After enzymatic digestion, cells were isolated from ventricles and calcium concentrations were raised stepwise to 1.8 mM. Cells were transferred to cell culture medium M199 (Sigma-Aldrich) containing penicillin 50 IU/ml, streptomycin 50 µg/ml (both Sigma-Aldrich), and maintained at 37°C under 5% CO_2. All experiments were performed on the day after isolation. For electrophysiological and calcium transient experiments cells were maintained in suspension. For PCR analysis, cells were transferred to Laminin (5 µg/ml) and L-ornithine (20 µg/ml) coated plates to separate viable cells from the dead cells.

2.8 Electrophysiological recordings and analysis

APs and transmembrane currents were recorded in the whole cell configuration of the patch-clamp technique using the amplifiers List L/M-EPC 7 (List, Darmstadt, Germany) and Axopatch 200B (Molecular Devices, CA, USA) and the A/D - D/A converters Digidata 1322A and Digidata 1200 (Molecular Devices LLC). Patch pipettes with the tip-resistance of 2-3 MΩ were used. pCLAMP software (Molecular Devices LLC) was used for data acquisition and analyses. Only quiescent rod-shaped myocytes with clear cross-striation were used for electrophysiological experiments. Cell membrane capacitance was determined by integration of the capacitive transient elicited by a 10 mV hyperpolarizing step from -50 mV and ion currents were normalized to cell membrane capacitance and expressed as pA/pF to compensate for cell size variations. In order to allow equilibration of the pipette solution with the cytosol current recordings were started 4 min after rupture of the membrane patch. Late

sodium current (I_{NaL}) current was measured at 22-23°C while all other currents were recorded at 36-37°C.

NT/N-pip solutions were used to record APs and steady state current (I_{ss})-voltage (I-V) relation. In some experiments Ba^{2+} (0.5 mM) was added to NT in order to measure inward rectifier potassium current (I_{K1}) as Ba^{2+}-sensitive current. CsT/Cs-pip solutions were used for L-type calcium current (I_{CaL}) and CsT containing 200 µM $CdCl_2$ for the non-selective cation current (I_{NS}). NaT/Na-pip solutions were used for measuring late sodium current (I_{NaL}).

For AP recordings cells were stimulated with minimal super-threshold current pulses (5 ms) at a frequency of 0.5 or 1 Hz. In order to exclude any initial transient behaviour, the effects were calculated after the run of 10 APs. Afterwards, 10 consecutive APs were averaged in each experiment to analyse AP parameters using Axotape software (Axon Instruments, Foster City, USA) (Zorn-Pauly et al., 2005).

$I_{Ca,L}$ was studied by voltage steps to potentials between -40 and +90mV (10 mV interval, 400 ms) preceded by a 50 ms prepulse to -40 mV from a holding potential of -80 mV in order to activate and voltage-inactivate sodium current). The amplitude of $I_{Ca,L}$ was measured as the difference between the peak inward current and the current at the end of the depolarization pulse (Zorn-Pauly et al., 2004). For determination of steady-state activation of $I_{Ca,L}$, peak values of $I_{Ca,L}$ were divided by the driving force and normalized with the maximal value. The reversal potential did not differ between control and treated groups and the mean reversal potential of all measured myocytes is +54 mV. Curves were fitted to the normalized data according to the equation (Pelzmann et al., 1998).

$$d_\infty = 1/\{1 + \exp[(V_{1/2\ act} - V)]/k]\}$$

Where d is the Boltzmann function, V is the membrane potential, $V_{1/2act}$ is the membrane potential of half maximum activation and *k* is the slope of the activation curve. The half maximum inactivation of control GPV cells was −8.76±0.54 mV.

For the determination of steady-state inactivation of I_{CaL} current was activated with test pulses to +10 mV (400 ms), which were preceded by conditioning pulses from -45 to +50 mV (5 mV interval, 400 ms) from a holding potential of -45 mV. The pulse pair was separated by a short 10 ms repolarizing step to -45 mV. $I_{Ca,L}$ during the test step was normalized and plotted as a function of prepulse potential. Curves were fitted to the normalized data according to the equation (Pelzmann et al., 1998).

$$f_\infty = 1/\{1 + \exp[V - V_{1/2\ \text{inact}})]/k]\}$$

Where f is the Boltzmann function, V is the membrane potential, $V_{1/2inact}$ is the membrane potential of half maximum inactivation and *k* is the slope of the inactivation curve. The half maximum inactivation of control GPV cells was −19.66±0.45 mV.

I_{ss} and I_{NS} recordings were performed using voltage ramps (-100 to +60 mV, duration 20 s). For I_{NS} measurements $CdCl_2$ (200 µM) was added to CaT solution to enable the current recording in the absence of K^+- and Ca^{2+}- conductance (Zorn-Pauly et al., 2005).

I_{K1} was measured as the Ba^{2+}-sensitive current (obtained by digital subtraction) elicited by hyperpolarizing voltage steps (3 s) from -40 mV to -130 mV (10 mV increments, holding potential -40 mV). For current analysis, currents (at the end of the pulse) measured in the presence of $BaCl_2$ were subtracted from the currents (at the end of pulse) measured in the absence of $BaCl_2$ for the same myocyte (Zorn-Pauly et al., 2005).

I_{NaL} was determined by a train of voltage pulses (5 pulses, basic cycle length 2 s, 1000 ms) to -20 mV from a holding potential of -120 mV. Each pulse was preceded by a 5 ms pre-pulse to +50 mV to optimize voltage control (Wagner et al., 2011). For analysis, time course of current inactivation was fitted bi-exponentially and the slow time constant (τ_{slow}) was analysed as an estimation of I_{NaL}.

2.9 Incubation of RAA with HOCl-LDL

Human RAAs were obtained from three patients undergoing cardiac surgery. Tissues were transferred to the laboratory in modified-Tyrode solution containing 2,3-butanedione 2-monoxime (5 mM) and low calcium (500 μM) to the laboratory. Tissues were cut into small pieces (1 mm^3) and transferred to modified-Tyrode containing nLDL or HOCl-LDL (200:1, 250 μg/ml) and incubated for 8 h with oxygen supply (37°C). Tissues were washed with cold PBS and homogenized in Trizol or RIPA buffer (150 mM NaCl, 50 mM Tris-HCl [pH 7.4], 1% NP-40, 0.1% SDS, 0.5% sodium deoxycholate, 1 mM EDTA, pH 7.4) for either PCR or Western blot analysis, respectively.

2.10 Western blot

HL-1 cells were lysed in ice-cold lysis buffer (50 mM HEPES, 150 mM NaCl, 1 mM EDTA, 10 mM $Na_4P_2O_7$, 2 mM Na_3VO_4, 10 mM NaF, 1% [v/v] Triton X-100, 10% [v/v] glycerol, pH 7.4) containing a protease inhibitor cocktail tablet (Sigma-Aldrich) for 10 min on ice. Cells were scraped and centrifuged at 10,000 rpm (4°C, 10 min) to pellet debris. Protein estimations of cell lysates or RAA tissues were performed using the BCA protein assay kit (Thermo Scientific, IL, USA). Fifty µg of total protein was added to 10 µl of 4x NuPAGE LDS sample buffer (Invitrogen, Lofer, Austria) containing 2 µl sample reducing agent (Invitrogen) and heated (70°C, 10 min). Proteins were separated by electrophoresis on NuPAGE 4-12% Bis-Tris gels and transferred to nitrocellulose membranes (Invitrogen) (Koyani et al., 2014). Membranes were blocked with 5% (w/v) non-fat milk in Tris-buffered saline containing Tween 20 (TBST, 25°C, 2 h) and incubated with following primary antibodies (diluted in 5% [w/v] bovine serum albumin (BSA)-TBST): anti-oxCaMKII (1:1000, Millipore-07-1387) or pCaMKII (1:1000, Abcam-ab32678) (overnight at 4°C). Membranes were washed and incubated with horseradish peroxidase-conjugated goat anti-rabbit IgG (1:200,000 Biomol-6293) (25°C, 2 h). Immunoreactive bands were visualized using Super Signal West Pico Chemiluminescent substrate (Thermo Scientific) and Bio-Rad

ChemiDoc MP Imaging System. For normalization, membranes were stripped with stripping buffer (58.4 g/L NaCl, 7.5 g/L glycine, pH 2.15) and incubated with anti-CaMKII (1:300 Santa Cruz-SC-9035) as primary antibody.

2.11 Real time quantitative PCR (qPCR)

Total RNA was isolated from HL-1/ GPV cardiomyocytes or human RAA using Direct-zol RNA MiniPrep (Zymo Research, Eichgraben, Austria). One µg of RNA was subjected to reverse transcription. Six ng cDNA per template was used for gene quantification using GoTaq qPCR Master Mix (Promega, Vienna, Austria) and gene specific primers. The real time qPCR protocol was performed using LightCycler 480 system (Roche Diagnostics, Vienna, Austria) (Koyani et al., 2014). Primer sequences are given above in Table 2. Relative gene expression levels compared to GAPDH were calculated using ΔΔCT method.

Table 2. Sequence of primers used in qPCR

Gene	Species	Forward primer (5'-3')	Reverse Primer (5'-3')
GAPDH	H	Hs_GAPDH_1_SG (Qiagen)	
	M	Mm_Gapdh_3_SG (Qiagen)	
	Gp	GTGAAGCAGGCATCAGAGGGC	GGCTCAGGTGGGGTCCACTTAC
Cav1.2	H	GAGAACAGCAAGTTTGACTTTGACAA	CGAAGGTGGAGACGGTGAA
	M	Mm_Cacna1c_1_SG (Qiagen)	
	Gp	GCGGACACAGAGGTGAGGGG	GTGGGGATGTGCTCAGGGGC
Cav3.2	H	GTTCGGGCAGAAGTGTTACCT	CTCACGTTGTGTCCGTCCAA
	M	CACATCACCAAGGAGTACTGGC	CAAATGAACGCTGAGCCTGA
	Gp	TGCTCAACATGTTCGTGGGTGTCG	CGTAGTAGGGTCGGCGCTGAGC
RyR2	H	GGCGAAGACGAGATCCAGTT	CTTTGTGGATGGTTGCGGTG
	M	CCATGGCTGATGCGGGCGAA	GCAGGGCCCGTACTGACAGG

NCX1	H	CTGGTGGAGATGAGTGAGAAGA	GGTTGGCCAAACAGGTATTTTC
	M	CCCTGTTGTTGAATGAGCTTGGTGG	TGCTGGTCAGTGGCTGCTTGT
	Gp	TCGCCCTCCACTGCCACTGT	TGACCTCCATGATGCCAATGCTCT
SERCA 2a	H	CCGCAACTACCTGGAACCTG	CACGCAACCGAACACCCTTA
	M	CACGTGCCTGGTGGAGAAGATGA	CCGGCTTGGCTTGTTTGGGG
	Gp	AGGTGCTGGGCCACTTCGGT	TTCAGCCGGTAACTCGTTGGAGC
Kir2.1	H	TTCAGTCACAATGCCGTGATT	GCTTTTCCGAAGATTGCCCA
	M	CCGACAACAGTGCAGGAGCCG	GAACAGCCAGGAGAGCACGAAGG
	Gp	TGTGTCCATGCTCCCGTGCC	TGCTGAGGACGCCAGTGCTT
Kir2.2	H	GCCCACTCAGCACCATTACA	CCTCCTCCGATGACACGATG
	M	GAGTCTGTGCCCACTGTGCCTG	TTGGGGTACTCAGACGCCGGG
	Gp	ACGCAGACCACCATCGGCTAC	GCCACCACCATGAAGACAGCCAC
Kir2.3	H	ACCTCAACGTGGGCTATGAC	CGTCGATCTCGTGGACAATGAT
	M	GACCCTCCTCGGACCTTACGCC	TGACAAAGCGGTTGCGGCGT
	Gp	GTCTTCCCAGGTGACACGCCG	TCTTGACGAAGCGGTTGCGG
NaV1.5	H	TCACCGCCATTTACACCTTTG	GGTCCCGAAGGAAAGTGAACG
	M	ATGGCAAACTTCCTGTTACCTC	CCACGGGCTTGTTTTTCAGC
	Gp	TTCCAGATCACCACATCGGC	GTTGGGCAAATTGGGGTCAC
SR-A1	M	TGAACGAGAGGATGCTGACTG	TGTCATTGAACGTGCGTCAAA
SR-B1	M	TTTGGAGTGGTAGTAAAAAGGGC	TGACATCAGGGACTCAGAGTAG
CD36	M	AGATGACGTGGCAAAGAACAG	CCTTGGCTAGATAACGAACTCTG
LOX-1	M	CAAGATGAAGCCTGCGAATGA	ACCTGGCGTAATTGTGTCCAC
MSRA	M	CACGCAATCCCACCTACAAAG	CGGGTCGTGATTCTCCCAG
MSRB	M	CTTCGGAGGCGAGGTTTTCC	TCTCAGGGCACTTGGTCACA

H: Human, M: Mouse and GP: Guinea Pig.

2.12 ROS measurement

Intracellular ROS levels were assessed using carboxy-H_2DCFDA (5-(and 6)-carboxy-2',7'-dichlorodihydrofluorescein diacetate, Invitrogen), a cell-permeable dye that becomes fluorescent upon oxidation by ROS. HL-1 cells were incubated with 10 µM DCFDA in PBS for 30 min at 37°C. Afterward, the cells were washed twice with ice-cold PBS and lysed with 300 µl of 3% (v/v) Triton X-100 in PBS (30 min) followed by addition of 50 µl absolute ethanol (15 min) with shaking (1350

rpm, 4°C). Lysates were centrifuged at 10,000 rpm (4°C, 10 min) to pellet debris. The supernatant (100 µl) was used to measure DCF (2',7'-dichlorofluorescein) fluorescence at emission and correction wavelengths of 485 and 540 nm respectively. A microtiter plate reader (Victor Multilabel Counter, Perkin-Elmer, Waltham, MA, USA) was used to detect fluorescence intensities (Koyani et al., 2014).

2.13 Scavenger receptor silencing by siRNA

HL-1 cells were transfected with four siRNAs specific for SR-A1, SR-B1, CD36 or LOX-1 (40 nM, SI04945962, SI02672971, SI00945063, SI02676765 Qiagen) or with a scrambled negative control siRNA (40 nM, 1022076, Qiagen). The siRNA transfections were performed using Lipofectamine 3000 (Invitrogen) according to the manufacturer's suggestions. Briefly, HL-1 cells were grown to 50% confluence and transfected with 500 µl medium (without penicillin/streptomycin) containing 3 µl of Lipofectamine 3000 and the respective siRNA (40 nM final concentrations) for 6 h at 37°C (Koyani et al., 2014). The transfection medium was aspirated and replaced with medium containing penicillin/streptomycin. Cells were grown for another 24 h, RNA was isolated and mRNA expression of scavenger receptors was measured using qPCR (see above). In parallel, transfected HL-1 cells were treated with HOCl-LDL at indicated concentrations and time periods to follow CaMKII oxidation by Western blot (see above).

2.14 Cell shortening and Ca^{2+} transient (CaT) measurements

GPV cardiomyocytes were treated with HOCl-LDL for indicated time periods. Cells were washed twice with NT and incubated with NT containing 1 µM Fura-2-AM (a fluorescent Ca^{2+} chelator, Invitrogen) and 1 µM Pluronic F-127 (Invitrogen) for 30 min at 37°C. Cell shortening and CaT were assessed simultaneously during field stimulation (electrode distance - 1 cm; pulse duration - 5 ms; super-threshold

pulse amplitude - 4 V/cm) at a frequency of 1 Hz using a video-based sarcomere length detection system (IonOptix Corporation, MA, USA) at 37°C. Fluorescence intensities were measured at 340 and 380 nm of excitation and at 510 nm of emission wavelengths using a dual excitation light source (Poteser et al., 2011). The F340/F380 ratio was used as an index of cytosolic Ca^{2+} concentration and to calculate CaT amplitude, CaT systolic ratio, CaT diastolic ratio, time to peak and relaxation time 50% (RT50). SR Ca^{2+} content was measured as the amplitude of the 20 mM caffeine-induced CaT. Relaxation tau of the caffeine-induced CaT was measured to assess NCX1 activity. Data were analyzed using Clampfit 10.2 and Microsoft Excel 2010.

2.15 Immunohistochemistry

Formalin-fixed paraffin embedded serial sections (3 μm) of infarcted and non-infarcted LV of healthy and MI patients were obtained from the Institute of Pathology, Medical University of Graz (Austria). Sections were deparaffinized in xylene and rehydrated in ethanol stepwise with the gradual decrease in % of ethanol. Sections were blocked with endogenous peroxidase (3% [v/v] H_2O_2 in methanol, 15 min) and incubated for 1 h at 25°C with following primary antibodies (diluted in Dako REAL Antibody Diluent, Dako, Vienna, Austria): anti-CD66 (1:10, Novocastra-NCL-CD66a), anti-MPO (1:400, Thermo Scientific-RB-373-A1), anti-apoB-100 (1:50, (Hazell et al., 1996)), anti-HOCl-modified epitopes (1:1, (Malle et al., 1995b)), anti-CaMKII (1:30, Santa Cruz-SC-9035) or anti-oxCaMKII (1:50, Millipore-07-1387). After washing three times with PBS sections were incubated for 30 min at 25°C with UltraVision LP Large Volume HRP Polymer (Thermo Scientific, IL, USA) to visualize the reaction. Detection was performed using AEC Substrate Chromogen (Dako, 5 min). Counterstaining was performed with hematoxylin (60 sec). Negative staining was performed in the absence of primary antibodies (Hoffmann et al., 2015).

2.16 Statistics

All values are represented as mean±SEM and n represents the number of experiments or cells. Statistical significances were tested by Student's t-test or one-way ANOVA with adequate post hoc tests (Tukey, Dunett), using IBM SPSS 20 software. P values ≤ 0.05 were considered statistically significant. All tests were 2-sided.

3. Results

3.1 Immunohistochemistry for neutrophils, MPO, apoB-100 and HOCl-modified epitopes in healthy and infarcted human LV

MPO has been used as a marker for neutrophil infiltration in various tissues including the heart (Mullane et al., 1985; Werner and Szelenyi, 1992) and various diseases such as CVDs (Alfakry et al., 2012; Loria et al., 2008). Therefore, we investigated whether the number of neutrophils is increased in infarcted heart tissue. Using immunohistochemistry we observed pronounced staining for CD66-positive cells (Figure 1, lower panel 1), indicating massive accumulation of neutrophils in the infarcted region of the myocardium. In parallel to the infiltration of neutrophils, intense staining of MPO was found within cells and also in some area of extracellular matrix (Figure 1, lower panel 2).

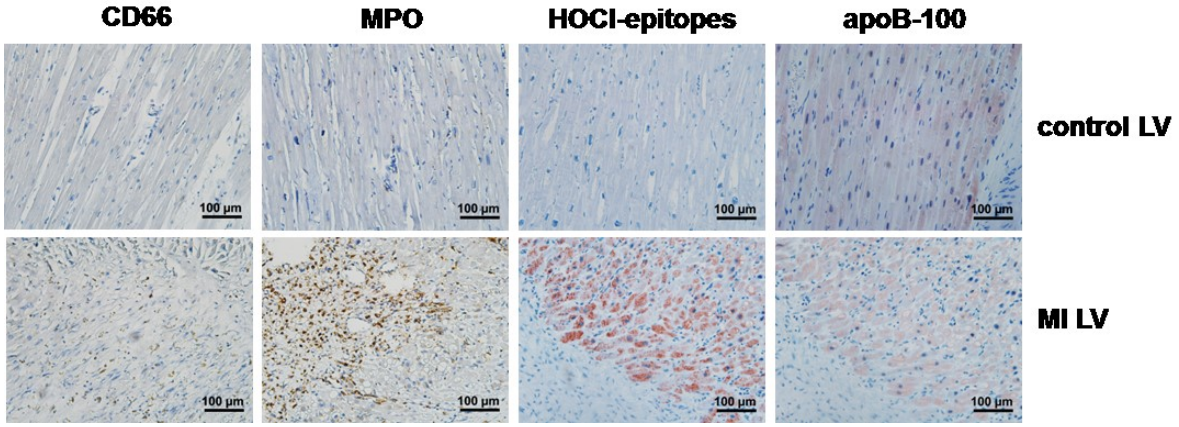

Figure 1. Immunostaining of neutrophils, MPO, HOCl-modified epitopes and apoB-100 in LV

Paraffin embedded serial sections of LV of healthy (control, upper panels) and infarcted hearts (lower panels) were stained with the specific antibodies recognizing CD66 (a marker for neutrophil), MPO, apoB-100 and HOCl-modified epitopes. Counterstaining was performed with hematoxylin to visualize nuclei. One representative immunostain from one out of four tissues is shown. Sections were kindly provided by Prof. G. Höfler, Department of Pathology, Medical University of Graz.

In contrast to diseased tissue, negligible staining for CD66 and MPO was observed in the myocardium of healthy LV (Figure 1, upper panel 1 and 2). Only at the region of blood vessels sporadic staining of CD66- and MPO-positive cells was observed.

Next, we investigated whether increased staining for MPO in the infarcted heart tissue is translated into accumulation of MPO-derived HOCl, a highly reactive oxidant that is known to modify (lipo)proteins in vivo and in vitro. Therefore, we used a monoclonal antibody that was raised against LDL modified by HOCl in vitro (Malle et al., 1995a). Abundant staining for HOCl-modified proteins/epitopes was found in the infarcted myocardium and staining was predominantly cell-associated (Figure 1, lower panel 3). Moreover, the pre-absorbed monoclonal antibody (with HOCl-LDL or HOCl-modified albumin in molar excess of 25:1) or omission of the primary antibody showed no immunostain (data not shown). This confirms that the staining is specific for HOCl-modified epitopes. In contrast to diseased tissue, no staining for HOCl-modified epitopes was detected in the myocardium of non-infarcted heart (Figure 1, upper panel 3).

The heart is reported to secret apoB-100-like lipoprotein particles (Boren et al., 1998). In another study, expression of apoB-100 at mRNA and protein levels were detected in cardiomyocytes (Nielsen et al., 1998). In line with these observations, we observed staining of apoB-100 in cardiomyocytes, whereby no apparent difference was observed for staining between control and infarcted LV (Figure 1, panel 4).

As LDL gets modified by HOCl under in vivo conditions, we hypothesized modification of lipoprotein particles by HOCl in the infarcted myocardium. Immunohistochemistry data confirmed correlation between staining of apoB-100 and HOCl-modified epitopes in serial sections of the infarcted heart (Figure 1, lower panel 3 and 4). From these data it is obvious that massive neutrophil accumulation is present in the infarcted heart. Moreover, detection of MPO, HOCl-modified epitopes and apoB-100 in serial section of MI LV provides strong evidence for oxidation of LDL in the myocardium by the MPO-H_2O_2-chloride system.

3.2 HOCl-LDL alters contractile function of human RAA trabeculae

Next, we planned to investigate whether HOCl-LDL, as detected by immunohistochemistry in the myocardium, might affect cardiac function adversely. Therefore, LDL was modified in vitro by HOCl and used to investigate its effect on contractile function of cardiac tissue. For these experiments we used RAA trabeculae obtained from patients undergoing cardiac surgery. Trabeculae were stimulated at a frequency of 1 Hz and after achievement of a preload by stretching trabeculae to an optimal length (baseline, 0 min, Figure 2), HOCl-LDL (100:1, 200:1 or 400:1, 250 µg/ml) was added at 15 min time point. Due to addition of modified-Tyrode alone or Tyrode-containing HOCl-LDL, we observed a negative inotropic effect in all trabeculae (Figure 2A-D, 18-27 min). This might occur due to change of volume or ionic composition of perfusion solution after addition of modified-Tyrode alone or Tyrode-containing HOCl-LDL.

In addition to a negative inotropic effect, we observed dysrhythmia in contractility of the trabeculae incubated with HOCl-LDL (200:1 and 400:1, Figure 2C/D, 18-27 min). These trabecuale could not follow contraction rhythm in response to 1 Hz stimulation; periods of drop in inotropy became apparent, which got recovered back to the maximum systole. Duration and amplitude of periods with loss of contractile rhythm were more pronounced in the trabeculae treated with HOCl-LDL modified using higher oxidant:lipoprotein molar ratio (400:1, Figure 2D, 18-27 min) compared to HOCl-LDL modified using lower oxidant:lipoprotein molar ratio (200:1, Figure 2C, 18-27 min). Longer exposure of trabeculae to HOCl-LDL led to an increase in diastolic tension as observed during 37-45 min (Figure 2B-D). With the increasing oxidant:lipoprotein molar ratio, an increase in the diastolic ratio (calculated from the ratio of diastolic to systolic force) became apparent. In parallel, we recorded separate contractile peaks. As shown in Figure 2 (right panel), we observed diastolic arrhythmia that became more pronounced with the increasing extent of oxidative modification of LDL (45 min vs. baseline).

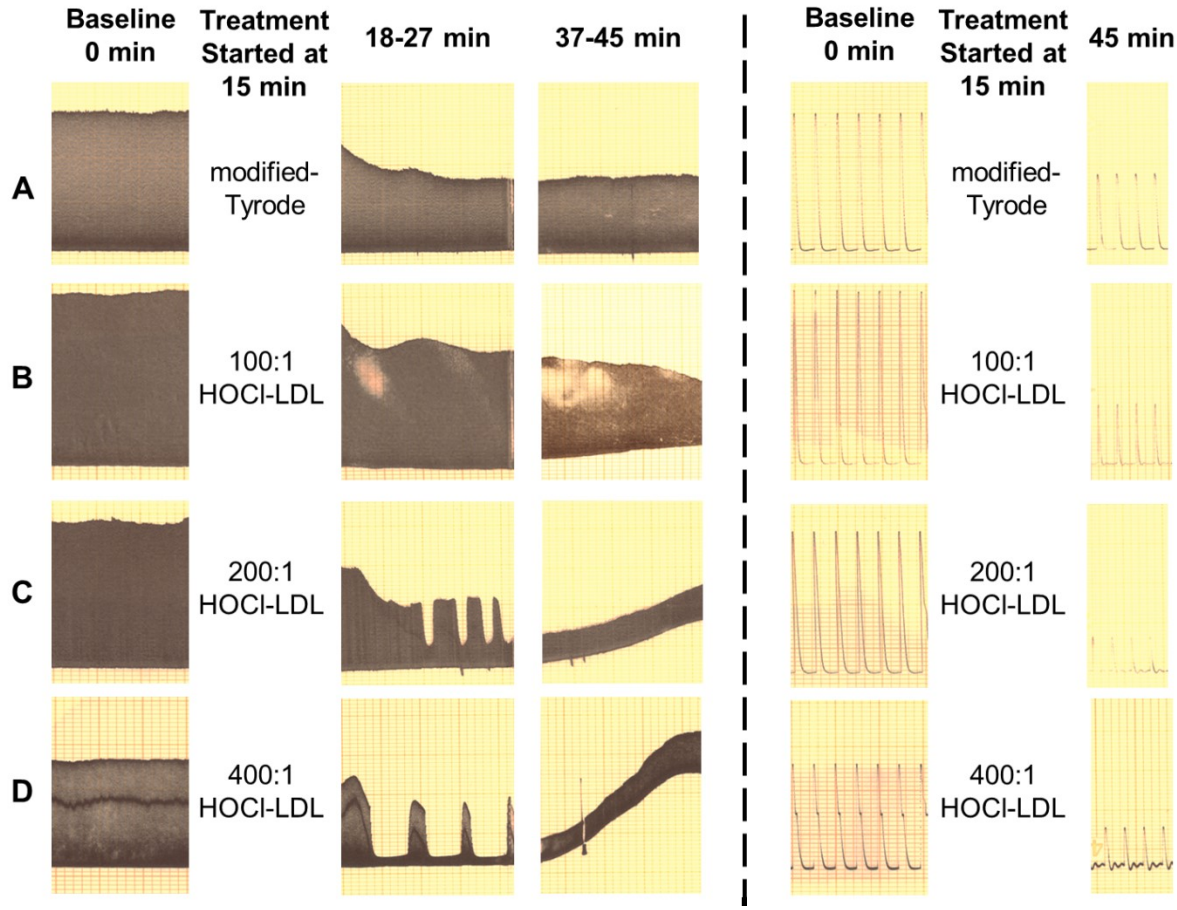

Figure 2. Original recordings of contractile response of human RAA trabeculae in response to HOCl-LDL

Human RAA trabeculae contractile response at baseline (0 min) and after treatment (started at 15 min) with (**A**) modified-Tyrode or Tyrode-containing HOCl-LDL (250 μg/ml) modified with the oxidant:lipoprotein molar ratio of (**B**) 100:1, (**C**) 200:1 or (**D**) 400:1 at indicated time periods. Trabeculae were stimulated at a frequency of 1 Hz. Original recordings of contractile response at 5 mm/min (left panel) and 250 mm/min (right panel) are shown (panels are separated by the dashed line). One representative recording out of three is shown.

Next, we aimed to investigate effects of HOCl-LDL on arrhythmic episodes and diastolic tension of trabeculae. For these experiments we used HOCl-LDL (200:1), as this oxidative modification showed pronounced effects on the contractile function of trabeculae (Figure 2C). Tissues were stimulated as shown in the protocol (Figure 3A) and spontaneous contractions in non-stimulation phase (0 Hz, 1 min at all indicated time periods) were counted as arrhythmic episodes. We observed arrhythmic episodes in some of the trabeculae even at baseline. This

might be a consequence of dissection of the trabeculae from RAA followed by hooking on the needles and stretching with mechanical force. Tissues were randomly selected for further interventions. Although, arrhythmic episodes in control trabeculae decreased after 15 min (Figure 3B), addition of HOCl-LDL (at 15 min) induced arrhythmic episodes that remained significantly higher compared to controls at all indicated further time points (45, 75 and 105 min, Figure 3B).

As shown in Figure 2 (37-45 min), HOCl-LDL treatment elevated diastolic tension. Data analysis revealed an increase in diastolic tension of the trabeculae incubated with HOCl-LDL by approx. 50% (Figure 3C). A negative diastolic tension observed in control group represents rundown (Figure 3B).

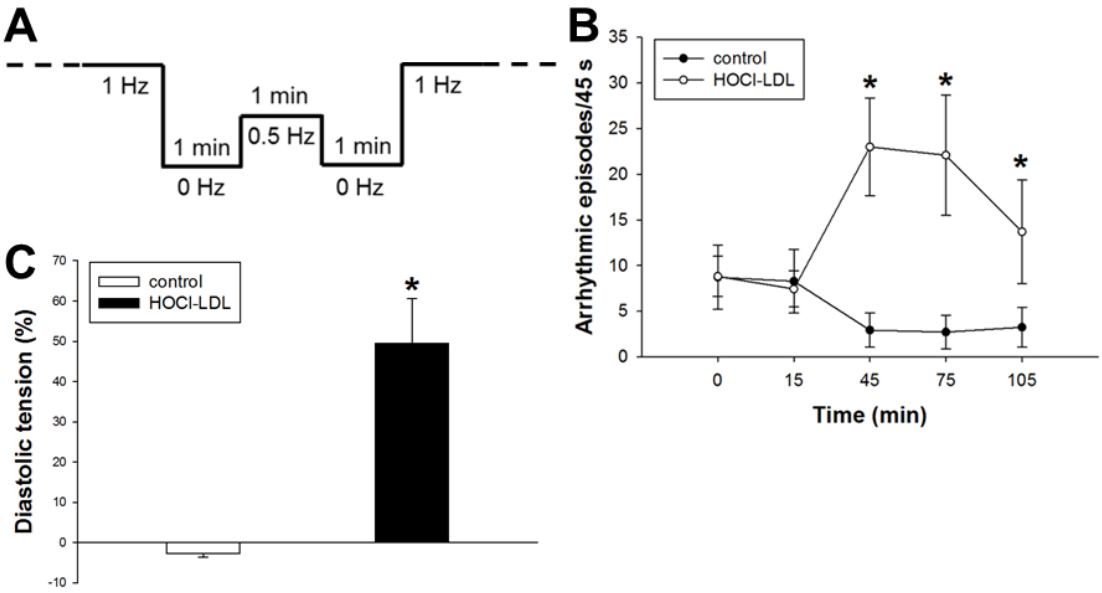

Figure 3. Arrhythmia and contractile dysfunction in human RAA trabeculae in response to HOCl-LDL

Human RAA trabeculae were stimulated at a frequency of 1 Hz for 105 min. HOCl-LDL (200:1, 250 μg/ml) was added at the 15 min time point. At indicated time periods stimulation was stopped (0 Hz) for 1 min followed by 0.5 Hz stimulation (1 min) and again 0 Hz (1 min) (stimulation protocol, **A**). During no-stimulation (0 Hz) period numbers of spontaneous contractions/45 s were counted as arrhythmic episodes (**B**). Diastolic tension (%) was calculated from the ratio of diastolic to systolic force at 30 min post-treatment with HOCl-LDL (**C**). Values are expressed as mean±SEM (n=8). *p≤0.05 vs. control.

3.3 HOCl-LDL alters electrophysiological characteristics of GPV myocytes

As we observed contractile dysfunction of trabeculae incubated with HOCl-LDL and contractile response of cardiomyocytes is strongly dependent on cellular excitability, we aimed to analyse APs. For these experiments, primary GPV cardiomyocytes were used. First, we measured APs of control and HOCl-LDL (200:1 or 400:1, 250 μg/ml, 12-16 h)-treated cardiomyocytes. Experiments performed at 4-8 h incubation time-periods did not show a significant difference in AP parameters between control and HOCl-LDL groups. Therefore, we chose an incubation time of 12-16 h for further experiments. Representative APs of a control myocyte stimulated at a frequency of 1 Hz is shown in Figure 4A.

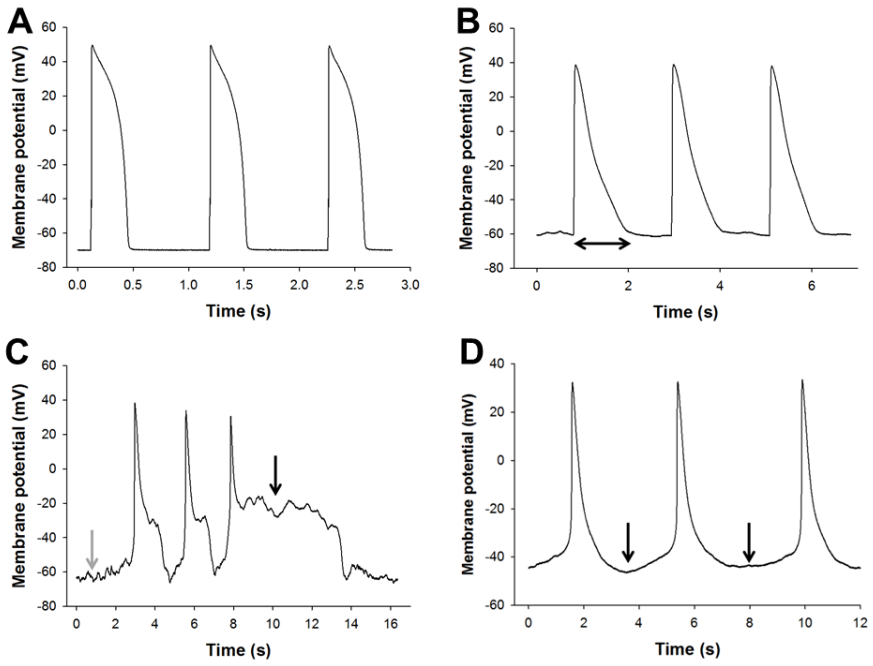

Figure 4. APs of GPV myocytes in response to HOCl-LDL

Representative APs of (**A**) control and (**B-D**) HOCl-LDL (400:1, 250 μg/ml)-treated (12-16 h) myocytes. Cells were patched using normal Tyrode (NT) and N-pip solutions and stimulated at a frequency of (**A**) 1 Hz, (**B**) 0.5 Hz or 0 Hz (**C** and **D**). Double-sided arrow in (**B**) represents prolongation of AP duration; black and grey arrows in (**C**) represent early- and delayed-afterdepolarization, respectively; arrows in (**D**) represent spontaneous diastolic depolarization of membrane potential.

Treatment of myocytes with HOCl-LDL resulted in prolongation of AP duration (APD, Figure 4B, double-sided arrow). Due to the prolongation of APD this cell could not follow the stimulation frequency of 1 Hz and therefore the cell was stimulated at a frequency of 0.5 Hz. In addition to APD prolongation, approx. 50% of the HOCl-LDL (400:1)-treated cells showed arrhythmic events even under non-stimulated condition (0 Hz). A representative AP with early afterdepolarizations (EADs, black arrow) and delayed afterdepolarizations (DADs, grey arrow) is shown in Figure 4C. Furthermore, Figure 4D shows spontaneous activity in APs of a cardiomyocyte with a highly depolarized resting membrane potential (arrows).

Next, we analysed AP parameters including APD (at 50% and 90% of repolarization), maximal upstroke velocity and resting membrane potential (V_{rest}) of cardiomyocytes treated with HOCl-LDL (200:1 and 400:1, 250 μg/ml, 12-16 h). Figure 5A shows a significant increase in APD at 50% of repolarization by 400:1 HOCl-LDL treatment (281±15 ms of control vs. 355±14 ms of HOCl-LDL). Moreover, HOCl-LDL (200:1 and 400:1)-treatment prolonged APD at 90% of repolarization from 325±17 ms (control) to 442±35 ms and 579±37 ms, respectively (Figure 5A).

Data analysis shows that HOCl-LDL treatment (200:1 and 400:1) reduced maximal upstroke velocity of APs significantly (348±19 V/s of control vs. 271±21 V/s of 200:1 HOCl-LDL and 138±17 V/s of 400:1 HOCl-LDL, Figure 5B). Moreover, resting membrane potential of control myocytes (69.21±1.10 mV) was depolarized under treated conditions (65.45±0.91 mV of 200:1 HOCl-LDL and 64.86±1.30 mV of 400:1 HOCl-LDL, Figure 5C). The extent of depolarization of resting membrane potential did not differ between both treatment groups. This is due to the fact that all cells treated with HOCl-LDL (200:1) showed APs while approx. 50% of HOCl-LDL (400:1)-treated cells showed arrhythmic events and therefore they were excluded from the analysis.

All these data confirm that HOCl-LDL altered cellular excitability of cardiomyocytes. In addition, arrhythmic events (EADs, DADs and spontaneous activity) observed in cardiomyocytes correlate with the HOCl-LDL-induced arrhythmic episodes in human RAA trabeculae.

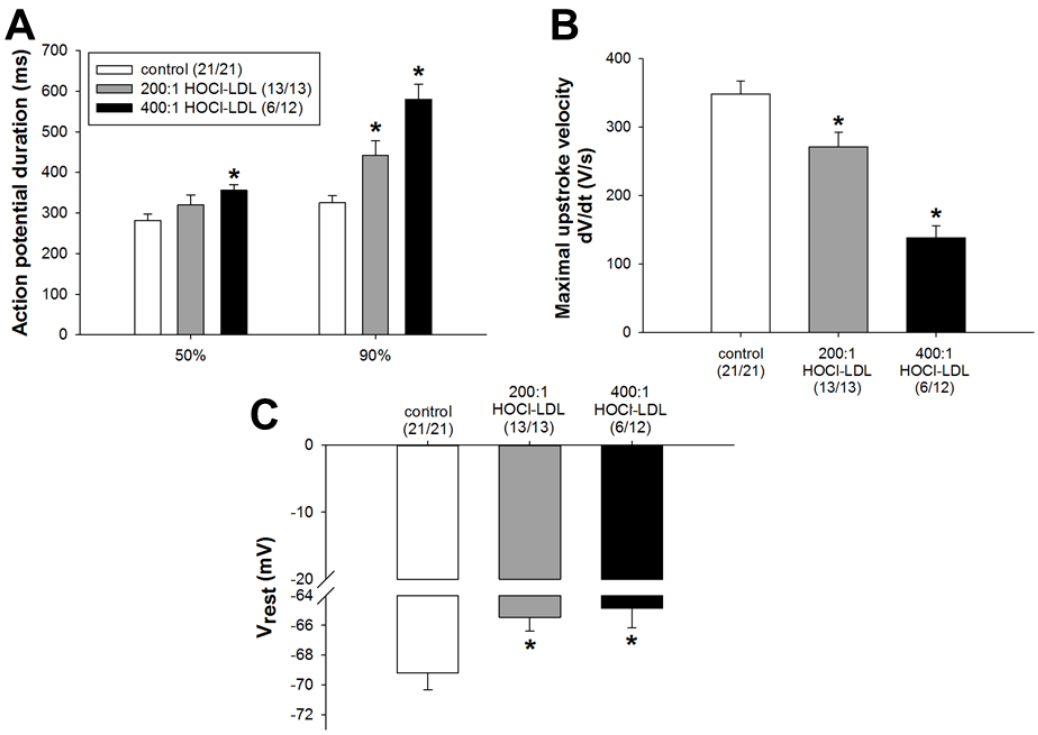

Figure 5. AP parameters of GPV myocytes in response to HOCl-LDL

Cardiomyocytes were incubated with HOCl-LDL (200:1 or 400:1, 250 μg/ml) for 12-16 h. Cells were patched and stimulated at a frequency of 1 Hz. (**A**) AP duration at 50% and 90% of repolarization, (**B**) upstroke velocity and (**C**) resting membrane potential were analysed. Values are expressed as mean±SEM. (n/n) represents number of cells showing APs elicited by external stimulus/total number of measured cells. Cells showing spontaneous activity or arrhythmic events were excluded from calculation. *p≤0.05 vs. control.

3.4 Modified-LDL oxidizes CaMKII

Since we observed alterations in contractility and cellular excitability in HOCl-LDL-treated cardiac tissue and myocytes, we intended to investigate the molecular mechanism(s) underlying the effects of HOCl-LDL. CaMKII plays a central role in regulation of ion channels, transporters and pumps that control EC coupling and electrophysiological characteristics of cardiomyocytes. Therefore, we investigated phosphorylation and oxidation status of CaMKII in response to HOCl-LDL. For these experiments, HL-1 cells, a murine atrial cardiomyocyte cell line, were used. For further experiments we used HOCl-LDL (200:1), as we observed pronounced effects using this modification degree.

Upon treatment of HL-1 cells with HOCl-LDL (250 µg/ml) we observed no change in phosphorylation (T^{287}, Figure 6A) but an increase in oxidation ($M^{281/282}$, Figure 6B) of CaMKII. In response to HOCl-LDL treatment, oxidation of CaMKII became apparent after 1 h and increased up to 24 h (Figure 6B).

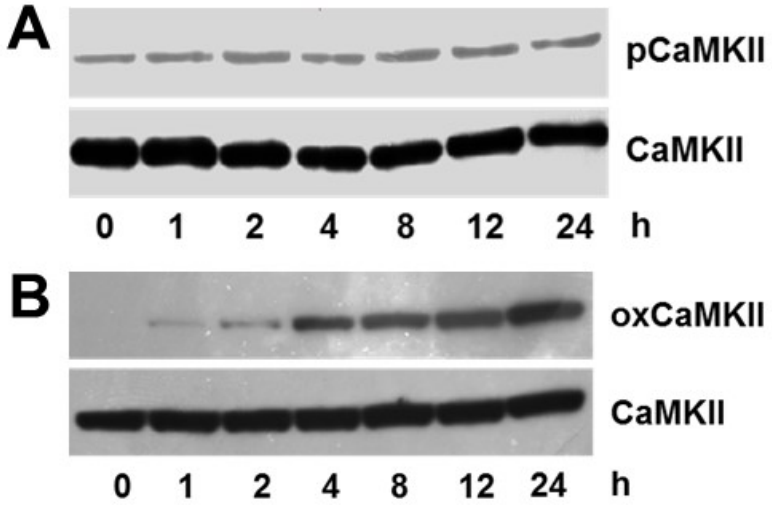

Figure 6. HOCl-LDL induces oxidation but not phosphorylation of CaMKII in HL-1 cells

HL-1 cells were incubated with HOCl-LDL (200:1, 250 µg/ml) for indicated time periods to follow (**A**) pCaMKII (phospho-CaMKII) and (**B**) oxCaMKII (oxidized-CaMKII) expression using Western blot analysis. CaMKII was used as a loading control. One representative blot out of three is shown.

To prove that CaMKII oxidation in response to HOCl-LDL is due to the modification of LDL, we examined effect of non-modified native LDL (nLDL). As shown in Figure 7A, nLDL (250 µg/ml, 12 h) had no effect on oxCaMKII expression. This data confirm that the observed change in CaMKII oxidation is mediated via the oxidative modification of LDL by HOCl.

Apart from modification of LDL by HOCl, we modified LDL by the MPO-H_2O_2-Cl^- system (MPO-LDL) to mimic in vivo conditions. LDL modified by both systems (HOCl added as a reagent or generated by the MPO-H_2O_2-Cl^- system) oxidized CaMKII to a similar extent in HL-1 cardiomyocytes. In addition, we used H_2O_2 (100 µM, 12 h) as a positive control for CaMKII oxidation; H_2O_2 is reported to oxidize CaMKII in cardiomyocytes (Wagner et al., 2011). A possibility of CaMKII oxidation by H_2O_2 that was used for the oxidative modification of LDL by the MPO-H_2O_2-Cl^- system can be ruled out, as H_2O_2 has a very short half-life (Giorgio et al., 2007) and LDL-modification by MPO was performed for 3 h at 37°C followed by incubation at 4°C overnight.

In the next set of experiments, we intended to evaluate efficacy of HOCl-LDL to oxidize CaMKII in cardiac tissue. Therefore, we incubated RAA obtained from 3 patients with either nLDL or 200:1 HOCl-LDL (250 µg/ml) for 8 h. HOCl-LDL treatment increased oxCaMKII expression in all RAA tissues compared to nLDL (Figure 7B). The data obtained from HL-1 cardiomyocytes and RAA tissues confirm that HOCl-LDL is a trigger for CaMKII oxidation in cardiac tissue as well as myocytes.

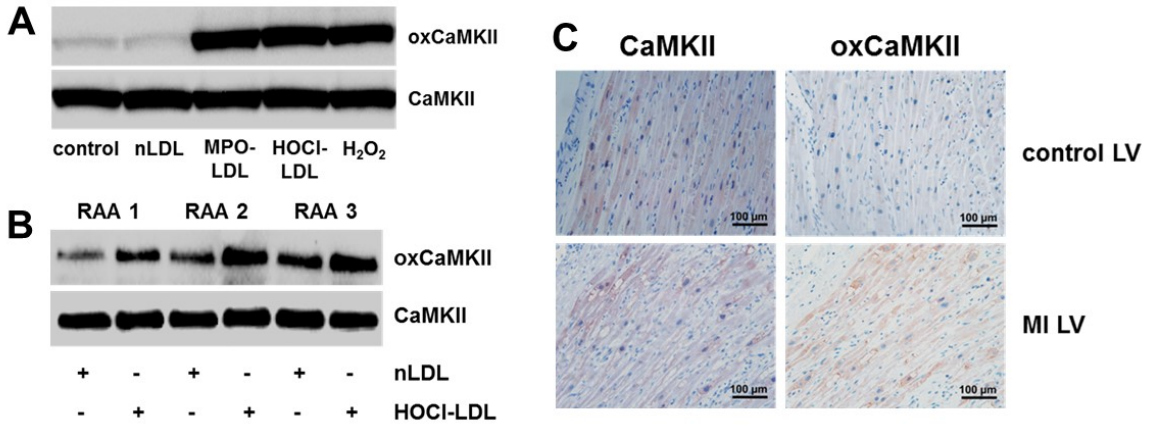

Figure 7. Oxidation of CaMKII by modified-LDL in human RAA/HL-1 cells and immunostaining of oxCaMKII in human LV myocardium

(**A**) HL-1 cells were treated with nLDL (250 μg/ml), LDL (250 μg/ml) modified by HOCl (200:1, HOCl-LDL) or MPO-H_2O_2-Cl^- system (MPO-LDL) or H_2O_2 (100 μM) for 12 h to follow oxCaMKII expression. (**B**) Human RAA from 3 patients (RAA 1-3) were incubated with nLDL or 200:1 HOCl-LDL (250 μg/ml) for 8 h with oxygen supply to follow oxCaMKII expression. (**C**) Paraffin embedded serial sections of LV of healthy (control, upper panel) and infarcted hearts (lower panel) were stained with anti-oxCaMKII or anti-CaMKII antibody. Counterstaining was performed with hematoxylin to visualize nuclei (n=4). (**A** and **B**) One representative blot out of three is shown and CaMKII was used as a loading control.

Next, we aimed to investigate the oxidation status of CaMKII in the infarcted myocardium. Immunohistochemistry data showed pronounced oxCaMKII expression in cardiomyocytes of the infarcted myocardium compared to healthy heart where no immunostaining was observed (Figure 7C). Similar cell-specific expression pattern of CaMKII was observed in serial sections of both, healthy and MI myocardium.

3.5 HOCl-LDL induces CaMKII oxidation via intracellular redox imbalance

Treatment of macrophages and T-cells with LDL modified by HOCl added as a reagent or generated by the MPO-H_2O_2-Cl^- system resulted in elevated ROS production (Calay et al., 2010; Resch et al., 2011). Therefore, we examined if this process might be operative also in cardiomyocytes. Treatment of HL-1 cells with HOCl-LDL (200:1, 250 μg/ml) resulted in a time-dependent activation of ROS production starting from 15 min and reaching a plateau after 120 min (Figure 8A). To identify specific reactive species, we used three ROS scavengers. Pre-treatment of HL-1 cells with Tempol (a superoxide anion blocker) and NAC (a non-specific blocker of superoxide and nitric oxide anions) blunted HOCl-LDL-induced ROS generation (Figure 8B, upper panel). In contrast, PDTC (a nitric oxide anion inhibitor) failed to inhibit the effect of HOCl-LDL on ROS production (Figure 8B, upper panel).

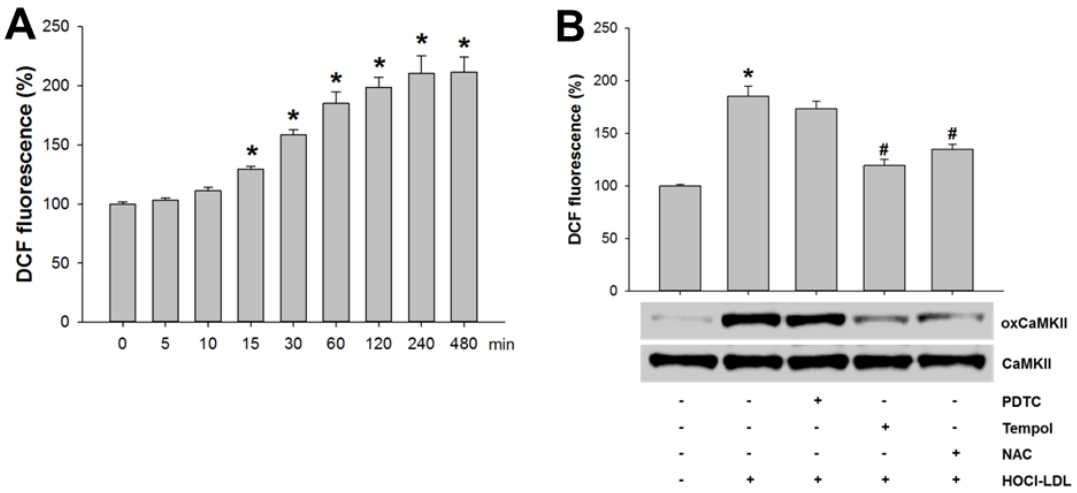

Figure 8. HOCl-LDL-induced intracellular redox imbalance leads to CaMKII oxidation

(**A**) HL-1 cells were stimulated with HOCl-LDL (200:1, 250 μg/ml) for indicated time periods to follow ROS levels by measuring DCF fluorescence. (**B**) Cells were incubated with ROS scavengers (PDTC [1 mM], Tempol [1 mM] or NAC [5 mM]) for 30 min prior to HOCl-LDL (200:1, 250 μg/ml) treatment to follow ROS levels (upper panel, 1 h) or CaMKII oxidation using Western blot analysis (lower level, 12 h). One representative blot out of three is shown. CaMKII was used as a loading control. DCF fluorescence intensity of vehicle (0.01% DMSO)-treated cells was set 100% and values are expressed as mean±SEM (n=6). *p≤0.05 vs. control and #p≤0.05 vs. HOCl-LDL.

Next, we tested if the redox imbalance is responsible for the oxidation of CaMKII, as ROS is known to oxidize CaMKII (Erickson et al., 2008). To confirm, we incubated HL-1 cells with ROS scavengers prior to HOCl-LDL (200:1, 250 μg/ml) treatment for 12 h. Figure 8B (lower panel) shows that both ROS scavengers, Tempol and NAC, blocked CaMKII oxidation in parallel to ROS activation (Figure 8B, upper panel). PDTC pre-treatment did not alter oxCaMKII expression in response to HOCl-LDL (Figure 8B, lower panel). These data confirm that HOCl-LDL induces CaMKII oxidation via elevation of intracellular superoxide anion level in cardiomyocytes.

3.6 Role of scavenger receptors in HOCl-LDL-induced CaMKII oxidation

HOCl-LDL is an agonist of various scavenger receptors. To investigate a possible role of various scavenger receptors in HOCl-LDL-mediated CaMKII oxidation, we adapted a siRNA approach to silence all four scavenger receptors in HL-1 cells. The silencing efficiency of siRNAs is shown in Figure 9A-D. The reduction in mRNA expression by gene specific siRNAs was found to be 52%, 41%, 58% and 62% for SR-A1, SR-B1, CD36 and LOX-1, respectively (Figure 9A-D). Scrambled siRNA (si-SCR) treatment did not alter expression of any of these scavenger receptors (Figure 9A-D).

In parallel, gene-silenced cells were incubated with HOCl-LDL (200:1, 250 μg/ml) for 12 h. Figure 9E reveals that silencing of SR-A1 and SR-B1 receptors did not alter HOCl-mediated oxCaMKII expression. In contrast, mainly the silencing of LOX-1 and partially the silencing of CD36 receptors inhibited HOCl-LDL-induced CaMKII oxidation (Figure 9E). These data reveal that HOCl-LDL-mediated CaMKII oxidation in cardiomyocytes is dependent mainly on LOX-1 and partially on CD36.

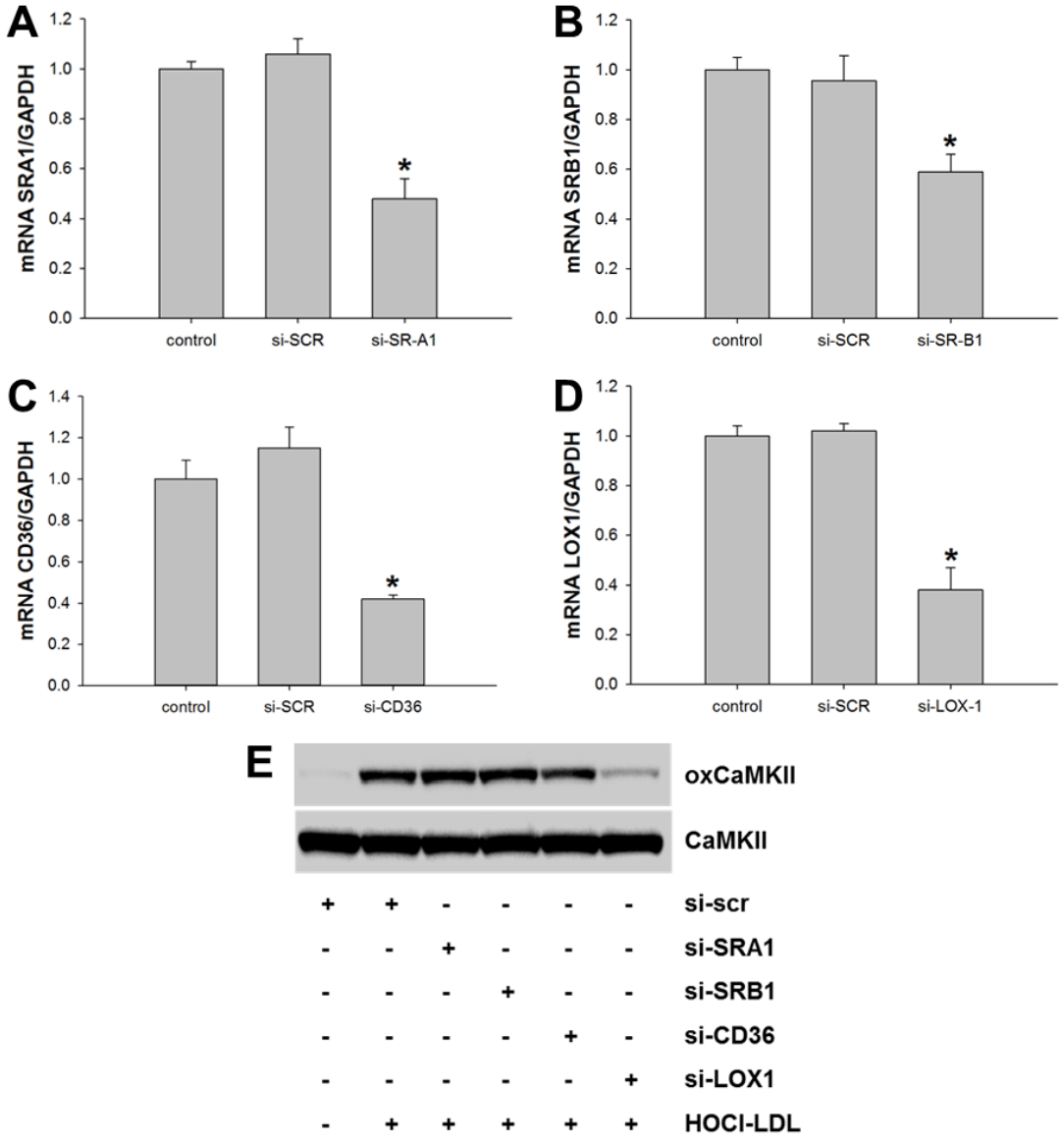

Figure 9. Impact of scavenger receptor silencing on HOCl-LDL-induced CaMKII oxidation

HL-1 cells were transfected with scrambled negative control siRNA (si-scr) (40 nM) or siRNA against SR-A1 (si-SRA1, **A** and **E**), SRB1 (si-SR-B1, **B** and **E**), CD36 (si-CD36, **C** and **E**) or LOX-1 (si-LOX-1, **D** and **E**) (40 nM). (**A**-**D**) Silencing efficiency of the respective siRNAs was followed using qPCR analysis. (**E**) Transfected cells were stimulated with HOCl-LDL (200:1, 250 µg/ml) for 12 h to follow oxCaMKII expression using Western blot analysis. One representative blot out of three is shown. CaMKII and GAPDH were used as loading controls for Western blot and PCR, respectively. Values are expressed as mean±SEM (n=6). *p≤0.05 vs. control.

3.7 Effect of HOCl-LDL on the expression of ion channels and pumps

As we observed contractile dysfunction and electrophysiological alterations induced by HOCl-LDL (Figure 3 and 4), we performed qPCR to determine expression level of various ion channels. Compared to nLDL, HOCl-LDL treatment decreased expression of CaV1.2, Kir2.2, RyR2 and NCX1, and increased expression of SERCA2a but did not alter expression of NaV1.5, CaV3.2, Kir2.1 or Kir2.3 in human RAA (Figure 10A). A similar expression pattern was observed in GPV myocytes treated with HOCl-LDL (Figure 10B).

To investigate if the altered expression pattern is due to CaMKII oxidation, we treated HL-1 cells with KN93 (5 μM, 30 min) prior to HOCl-LDL-treatment (200:1, 250 μg/ml) for 12 h. KN93 is a CaMKII inhibitor that has been used to study role of CaMKII oxidation in various in vitro and in vivo studies (Anderson et al., 1998; Ronkainen et al., 2011; Singh et al., 2009). KN93-pretreatment inhibited the effect of HOCl-LDL on expression levels of CaV1.2, Kir2.2, SERCA2a, NCX1 and RyR2 (Figure 10C). HOCl-LDL had no effect on the expression of CaV3.2, Kir2.1, Kir2.3 or NaV1.5 channels in HL-1 cells (Supplement Figure I).

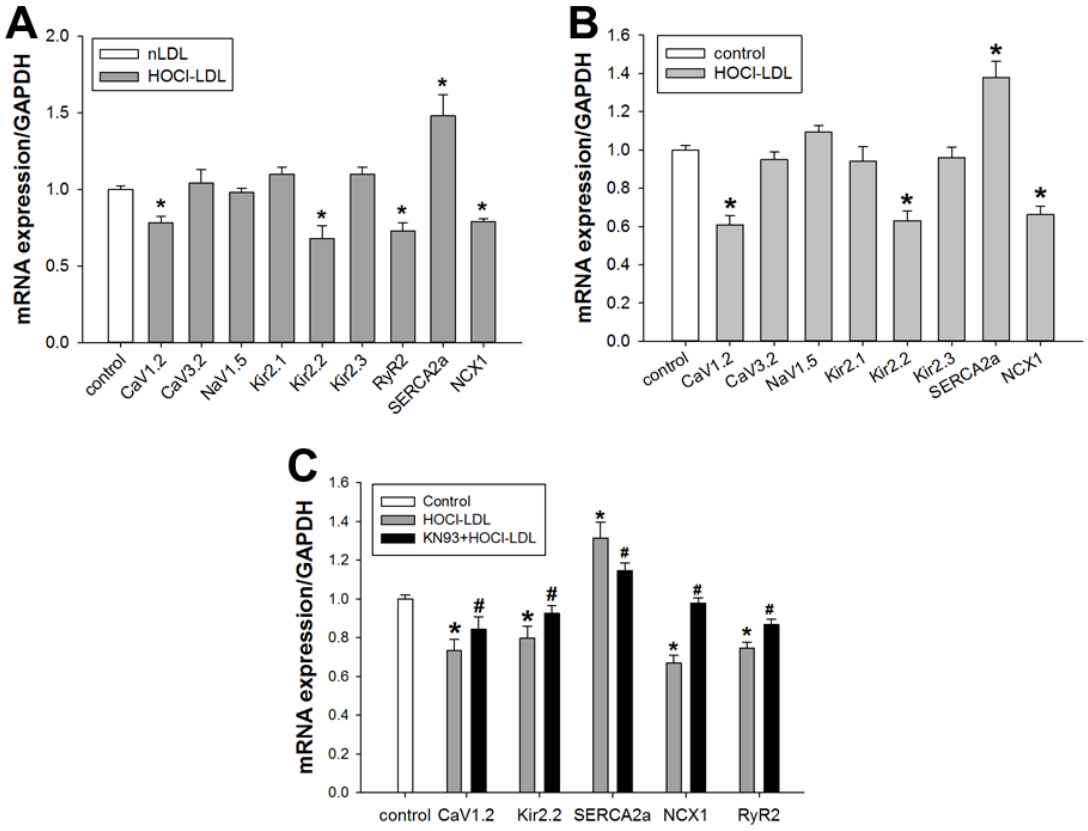

Figure 10. HOCl-LDL alters ion channel expression

Expression pattern of the indicated ion channels in (**A**) human RAA, (**B**) GPV and (**C**) HL-1 cells in response to HOCl-LDL (200:1, 250 µg/ml) is shown. The impact of HOCl-LDL on expression of ion channels is reversed by KN93 in HL-1 cells (**C**). (**A**) Human RAA trabeculae were incubated for 8 h with nLDL (250 µg/ml) or HOCl-LDL (200:1, 250 µg/ml) with oxygen supply. (**B**) GPV cells were incubated for 14 h with HOCl-LDL (200:1, 250 µg/ml). (**C**) HL-1 cells were incubated with KN93 (5 µM, 30 min) prior to HOCl-LDL (200:1, 250 µg/ml) treatment for 12 h. Tissues were homogenized and cells were lysed, RNA was isolated and qPCR was performed to follow mRNA expression levels of the respective ion channels. Values are expressed as mean±SEM [n=3 (**A**); n=6 (**B** and **C**)]. *p≤0.05 vs. control, $^{\#}$p≤0.05 vs. HOCl-LDL.

3.8 HOCl-LDL reduces $I_{Ca,L}$ density via CaMKII oxidation

As shown in Figure 2 and 3, HOCl-LDL treatment led to contractile dysfunction in RAA trabeculae. Moreover, HOCl-LDL decreased CaV1.2 expression level in RAA, GPV and HL-1 cells (Figure 10). Therefore, we aimed to estimate $I_{Ca,L}$ density in GPV cardiomyocytes. Treatment of cells with nLDL (250 μg/ml, 12-16 h) did not alter $I_{Ca,L}$ density (Figure 11A). In parallel to CaV1.2 expression (Figure 10B), HOCl-LDL (200:1, 250 μg/ml, 12-16 h) significantly decreased $I_{Ca,L}$ density in GPV cardiomyocytes at 0, +10, +20 and + 30 mV membrane potentials (Figure 11B). Control GPV cells had the peak $I_{Ca,L}$ density (11.42±0.54 pA/pF) at 0 mV whereby $I_{Ca,L}$ density in HOCl-LDL-treated cells was 7.49±0.67 pA/pF. Next, we analysed steady-state activation and inactivation parameters of $I_{Ca,L}$. The steady-state activation and inactivation of $I_{Ca,L}$ did not differ between control and HOCl-LDL groups (Figure 11C/D). HOCl-LDL treatment did not alter either the half-activation potential ($V_{1/2}$, -8.75±0.54 mV of control vs. -9.30±0.86 of HOCl-LDL) or the slope factor (*k*, 6.01±0.49 mV of control vs. 6.13±0.47 mV of HOCl-LDL). Similarly, HOCl-LDL treatment did alter neither the half-inactivation potential ($V_{1/2}$, -19.66±1.45 mV of control vs. -21.47±1.04 of HOCl-LDL) nor the slope factor (*k*, 4.59±0.15 mV of control vs. 5.12±0.33 mV of HOCl-LDL).

As KN93 inhibited HOCl-LDL-induced decrease in CaV1.2 expression in HL-1 cells (Figure 10C), we incubated GPV myocytes with KN93 (5 μM) prior to HOCl-LDL (200:1, 250 μg/ml) treatment for 12-16 h. Patch clamp analysis revealed that KN93-pretreatment prevented a decrease of $I_{Ca,L}$ density in response to HOCl-LDL at 0 and +10 mV membrane potentials significantly (Figure 11B). The peak $I_{Ca,L}$ densities (at 0 mV) were found to be 11.42±0.54 pA/pF (control), 7.49±0.67 pA/pF (HOCl-LDL) and 10.68±0.77 pA/pF (KN93 + HOCl-LDL). KN93 alone increased $I_{Ca,L}$ density in GPV myocytes (Supplement Figure II).

To sum up, HOCl-LDL decreased CaV1.2 expression and $I_{Ca,L}$ density via oxidation of CaMKII.

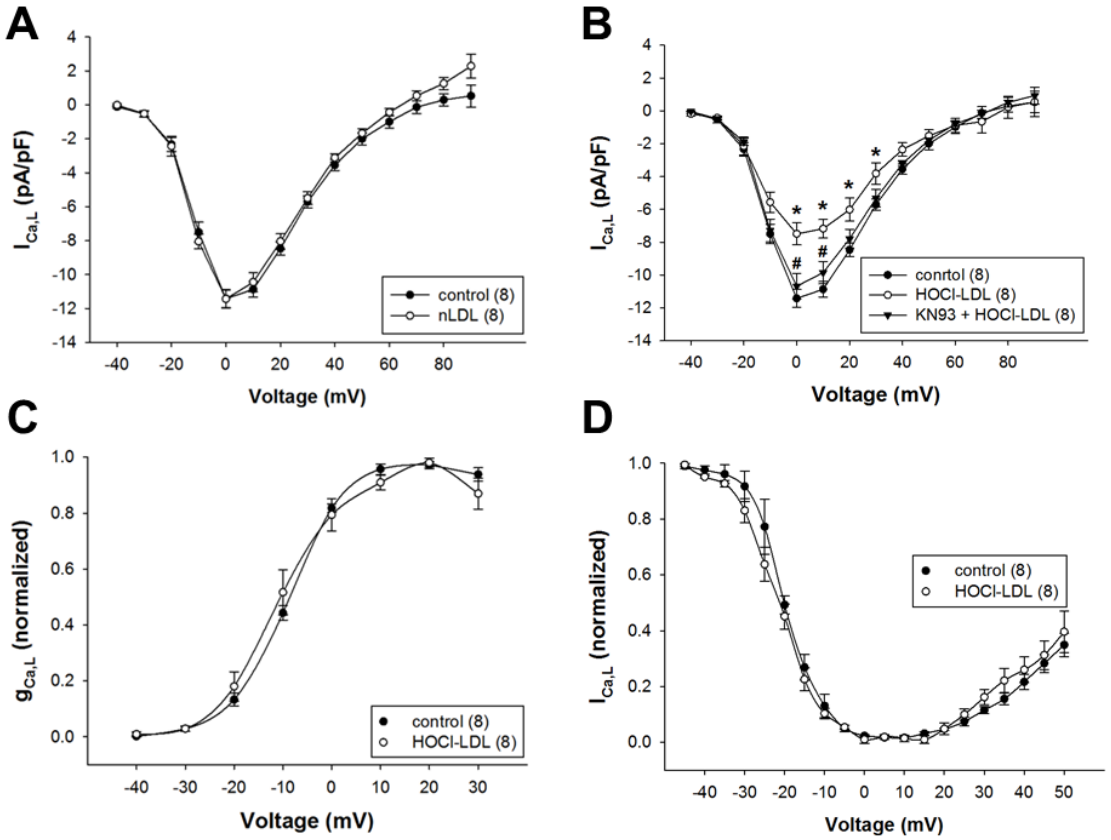

Figure 11. HOCl-LDL decreases L-type Ca^{2+} current ($I_{Ca,L}$) density via CaMKII oxidation

GPV cells were treated (12-16 h) with (**A**) nLDL (250 μg/ml) or (**B-D**) HOCl-LDL (200:1, 250 μg/ml) in the absence or presence of KN93 (5 μM) (**B**) to follow (**A** and **B**) $I_{Ca,L}$ density, steady-state (**C**) activation and (**D**) inactivation of $I_{Ca,L}$. Cardiomyocytes were patched using Cs-T and Cs-pip solutions. After inactivation of I_{Na} achieved by a prestep from -80 to -40 mV (50 ms), $I_{Ca,L}$ was elicited by voltage steps from -40 to +90 mV (10 mV increments, 400 ms). $I_{Ca,L}$ peak values were divided by the driving force and normalized to describe steady-state activation. In order to determine steady-state inactivation $I_{Ca,L}$ was activated with test pulses to +10 mV (400 ms), which were preceded by conditioning pulses from -45 to +50 mV (5 mV interval, 400 ms). Peak $I_{Ca,L}$ elicited by the test pulse was normalized and plotted as a function of prepulse potential. Values are expressed as mean±SEM; (n) represents number of cells. *p≤0.05 vs. control, $^{\#}$p≤0.05 vs. HOCl-LDL.

3.9 CaT and cell shortening in response to nLDL and HOCl-LDL

As HOCl-LDL impaired CaV1.2 expression (Figure 10B) and $I_{Ca,L}$ density (Figure 11B) in GPV cells, we decided to explore calcium homeostasis. At first we measured EC coupling in nLDL-treated cells. Figure 12 reveals that nLDL (250 μg/ml, 12-16 h)-treatment did not alter cell shortening (A), CaT amplitude (B), systolic calcium level (C), diastolic calcium level (D), time to peak (E) or relaxation time (50%, F).

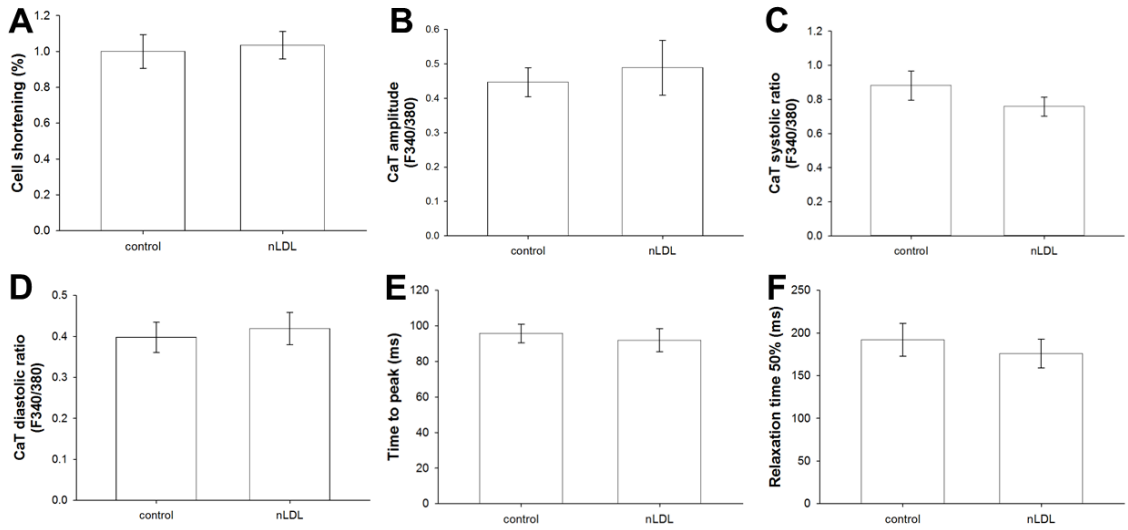

Figure 12. Impact of nLDL on calcium homeostasis of GPV cardiomyocytes

Cells were incubated with nLDL (200:1, 250 μg/ml) for 14 h. (**A**) Cell shortening, (**B**) CaT amplitude, (**C**) CaT systolic ratio, (**D**) CaT diastolic ratio, (**E**) Time to peak and (**F**) Relaxation time (50%) were analyzed. Cells were loaded with Fura-2-AM (1 μM) and Pluronic F-127 (1 μM) for 30 min. Cell shortening and CaT were assessed simultaneously during field stimulation (electrode distance: 1 cm; pulse duration: 5 ms; super-threshold pulse amplitude: 4 V/cm) at a frequency of 1 Hz. Fluorescence intensities were measured at 340 and 380 nm of excitation and at 510 nm of emission wavelengths. Values are expressed as mean±SEM (n=12).

In parallel, cardiomyocytes were incubated with HOCl-LDL (200:1, 250 μg/ml) for 12-16 h. As expected, HOCl-LDL treatment decreased cell shortening (approx. 30%) and CaT amplitude (0.44±0.4 F340/380 of control vs. 0.30±0.01 F340/380 of HOCl-LDL) in GPV cells (Figure 13A/B). A decrease in systolic (0.85±0.05 F340/380 of control vs. 0.69±0.03 F340/380 of HOCl-LDL) but not diastolic calcium level was observed in HOCl-LDL incubated cells compared to controls (Figure 13C/D). This is in line with decreased $I_{Ca,L}$ density (Figure 11B) and CaV1.2 expression (Figure 10B). Treated cells showed increased time to peak (95.75±5.24 ms of control vs. 139.20±12.51 ms of HOCl-LDL) and a decrease in relaxation time 50% (197.39±13.54 ms of control vs. 160.13±5.48 ms of HOCl-LDL) (Figure 13E/F). These data correlate with HOCl-LDL-induced decrease in RyR2 and increase in SERCA2a expression (Figure 10B). To measure sarcoplasmic reticulum calcium content, we perfused cells with caffeine (20 mM). Caffeine CaT amplitude was observed lower in HOCl-LDL incubated cells (Figure 13G, 1.11±0.09 F340/380 of control vs. 0.70±0.08 F340/380 of HOCl-LDL). This implicates that HOCl-LDL treatment led to a decrease in the calcium content of sarcoplasmic reticulum that might contribute to the decreased cell shortening and CaT (Figure 13A/B). Caffeine relaxation τ was measured as an index of NCX1 activity. Figure 13H reveals that HOCl-LDL slowed caffeine relaxation phase (685.48±35.89 ms of control vs. 1072.69±109.85 ms of HOCl-LDL), which implicates lower NCX1 activity that parallels with the decreased NCX1 expression in response to HOCl-LDL (Figure 10B).

Since KN93 protected cardiomyocytes against HOCl-LDL-induced changes in expression of ion channels (Figure 10C) and decrease in $I_{Ca,L}$ density (Figure 11B), we tested the effect of KN93 on HOCl-LDL-induced alteration of EC coupling. Pre-treatment of GPV cells with KN93 inhibited the effects of HOCl-LDL on cell shortening (70% contraction of HOCl-LDL vs. 97% contraction of KN93+HOCl-LDL, Figure 13A), CaT amplitude (0.30±0.01 F340/380 of HOCl-LDL vs. 0.39±0.02 F340/380 of KN93+HOCl-LDL, Figure 13B), systolic calcium level (0.69±0.03 F340/380 of HOCl-LDL vs. 0.82±0.06 F340/380 of KN93+HOCl-LDL, Figure 13C), time to peak (139.20±12.51 ms of HOCl-LDL vs. 108.83±6.53 ms of KN93+HOCl-LDL, Figure 13E), relaxation time 50% (160.13±5.48 ms of HOCl-LDL vs. 186.39±6.58 ms of KN93+HOCl-LDL, Figure 13F), caffeine CaT amplitude

(0.70±0.08 F340/380 of HOCl-LDL vs. 1.04±0.15 F340/380 of KN93+HOCl-LDL, Figure 13G) and caffeine relaxation τ (1072.69±109.85 ms of HOCl-LDL vs. 811.46±48.31 ms of KN93+HOCl-LDL, Figure 13G).

These data confirm that HOCl-LDL-induced contractile dysfunction in cardiomyocytes is dependent on CaMKII oxidation.

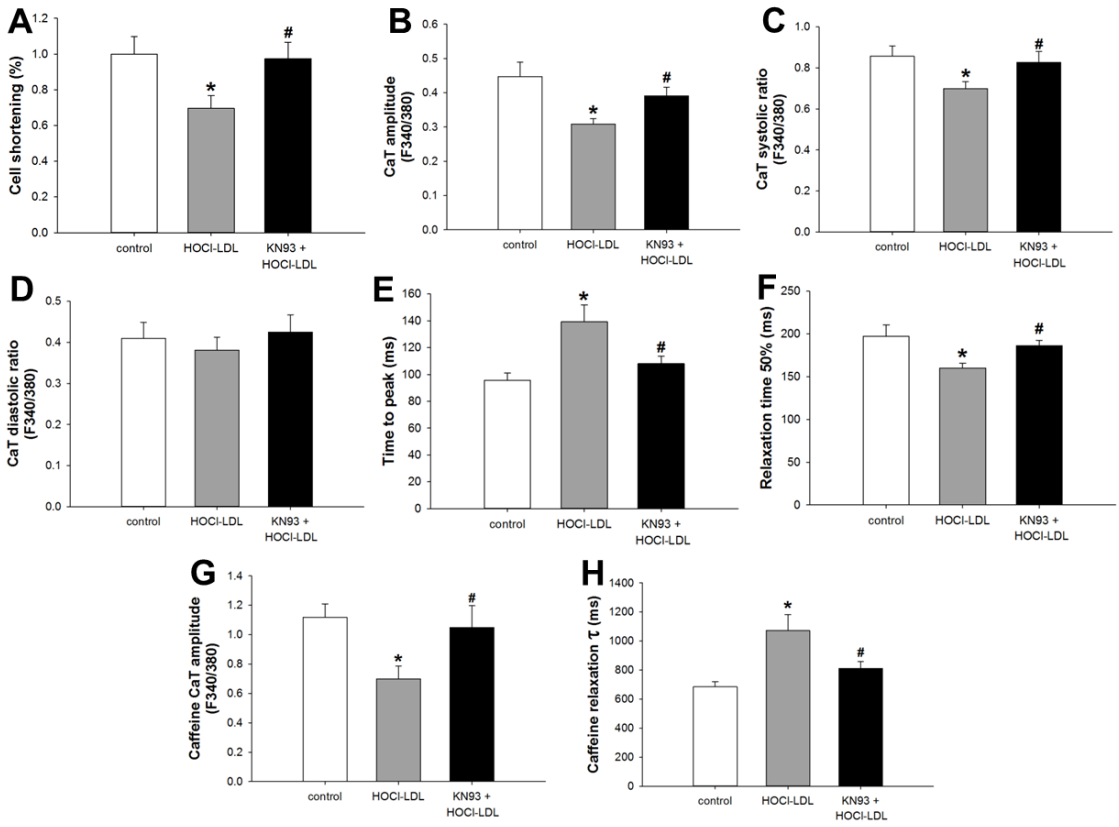

Figure 13. HOCl-LDL alters calcium homeostasis via CaMKII oxidation

GPV cardiomyocytes were incubated with KN93 (5 μM, 30 min) prior to HOCl-LDL (200:1, 250 μg/ml, 14 h) addition. (**A**) Cell shortening, (**B**) CaT amplitude, (**C**) CaT systolic ratio, (**D**) CaT diastolic ratio, (**E**) Time to peak, (**F**) Relaxation time (50%), (**G**) Caffeine CaT amplitude and (**H**) Caffeine relaxation τ were analyzed. Cells were loaded with Fura-2-AM (1 μM) and Pluronic F-127 (1 μM) for 30 min. Cell shortening and CaT were assessed simultaneously during field stimulation (electrode distance: 1 cm; pulse duration: 5 ms; super-threshold pulse amplitude: 4 V/cm) at a frequency of 1 Hz. Fluorescence intensities were measured at 340 and 380 nm of excitation and at 510 nm of emission wavelengths. Values are expressed as mean±SEM (n=22). *p≤0.05 vs. control, $^{\#}$p≤0.05 vs. HOCl-LDL.

3.10 Alteration in I_{ss} curve in response to HOCl-LDL

As HOCl-LDL altered AP parameters of GPV myocytes (Figure 5), we aimed to measure steady state current (I_{ss})-voltage relationship using a slow voltage ramp (20 s) from -100 mV to +60 mV.

Treatment of GPV cells with nLDL (250 μg/ml, 12-16 h) did not alter I_{ss} (Figure 14A). In HOCl-LDL incubated cells (200:1, 250 μg/ml, 12-16 h), I_{ss} density was significantly altered between membrane potentials ranging from -60 mV (1.22±0.25 pA/pF of control vs. 0.08±0.025 pF/pF of HOCl-LDL) to -80 mV (-2.10±0.36 pA/pF of control vs. -3.67±0.029 pF/pF of HOCl-LDL, Figure 14B). These alterations implicate an involvement of I_{K1}, since I_{K1} is the most prominent potassium current within this potential range ensuring the final repolarization phase of the action potential and the determining the resting membrane potential. In addition, HOCl-LDL treatment increased outward current density at positive membrane potentials from +30 mV (4.06±0.35 pA/pF of control vs. 5.96±0.48 pF/pF of HOCl-LDL) to +60 mV (9.19±0.73 pA/pF of control vs. 14.55±0.89 pF/pF of HOCl-LDL, Figure 14B). This effect is in contrast to HOCl-LDL-induced prolongation in APD (Figure 5A), as increased repolarizing outward current at positive membrane potential causes shortening of AP.

Next, we incubated cells with KN93 prior to HOCl-LDL treatment. KN93 pre-treatment reversed the changes in I_{ss} observed at negative membrane potentials from -60 mV (0.08±0.025 pF/pF of HOCl-LDL vs. 0.77±0.024 pA/pF of control) to -80 mV (-3.67±0.029 pF/pF of HOCl-LDL vs. -2.51±0.31 pA/pF of control, Figure 14B). However, no change in the outward current density at positive membrane potential was observed between KN93+HOCl-LDL and HOCl-LDL groups (Figure 14B). KN93 alone increased outward I_{ss} current at -60 and -70 mV significantly (Supplement Figure III). These data implicate that the effects of HOCl-LDL on I_{ss} within negative membrane potential range is due to CaMKII oxidation, while the effect at positive membrane potentials is CaMKII-independent.

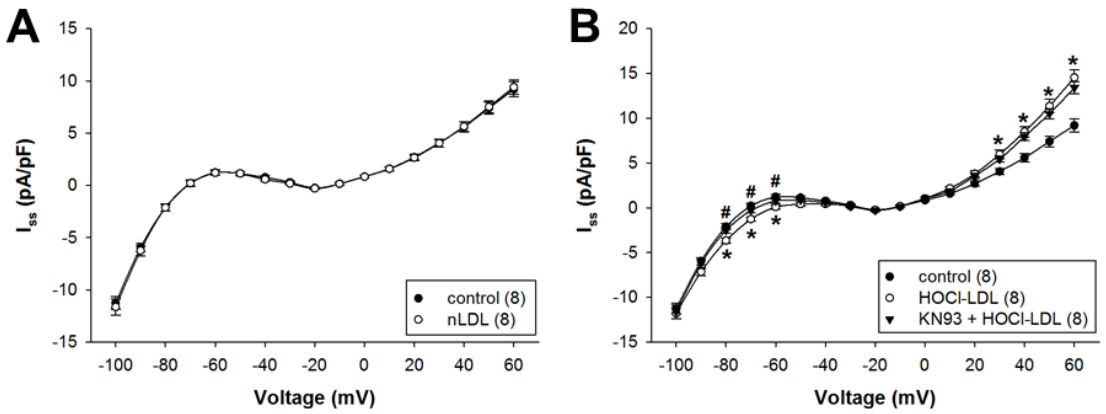

Figure 14. Steady-state current (I_{ss})-voltage relationship in response to nLDL and HOCl-LDL

GPV cardiomyocytes were treated (12-16 h) with (**A**) nLDL (250 μg/ml) or (**B**) HOCl-LDL (200:1, 250 μg/ml) in the absence or presence of KN93 (5 μM) (**B**). Cardiomyocytes were patched using NT and N-pip solutions. I_{ss} was elicited by voltage ramps (-100 to +60 mV, duration 20 s). Values are expressed as mean±SEM (each ramp current was discretized at 10 mV intervals by averaging 3 adjacent data points); (n) represents number of cells. *p≤0.05 vs. control, $^{\#}$p≤0.05 vs. HOCl-LDL.

3.11 HOCl-LDL-induced CaMKII oxidation reduces I_{K1}

As HOCl-LDL treatment decreased Kir2.2 expression (Figure 10B) and impaired I_{ss} from -60 to -80 mV (Figure 15B), we intended to measure I_{K1} in GPV cells. Figure 15A reveals that nLDL treatment (250 μg/ml, 12-16 h) had no effect on I_{K1}. As expected, outward directed I_{K1} density was significantly reduced or even inward directed at membrane potentials ranging from -40 mV (0.82±0.12 pA/pF of control vs. 0.28±0.08 pA/pF of HOCl-LDL) to -80 mV (-1.95±0.39 pA/pF of control vs. -2.64±0.23 pA/pF of HOCl-LDL, Figure 15B) under HOCl-LDL treatment. The inset in Figure 15B reveals a prominent shift of I_{K1} reversal potential ranging from approx. -70 mV to -60 mV in HOCl-LDL-incubated myocytes. The shift of I_{K1} reversal potential towards positive membrane potential contributes to the depolarization of resting membrane potential as observed in Figure 5C. The

reduced outward directed I_{K1} density possibly accounts for the prolongation of AP at 90% of repolarization (Figure 5A).

As, KN93 pre-treatment prevented a decrease of Kir2.2 expression in response to HOCl-LDL treatment (Figure 10C), we investigated effect of KN93 pre-treatment on I_{K1} density in response to HOCl-LDL. Figure 15B reveals a protective effect of KN93 against HOCl-LDL-impaired I_{K1} density from -40 mV (0.28±0.08 pA/pF of HOCl-LDL vs. 0.72±0.12 pA/pF of KN93+HOCl-LDL) to -70 mV (0.90±0.04 pA/pF of HOCl-LDL vs. -0.01±0.006 pA/pF of KN93+HOCl-LDL). Moreover, the reversal potential of I_{K1} in KN93 pre-treated myocytes did not differ from control cells (Figure 15B, inset). KN93 alone increased I_{K1} in GPV myocytes (Supplement Figure IV). These data suggest that HOCl-LDL impairs I_{K1} density thereby shifting reversal potential towards positive membrane potential via CaMKII oxidation.

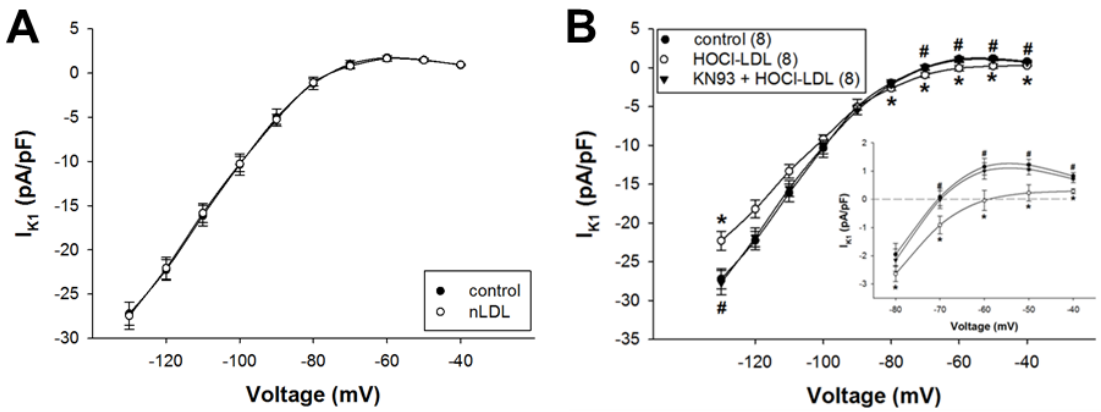

Figure 15. HOCl-LDL-induced inward-rectifier potassium current (I_{K1}) impairment is reversed by KN93

Cells were treated (12-16 h) with (**A**) nLDL (250 μg/ml) or (**B**) HOCl-LDL (200:1, 250 μg/ml) in the absence or presence of KN93 (5 μM) (**B**). Cardiomyocytes were patched using N-pip and NT solutions (with and without 0.5 mM $BaCl_2$). I_{K1} was measured as the Ba^{2+}-sensitive current (obtained by digital subtraction) elicited by hyperpolarizing voltage steps (3 s) from -40 mV to -130 mV (10 mV increments, holding potential -40 mV). Inset in (**B**) represents I_{K1} current density from -80 to -40 mV. Dashed line in the inset illustrates a prominent shift of I_{K1} reversal potential towards positive membrane potential. Values are expressed as mean±SEM; (n) represents number of cells. *p≤0.05 vs. control, $^{\#}$p≤0.05 vs. HOCl-LDL.

3.12 I_{NS} in response to HOCl-LDL

In this set of experiments we measured I_{NS} in response to nLDL (250 μg/ml) and HOCl-LDL (200:1, 250 μg/ml) treatment for 12-16 h. Figure 16A shows that nLDL had no effect on I_{NS}. However, HOCl-LDL increased inward I_{NS} density at negative membrane potentials ranging from -60 mV (-0.31±0.08 pA/pF of control vs. -0. 81±0.06 pA/pF of HOCl-LDL) to -100 mV (-1.05±0.17 pA/pF of control vs. -1.92±0.13 pA/pF of HOCl-LDL, Figure 16B). In addition, an increase in I_{NS} density was observed at membrane potentials from 0 mV (0.61±0.14 pA/pF of control vs. 1.42±0.18 pA/pF of HOCl-LDL) to +60 mV (3.23±0.58 pA/pF of control vs. 7.13±0.51 pA/pF of HOCl-LDL, Figure 16B). These changes might contribute to the observed alterations in I_{ss} at positive membrane potentials in response to HOCl-LDL (Figure 14B).

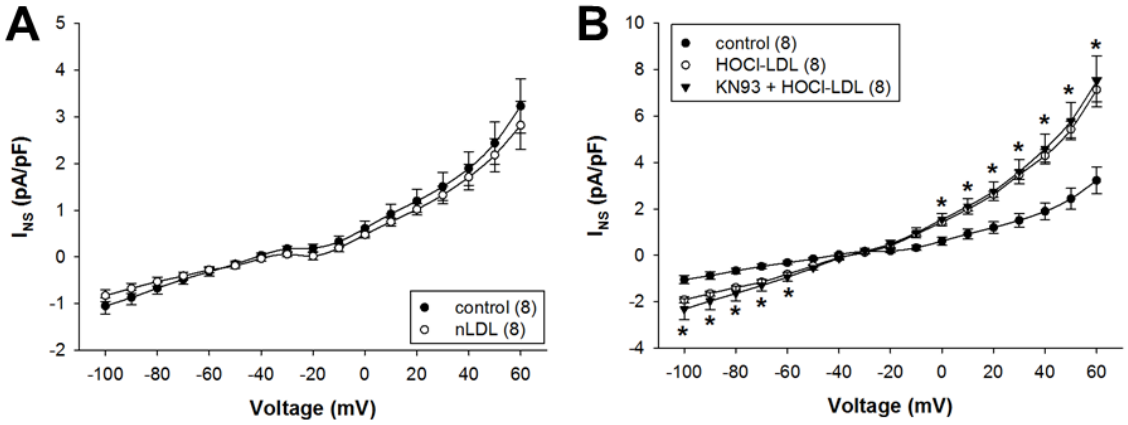

Figure 16. Non-selective cation current (I_{NS}) in response to nLDL and HOCl-LDL

GPV cardiomyocytes were treated (12-16 h) with (**A**) nLDL (250 μg/ml) or (**B**) HOCl-LDL (200:1, 250 μg/ml) in the absence or presence of KN93 (5 μM) (**B**). Cardiomyocytes were patched using Cs-pip and $CdCl_2$ (200 μM)-containing CsT solutions. I_{NS} was elicited by voltage ramps (-100 to +60 mV, duration 20 s). Values are expressed as mean±SEM (each ramp current was discretized at 10-mV intervals by averaging 3 adjacent data points); (n) represents number of patched cells. *p≤0.05 vs. control, $^{\#}$p≤0.05 vs. HOCl-LDL.

Next, we incubated cardiomyocytes with KN93 prior to addition of HOCl-LDL. No change in I_{NS} density-voltage relationship was observed between HOCl-LDL and KN93+HOCl-LDL groups (Figure 16B). Moreover, KN93 alone had no effect on I_{NS} (Supplement Figure V). These data reveal that HOCl-LDL altered I_{NS} density independent of CaMKII oxidation.

3.13 HOCl-LDL induces I_{NaL} in GPV myocytes

As HOCl-LDL induced arrhythmic events (EADs, DADs and spontaneous activity) in GPV myocytes (Figure 4C/D) and I_{NaL} is reported to play a pivotal role during cardiac arrhythmia (Asakura et al., 2014; Shryock, 2011), we measured I_{NaL} in response to HOCl-LDL-treatment (200:1, 250 μg/ml, 12-16 h). The time course of I_{Na} inactivation was analyzed and the time constant of the slow inactivation phase (τ_{slow}) was taken as a measure of I_{NaL}. Indeed, HOCl-LDL treatment slowed the inactivation phase of I_{Na}. As shown in Figure 17C, HOCl-LDL increased τ_{slow} in GPV myocytes (6.79±0.13 ms of control vs. 12.36±0.10 ms of HOCl-LDL, Figure 17A).

Next, we intended to clarify the role of KN93 in HOCl-LDL-induced I_{NaL}. Pre-treatment of myocytes with KN93 did not inhibit HOCl-LDL-induced I_{NaL} (Figure 17A/C). As a positive control we used Ranolazine, a blocker of I_{NaL} (Makielski and Valdivia, 2006). Ranolazine pre-treatment abolished HOCl-LDL-induced increase of I_{NaL} (12.36±0.10 ms of HOCl-LDL vs. 8.86±0.15 ms of KN93+HOCl-LDL, Figure 17B/C).

These data suggest that HOCl-LDL induces I_{NaL} in cardiomyocytes independent of CaMKII oxidation.

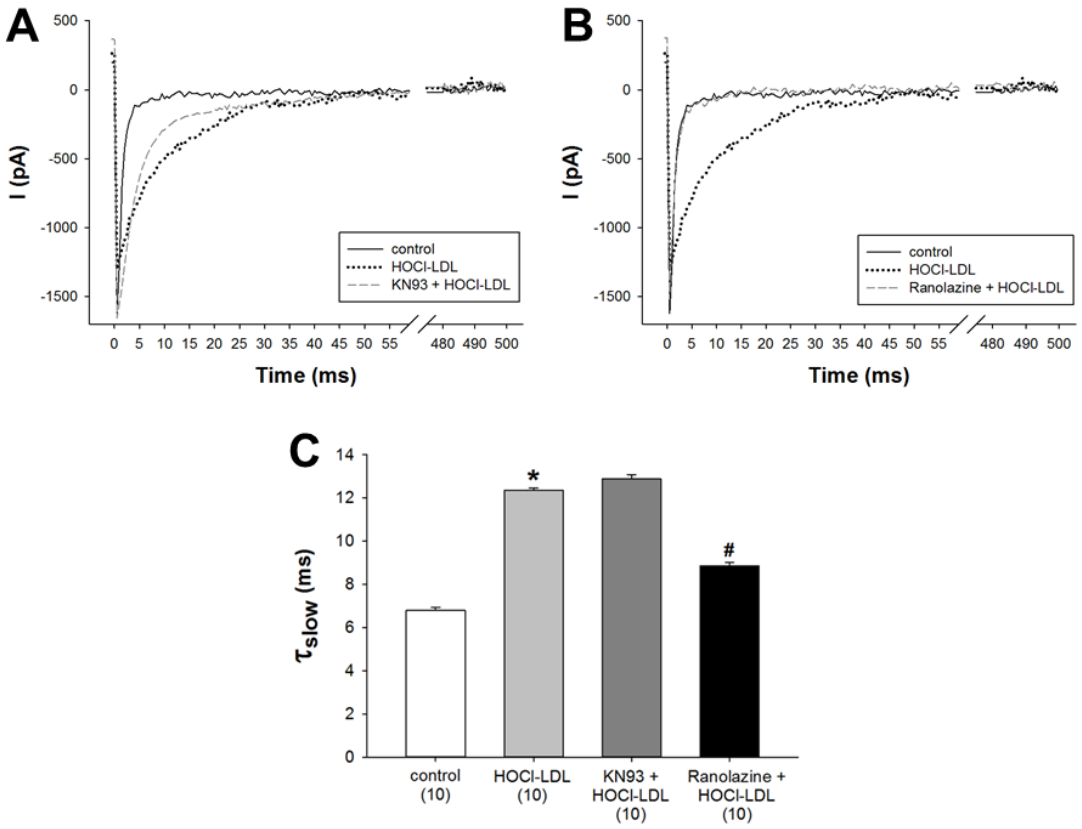

Figure 17. HOCl-LDL-induced late sodium current (I_{NaL}) is reversed by Ranolazine but not KN93

(**A**) Representative current traces of I_{NaL} of GPV cardiomyocytes. Cells were incubated (12-16 h) with HOCl-LDL (200:1, 250 μg/ml), in the absence or presence of either KN93 (5 μM, **A** and **C**) or Ranolazine (10 μM, **B** and **C**). Cardiomyocytes were patched using NaT and Na-pip solutions. I_{Na} was elicited by a train of voltage pulses to -20 mV from a holding potential of -120 mV (5 pulses, basic cycle length 2 s, 1000 ms). To optimize voltage control, each pulse was preceded by a 5 ms pre-pulse to +50 mV. The representative current traces are shown from the time point when pulses of -20 mV were applied. Time course of current inactivation was fitted bi-exponentially and the slow time constant (τ_{slow}, **C**) was taken as an estimation of I_{NaL}. Values are expressed as mean±SEM; (n) represents number of cells. *p≤0.05 vs. control, $^{\#}$p≤0.05 vs. HOCl-LDL.

3.14 Contribution of I_{NaL} in HOCl-LDL-induced arrhythmia

Ranolazine is clinically used to cure cardiac arrhythmia (Saad et al., 2015) and increased I_{NaL} is reported to promote arrhythmic events in cardiomyocytes (Song et al., 2008). Therefore, we tested whether Ranolazine could rescue HOCl-LDL-induced arrhythmic events in GPV myocytes. We used HOCl-LDL (400:1), as arrhythmic events became apparent in myocytes incubated with HOCl-LDL (400:1) but not HOCl-LDL (200:1, Figure 5B/C, number of cells shown below bars). Figure 18A shows representative APs of a HOCl-LDL-treated (400:1, 250 μg/ml, 12-16 h) cell showing arrhythmic events. This cardiomyocyte had a resting membrane potential of approx. -54 mV.

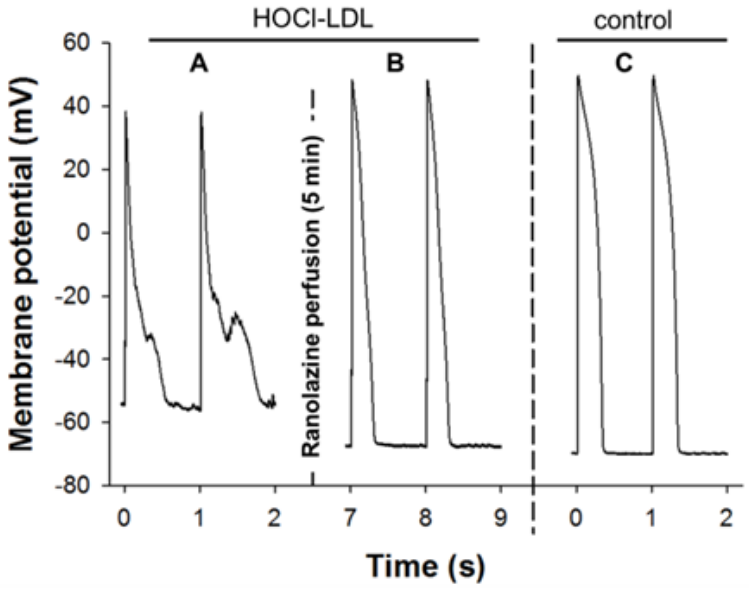

Figure 18. Reversal of HOCl-LDL-induced EADs, DADs and depolarized resting membrane potential by acute superfusion with Ranolazine

GPV cells were treated (12-16 h) with HOCl-LDL (400:1, 250 μg/ml). Cells were patched using NT and N-pip solutions and stimulated at a frequency of 1 Hz. Representative APs (one out of three) recorded in the same cell are shown before (**A**) and after (**B**) superfusion with NT-containing Ranolazine (10 μM, 5 min). For comparative purpose representative APs of a control cardiomyocyte are shown (**C**).

Superfusion of the same cell (as shown in Figure 18A) with NT-containing Ranolazine (10 µM, 5 min) blocked HOCl-LDL-induced arrhythmia completely (Figure 18B). Moreover, the resting membrane potential was repolarized to approx. -67 mV after superfusion with Ranolazine. Control GPV myocytes have a resting membrane potential of approx. -69 mV. For a comparative purpose APs of a control myocyte are shown in Figure 18C.

3.15 Reversal of altered AP parameters by KN93 and Ranolazine

As KN93 inhibited the effects of HOCl-LDL on electrophysiological characteristics and Ranolazine blocked HOCl-LDL-induced arrhythmic events, we aimed to reveal effects of KN93 and Ranolazine on HOCl-LDL-induced alterations in AP parameters. KN93 prevented increased of APD 90% (579.93±37.96 ms of HOCl-LDL vs. 455.58±29.51 ms of KN93+HOCl-LDL, Figure 19A) and decrease of upstroke velocity (138.75±17.73 V/s of HOCl-LDL vs. 260.08±13.07 V/s of KN93+HOCl-LDL Figure 19B) in HOCl-LDL (400:1, 250 µg/ml, 12-16 h) incubated myocytes. However, KN93 could not block arrhythmic events completely (Figure 19, number of cells below black bars). Approx. 35% cells showed arrhythmic events in KN93+HOCl-LDL group compared to approx. 50% cells in HOCl-LDL group.

Protective effects of KN93 on AP parameters are most likely due to the reversal of HOCl-LDL-induced decrease of I_{K1} by KN93. I_{K1} inhibition has been shown to prolong APD in cardiomyocytes (Williams et al., 1999). Moreover, shift of I_{K1} reversal potential towards positive membrane potentials (Figure 15B, inset) leads to depolarization of resting membrane potential. As a consequence of depolarization of resting membrane potential, a decrease in maximal upstroke velocity was observed in cardiac Purkinje fibers (Arita and Surawicz, 1973). To sum up, KN93 pre-treatment reversed impairment of I_{K1} density and its reversal potential that led to repolarization of resting membrane potential and in turn an increase of upstroke velocity.

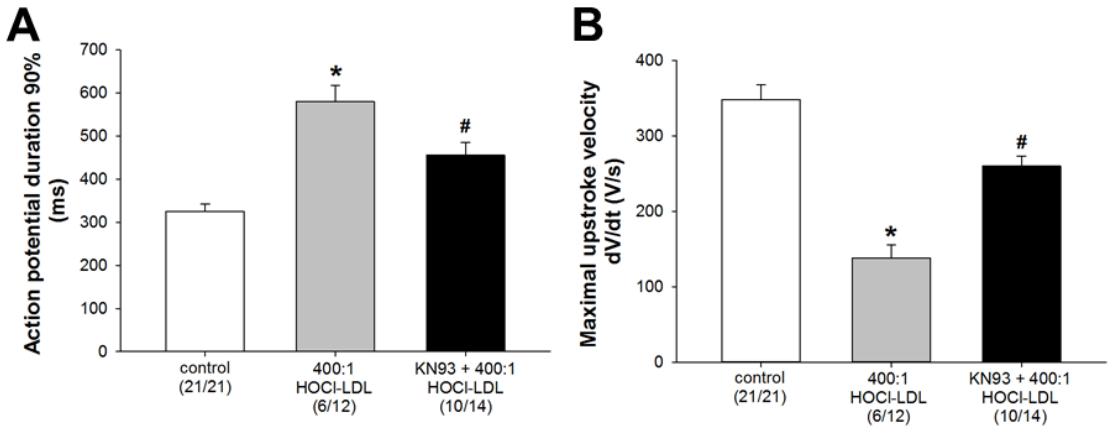

Figure 19. Reversal of the impact of HOCl-LDL on action potential parameters by KN-93

GPV cardiomyocytes were treated (12-16 h) with HOCl-LDL (400:1, 250 μg/ml) in the absence or presence of KN93 (5 μM). Cells were patched using NT and N-pip solutions and stimulated at a frequency of 1 Hz. (**A**) AP duration at 90% of repolarization and (**B**) upstroke velocity were analyzed. Values are expressed as mean±SEM. (n/n) represents number of cells showing APs elicited by external stimulus/total number of measured cells. Cells showing spontaneous activity or arrhythmic events were excluded from the calculation. *p≤0.05 vs. control, $^{\#}$p≤0.05 vs. HOCl-LDL.

Like KN93, also Ranolazine reversed the effects of HOCl-LDL treatment (400:1, 250 μg/ml, 12-16 h) on APD 90% (579.93±37.96 ms of HOCl-LDL vs. 406.12±25.10 ms of Ranolazine+HOCl-LDL, Figure 20A) and upstroke velocity (138.75±17.73 V/s of HOCl-LDL vs. 291.90±15.76 V/s of KN93+HOCl-LDL, Figure 20B) significantly. Our data show the protective effect of Ranolazine against HOCl-LDL-induced elevation in APD (Figure 20A). This might be due to the fact that Ranolazine is capable to decrease APD (Song et al., 2004). As, shown in Figure 20, HOCl-LDL treatment induced arrhythmic events in approx. 50% cardiomyocytes (number of cells below grey bars). Ranolazine pre-treatment abolished arrhythmic events completely (number of cells below black bars, Figure 20). These data show that Ranolazine is protective against HOCl-LDL-induced alteration in AP parameters and arrhythmic events.

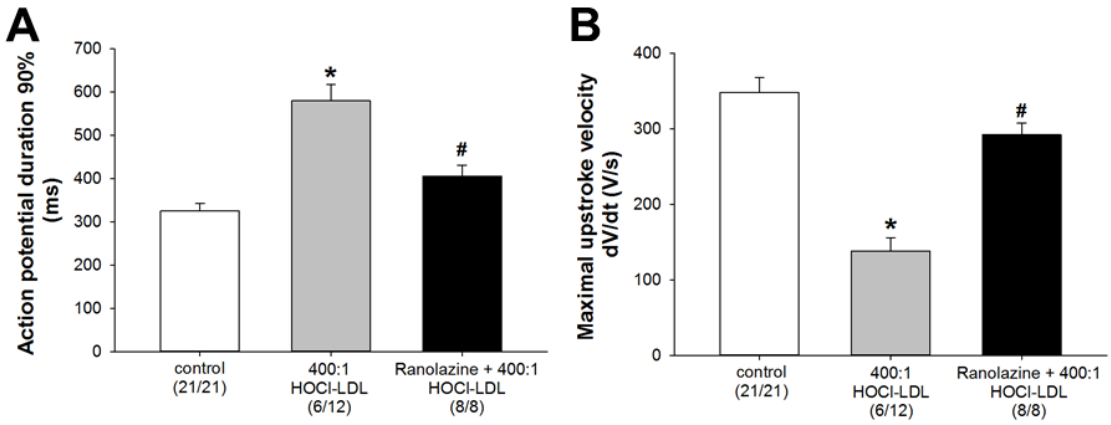

Figure 20. Reversal of the impact of HOCl-LDL on action potential parameters by Ranolazine

GPV cardiomyocytes were treated (12-16 h) with HOCl-LDL (400:1, 250 μg/ml) in the absence or presence of Ranolazine (10 μM). Cells were patched using NT and N-pip solutions and stimulated at a frequency of 1 Hz. (**A**) AP duration at 90% of repolarization and (**B**) upstroke velocity were analyzed. Values are expressed as mean±SEM. (n/n) represents number of cells showing AP elicited by external stimulus/total number of measured cells. Cells showing spontaneous activity or arrhythmic events were excluded from the calculation. *p≤0.05 vs. control, $^{\#}$p≤0.05 vs. HOCl-LDL.

3.16 Effect of KN93, KN92 and Ranolazine on AP parameters

In this set of experiments we aimed to evaluate effects of KN93, KN92 (an inactive homologue of KN93) and Ranolazine on AP parameters. None of these compounds altered APD (Figure 21A). However, KN93 significantly reduced upstroke velocity (348±19 V/s of control vs. 225±51 V/s of KN93, Figure 21B), while KN92 or Ranolazine showed no effect (Figure 21B). Furthermore, both KN93 and KN92 induced arrhythmia in 2 out of 11 and 3 out of 10 cells, respectively (number of cells below bars). These data suggest that KN93 and KN92 affected cellular excitability, while Ranolazine had no significant effect. This might be due to the fact that KN93 inhibits basal CaMKII activity in control myocytes. Moreover, KN93 and KN92 are reported to possess CaMKII independent activity (Gao et al., 2006) that might be responsible for the observed effects.

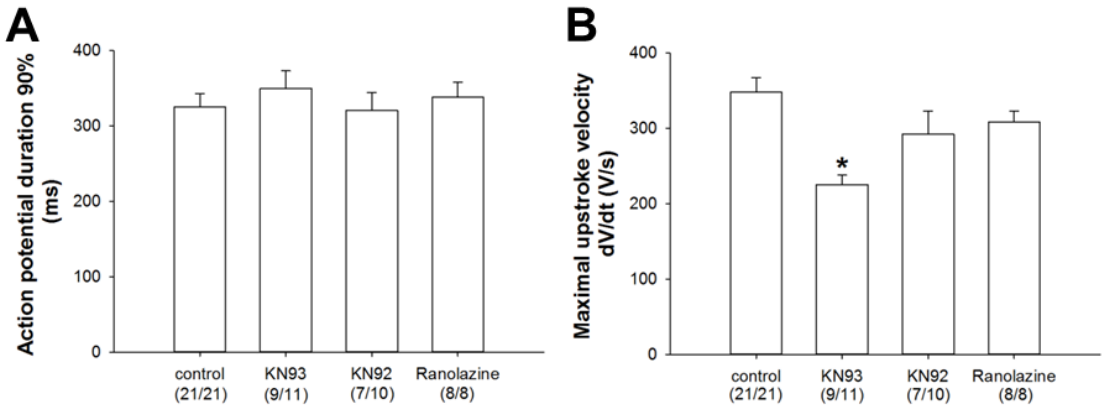

Figure 21. Action potential parameters in response to KN93, KN92 and Ranolazine

GPV cardiomyocytes were treated (12-16 h) with KN93 (5 μM), KN92 (5 μM) or Ranolazine (10 μM). Cells were patched using NT and N-pip solutions and stimulated at a frequency of 1 Hz. (**A**) AP duration at 90% of repolarization and (**B**) upstroke velocity were analyzed. Values are expressed as mean±SEM. (n/n) represents number of cells showing APs elicited by external stimulus/total number of measured cells. Cells showing spontaneous activity or arrhythmic events were excluded from the calculation. *p≤0.05 vs. control.

3.17 KN93 and Ranolazine protected human atrial trabeculae against HOCl-LDL-induced contractile dysfunction and arrhythmia

KN93 protected cardiomyocytes against HOCl-LDL-induced alterations in AP parameters, $I_{Ca,L}$ (Figure 11B), I_{K1} (Figure 15B), I_{ss} (Figure 14B), EC coupling (Figure 13A-H) and ion channel expression (Figure 10C). Moreover, Ranolazine protected cardiomyocytes against HOCl-LDL-induced arrhythmia (Figure 18B), I_{NaL} (Figure 17B/C) and alterations in AP parameters (Figure 20A/B). Therefore, we intended to evaluate effects of KN93 and Ranolazine on HOCl-LDL-mediated contractile dysfunction and arrhythmia in human atrial trabeculae. Figure 22A shows that HOCl-LDL failed to induce arrhythmic episodes in KN93- or Ranolazine-pretreated trabeculae. Moreover, arrhythmic episode count stayed higher in control group (3.25±2.19 counts) compared to KN93 (0.20±0.13 counts) or Ranolazine (0 count) treated trabeculae at 105 min, even though trabeculae from Ranolazine group have the highest arrhythmic episodes at baseline (0 min, 12.91±4.35 counts of Ranoalzine+HOCl-LDL vs. 8.71±3.52 counts of control, Figure 22A).

In addition to arrhythmic episodes, we observed protective effects of KN93 and Ranolazine against elevation of diastolic tension in response to HOCl-LDL. As shown in Figure 22B, both pre-treatments blocked detrimental effect of HOCl-LDL on diastolic tension. However, rundown of diastolic force was higher in both pre-treatment groups compared to control.

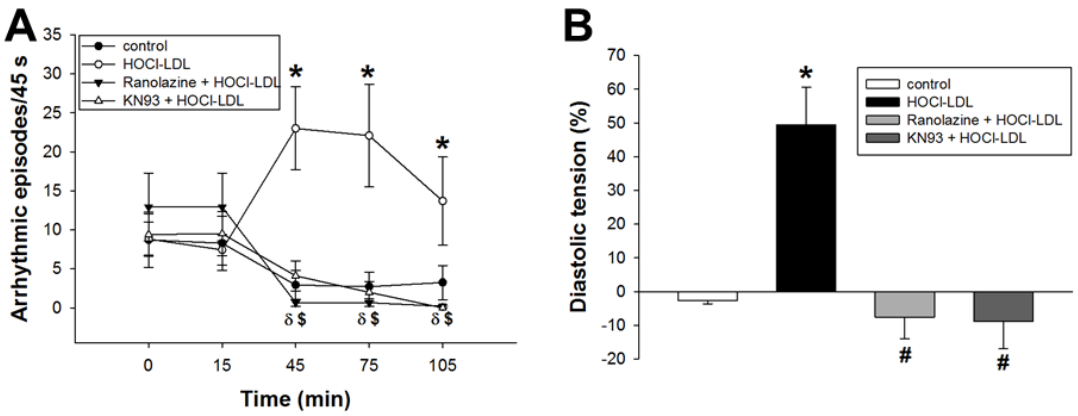

Figure 22. Arrhythmia and contractile dysfunction in RAA trabeculae in response to HOCl-LDL

Human RAA trabeculae were incubated for 15 min with KN93 (5 μM) or Ranolazine (10 μM) at 0 min prior to HOCl-LDL (200:1, 250 μg/ml) addition at 15 min. Muscle strips were stimulated at a frequency of 1 Hz. At indicated time periods stimulation was stopped for 1 min followed by 0.5 Hz stimulation (1 min) and 0 Hz (1 min) (stimulation protocol see Figure 3C). During no-stimulation period numbers of spontaneous contractions/45 s were counted as arrhythmic episodes (**A**). Diastolic tension (%) was calculated from the ratio of diastolic to systolic force at 30 min post-treatment with HOCl-LDL (**B**). Values are expressed as mean±SEM (n=8). *p≤0.05 HOCl-LDL vs. control, $^{\delta}$p≤0.05 KN93+HOCl-LDL vs. HOCl-LDL, $^{\$}$p≤0.05 ranolazine+HOCl-LDL vs. HOCl-LDL, $^{\#}$p≤0.05 vs. HOCl-LDL.

4. Discussion

Clinical trials suggest detrimental roles of infiltration of neutrophils and accumulation of enzymatically active leucocyte-derived MPO in CVDs including MI, HF and CAD (Haumer et al., 2005; Nicholls and Hazen, 2005; Siminiak and Ozawa, 1993). Activated MPO in the presence of H_2O_2 and Cl^- generates HOCl. This potent oxidant (commonly known as bleach) reacts with a variety of biological molecules such as thiols, sulphides and disulphides, DNA, nucleotides, proteins and lipids (Prutz, 1996). Most importantly, HOCl reacts with lipoproteins of low- and high-density (HDL) range (Malle et al., 2006a; Malle et al., 2006b). Both, LDL and HDL play a pivotal role in the development of CVDs. LDL, a biomarker for cardiovascular risk, gets oxidized by enzymes including lipooxygenase, NADPH oxidase and MPO under in vivo conditions. Oxidized LDL is a circulating risk factor for CVDs including atherosclerosis. Although apoB-100-containing lipoprotein particles are primarily secreted by the liver, cardiomyocytes are also capable to generate LDL-like particles. Therefore, the presence of elevated levels of neutrophil-derived MPO and its product, HOCl, in the myocardium reveals a direct interaction of HOCl with LDL in the myocardium during CVDs. Our immunostaining data showed a correlation between the staining of apoB-100 and HOCl-modified epitopes in the infarcted myocardium. In response to HOCl-LDL, intracellular superoxide anion levels were increased in cardiomyocytes that promoted oxidation of CaMKII. Gene-silencing experiments confirmed involvement of LOX-1 and CD36 in HOCl-LDL-mediated oxidation of CaMKII. Effects of HOCl-LDL on expression of ion channels/pump, contractility and electrophysiological characteristics are given in Table 3. Pharmacological inhibition of CaMKII activity by KN93 as well as I_{NaL} by Ranolazine protected cardiac tissue and myocytes against HOCl-LDL-induced arrhythmia, contractile dysfunction and alterations in electrophysiological characteristics.

Table 3. Effect of HOCl-LDL on cardiac tissue and myocytes

Parameter	Effect of HOCl-LDL
CaV1.2, Kir2.2, NCX1, RyR2 expression	↓
SERCA2a expression	↑
CaV3.2, Kir2.1, Kir2.3, NaV1.5 expression	↔
$I_{Ca,L}$ and I_{K1} density	↓
I_{K1} reversal potential	Shifted towards positive membrane potential
I_{ss} and I_{NS}, inward current density	Increased
I_{ss} and I_{NS}, outward current density	Increased
I_{NaL} and arrhythmic events	↑
CaT and cell shortening	↓
Systolic Ca^{2+} level	↓
Diastolic Ca^{2+} level	↔
Diastolic tension	↑
Time to peak	↑
Relaxation time 50%	↓
APD	Prolonged
Resting membrane potential	Depolarized
Maximal upstroke velocity	↓

Amongst known risk factors for cardiovascular mortality, LDL-cholesterol, apoB-100 and oxidized-LDL are clinical markers to predict cardiovascular events (Boekholdt et al., 2012; Holvoet et al., 2001). LDL-lowering properties of statins and PCSK9 inhibitors are suitable therapeutic approaches to lower dyslipidaemia-induced CVDs (Ebrahim et al., 2014; Tavori et al., 2015). A number of studies reported detrimental effects of modified LDL on various cells and organs (Levitan et al., 2010). Although various methods have been used to modify LDL in vitro, it is of importance to use in vivo relevant LDL-modification approach (Steinberg and Witztum, 2002). Out of known biological molecules modifying LDL in vivo, MPO and its oxidants, are found to be present in human atherosclerotic lesions (Arnhold and Flemmig, 2010; Hazell et al., 1996; Malle et al., 2000). In the present study,

we have observed neutrophil infiltration and MPO accumulation in the myocardium of MI patients (Figure 1). Most importantly, HOCl-modified LDL was found to be present in human atherosclerotic lesion (Hazell et al., 1996) and our data show correlation of apoB-100 staining with HOCl-modified epitopes in cardiomyocytes of infarcted LV (Figure 1). The antibody used in the present study to detect HOCl-modified epitopes was raised against LDL modified by HOCl in vitro (Malle et al., 1995a). It is worth mentioning that the used monoclonal antibody does not only react with LDL modified by HOCl in vitro (Malle et al., 1995a) but also recognizes LDL/apoB-100 modified by the MPO-H_2O_2-chloride system in vivo (Hazell et al., 1996). All these data postulate the presence of HOCl-modified low-density (lipo)proteins in the myocardium under in vivo conditions.

HOCl-LDL triggers cellular signalling via its binding to scavenger receptors that have been reported to affect cardiac function. SR-$A^{-/-}$ mice had higher mortality compared to WT mice in a left anterior descending (LAD) coronary artery ligation model (Hu et al., 2011). In contrast, another study of LAD ligation in mice proved detrimental role of SR-A against LAD ligation, whereby improved EF and fractional shortening were observed in SR-$A^{-/-}$ mice compared to WT mice (Ren et al., 2013). On the other hand, $CD36^{-/-}$ mice showed impaired EC coupling and AP parameters that led to sudden death (Pietka et al., 2012). Pietka and co-workers (Pietka et al., 2012) further reported that CD36 knockdown in HL-1 cells led to decreased SERCA2a activity resulting in delayed removal of Ca^{2+} from the cytoplasm after systole. Furthermore, expression of LOX-1 was found to be upregulated during myocardial ischemia/reperfusion injury (Li et al., 2002). Administration of an antibody against LOX-1 in mice resulted in approx. 50% reduction in infarct size in a coronary artery ligation model (Kataoka et al., 2003). In line, Hu and co-workers (Hu et al., 2008) reported that LOX-1 deletion protected mice against coronary artery occlusion. In the present study we reported that silencing of mainly LOX-1 and partially CD36 but not SR-A1/B1 impaired HOCl-LDL-induced CaMKII oxidation that triggered contractile and electrophysiological dysfunctions (Figure 9E).

CaMKII plays a pivotal role in the maintenance of cardiac physiological functions and hyperactivity of the enzyme is reported in various CVDs (Couchonnal and Anderson, 2008). CaMKII activity is tightly under control of intracellular Ca^{2+} levels and its binding to Ca^{2+}/CaM complex. In the presence of ATP, CaMKII undergoes autophosphorylation at T^{287} residue that permits persistent activity of the enzyme even after Ca^{2+}/CaM dissociation. In the present study we did not observe any change in the phosphorylation state of CaMKII (Figure 6A). This confirms that the binding of Ca^{2+}/CaM to CaMKII is not affected by HOCl-LDL.

Recently, CaMKII was reported to get oxidized via redox imbalance, whereby activation of CaMKII activity was found to be independent of Ca^{2+} (Erickson et al., 2008). Our data show that intracellular HOCl-LDL-mediated elevation of ROS triggers oxidation of CaMKII at $M^{281/282}$ residues in cardiomyocytes (Figure 6B). Like phosphorylation, also oxidation of CaMKII activates signalling cascades that are crucial for cardiac physiology as well as pathophysiology. CaMKII oxidation in the heart induced mortality after MI in diabetic mice (Luo et al., 2013). We observed oxCaMKII expression in the infarcted LV compared to healthy myocardium (Figure 7C). Under physiological conditions CaMKII phosphorylation is reversed by phosphatases (Strack et al., 1997). On the other hand, the oxidation status of CaMKII undergoes reduction by two isoforms of methionine sulfoxide reductase (MSRA and MSRB), enzymes that are abundantly expressed in cardiomyocytes (Fomenko et al., 2009; Prentice et al., 2008). However, HOCl-LDL did not modulate expression of any isoform of the enzyme (Supplement Figure VI).

A number of studies indicate a crucial role of oxidative stress in the development and progression of CVDs (Dhalla et al., 2000; Fearon and Faux, 2009). Serum and biopsy samples from CVD patients showed elevated oxidative DNA damage (Kono et al., 2006). Moreover, lipid peroxidation and glutathione oxidation were induced in LV of failing heart of rats (Hill and Singal, 1997). Cardiac hypertrophy induced by angiotensin II was mediated via NADPH oxidase-induced generation of ROS (Bendall et al., 2002). NADPH oxidase is the major source for superoxide anion production in various cell types including cardiomyocytes (Brennan et al., 2009; Kuroda et al., 2010). Furthermore, copper-oxidized LDL (a

non-physiological oxidative modification of LDL) increased superoxide anion production via its binding to LOX-1 on endothelial cells, whereby anti-LOX-1 antibody inhibited synthesis of superoxide anion (Cominacini et al., 2001). In the present study, we observed superoxide anion-induced CaMKII oxidation (Figure 8B) that was inhibited by silencing of LOX-1 (Figure 9E). Superoxide anions produce H_2O_2 by either spontaneous dismutation or superoxide dismutase (SOD) (Marklund, 1976). Both, superoxide anion and H_2O_2 are known to generate oxidative stress in CVDs whereby elevation in superoxide anion level was observed in the failing heart (Munzel and Harrison, 1999). Moreover, increased H_2O_2 levels were observed in rat hearts undergoing ischemia (Slezak et al., 1995). H_2O_2 treatment increased oxidation of isolated CaMKII (Erickson et al., 2008) as well as intracellular CaMKII in cardiomyocytes (Xie et al., 2009). Our results show oxidation of CaMKII by HOCl-LDL in human RAA cardiac tissue and atrial myocytes (Figure 7A/B).

A growing number of studies suggest that CaMKII regulates function and/or expression of most of the ion channels of cardiomyocytes in a direct or indirect manner. CaMKII regulates phosphorylation of L-type calcium channels that facilitates entry of Ca^{2+} into cardiomyocytes. This process requires phosphorylation of T^{498} residue of the β2a subunit of L-type calcium channel (Grueter et al., 2006). Several studies showed that CaMKII phosphorylation increases $I_{Ca,L}$ and slowed down the inactivation of CaV1.2 (Dzhura et al., 2000). $I_{Ca,L}$ density has been reported to be decreased or unaffected during the majority of the studies of CVDs (Benitah et al., 2002). Treatment of hamster cardiomyocytes with HOCl resulted in a dose-dependent decrease in $I_{Ca,L}$, while no alteration was observed in reversal potential as well as in voltage-dependence of activation or inactivation parameters of the current (Hammerschmidt and Wahn, 1998). Moreover, copper-oxidized LDL increased $I_{Ca,L}$ in GPV cardiomyocytes without affecting voltage-dependence of activation or inactivation (Zorn-Pauly et al., 2005). In the present study we have used a physiologically relevant oxidative LDL modification. Using HOCl-LDL we observed impairment of $I_{Ca,L}$ density by CaMKII oxidation but no alteration in voltage-dependence of either activation or inactivation of the current in GPV myocytes (Figure 11B).

Moreover, adenovirus-mediated CaMKII overexpression in rabbit myocytes increased $I_{Ca,L}$ density (Kohlhaas et al., 2006). In contrast, CaMKII$\delta^{-/-}$ mice have higher CaV1.2 expression as well as $I_{Ca,L}$ compared to WT mice (Xu et al., 2010). Although the underlying mechanisms behind these phenomenons remain widely unknown, one can conclude that CaMKII is able to modulate CaV1.2 expression. CaMKII over-expression decreased CaV1.2 expression in HL-1 cells, whereby KN93 elevated $I_{Ca,L}$ (Ronkainen et al., 2011). In line, our data show that HOCl-LDL-induced CaMKII oxidation (an indicator of increased CaMKII activity) decreased CaV1.2 expression in cardiac tissue and myocytes, and $I_{Ca,L}$ density in cardiomyocytes. This phenomenon was blocked by an inhibitor of CaMKII activity, KN93. Similarly, increased expression of CaV1.2 by KN93 treatment was observed in rat neonatal cardiomyocytes, whereby KN92 was ineffective (Ronkainen et al., 2011).

CaMKII regulates all channels and pumps that regulate EC coupling and it acts as an intermediate junction that helps to coordinate the inter-relationship between membrane excitation and sarcoplasmic reticulum Ca^{2+} release/uptake (Maier and Bers, 2007). CaMKII catalyses phosphorylation of RyR2 (Hain et al., 1995) that leads to release of sarcoplasmic reticulum Ca^{2+} into the cytosol. Overexpression of CaMKII increased sarcoplasmic reticulum Ca^{2+} release in murine cardiomyocytes (Maier et al., 2003). In contrast, Ronkainen and co-workers (Ronkainen et al., 2011) did not observe any change in either RyR2 expression or sarcoplasmic reticulum Ca^{2+} release by CaMKII overexpression in HL-1 cells. In a recent study, digitoxin-mediated CaMKII oxidation was shown to increase phosphorylation of RyR2 at S^{2814} residue (Ho et al., 2014). Our data show that HOCl-LDL-induced CaMKII oxidation led to decreased RyR2 mRNA expression in cardiac tissue and myocytes (Figure 10). In parallel, time to peak of CaT was increased in HOCl-LDL-treated cells whereby KN93 pre-treatment was protective (Figure 13E). Upon release of Ca^{2+} from the sarcoplasmic reticulum during systole, cytosolic Ca^{2+} levels increase and results in contraction. Cytosolic Ca^{2+} and cell shortening were impaired by HOCl-LDL (Figure 13C). Increasing evidences suggest that decreased Ca^{2+} release in failing myocytes is a result of dysfunction of one or more Ca^{2+}-handling channels including CaV1.2 and RyR2; both of them are targets of oxCaMKII in response to HOCl-LDL. Moreover, CaMKII

overexpression decreased CaT amplitude in mouse cardiomyocytes (Maier et al., 2003) and CaMKII oxidation decreased CaT in GPV myocytes (Figure 13B). This observation can be translated into impairment of cell shortening as observed in HOCl-LDL-incubated myocytes (Figure 13A).

During relaxation phase, cytosolic Ca^{2+} is sequestered mainly to the sarcoplasmic reticulum by SERCA2a. CaMKII enhances Ca^{2+} uptake by SERCA2a via phosphorylation of PLB, an inhibitor of SERCA2a. Unphosphorylated PLB inhibits SERCA2a activity, while its phosphorylation at T^{17} by CaMKII results in elevated SERCA2a activity as observed in rat cardiomyocytes (Hagemann et al., 2000). In contrast, HOCl-LDL-mediated CaMKII oxidation elevated SERCA2a expression (Figure 10) and decreased RT50 (Figure 13F) without any alteration in the phosphorylation state of PLB at S^{16} or T^{17} residues (Supplement Figure VII). CaMKII inhibition reversed SERCA2a expression as well as RT50. These data are in line with a previous study where CaMKII inhibition led to a decrease in SERCA2a activity (Picht et al., 2007). Even though sarcoplasmic reticulum Ca^{2+} refilling was faster in HOCl-LDL-treated myocytes, caffeine CaT was significantly reduced in the treated cells. CaMKII inhibition restored caffeine CaT and cell shortening (Figure 13A/B) that is in line with the previous findings where CaMKII overexpression decreased caffeine CaT (Maier et al., 2003). Thus, our data suggest that HOCl-LDL treatment decreases CaT amplitude due to reduction of $I_{Ca,L}$ (Figure 11B), reduced sarcoplasmic reticulum Ca^{2+} content (Figure 13G) and increased time to peak (Figure 13E) possibly as a result of decreased RyR2 mRNA expression (Figure 10) that could be reversed by KN93. Moreover, caffeine relaxation τ, a measure of NCX1 activity, was increased in HOCl-LDL-treated myocytes (Figure 13H). NCX1 regulates intracellular Na^{+} and Ca^{2+} levels via bidirectional transportation. CaMKII overexpression increased NCX1 expression via histone deacetylase (HDAC)/myocyte enhancer factor-2 (MEF2)-mediated signalling in mouse cardiomyocytes (Lu et al., 2011). In the present study, we observed a reduction of NCX1 expression followed by HOCl-LDL-induced CaMKII oxidation.

HOCl-LDL treatment induced oxCaMKII-dependent decrease in Kir2.2 channels underlying I_{K1} that is responsible for shaping the initial depolarization phase, final repolarization and stabilization of resting membrane potential in ventricular and atrial myocytes. Reduced I_{K1} density (approx. 40-50%) was observed in failing cardiomyocytes (Beuckelmann et al., 1993; Pogwizd et al., 2001). Chronically enhanced CaMKII activity, as observed in the failing heart, is predicted to be involved in the observed decrease of I_{K1}. Enhanced CaMKII activity decreased Kir2.1 expression in mouse cardiomyocytes and resulted in reduced I_{K1} (Wagner et al., 2006). Our data parallel these findings as CaMKII oxidation reduced Kir2.2 expression (Figure 10) and I_{K1} density (Figure 15B) in HOCl-LDL-treated GPV myocytes. Moreover, CaMKII inhibition with KN93 resulted in reversal of I_{K1} density under treatment conditions (Figure 15B). These might be explained by previously reported data where inhibition of CaMKII was able to increase I_{K1} density in mouse ventricular myocytes (Li et al., 2006). Under our experimental conditions, CaMKII inhibition by KN93 elevated I_{K1} density in control myocytes (Supplemental Figure IV).

The I_{K1} reversal potential determines resting membrane potential of ventricular myocytes. In the present study, we observed I_{K1} reversal potential of control GPV myocytes at approx. -70 mV and resting membrane potential at -69.21±1.10 mV (Figure 15B, inset). Under treatment conditions reversal potential was shifted towards positive membrane potentials that is most likely responsible for the depolarization of resting membrane potential by HOCl-LDL (Figure 5C). CaMKII inhibition restored the reversal potential of I_{K1} in HOCl-LDL-treated myocytes (Figure 15B, inset). In parallel to I_{K1} reduction, chronic CaMKII activation prolonged APD in mice cardiomyocytes but shortened APD in rabbit myocytes (Wagner et al., 2009). We observed a prolongation of APD by HOCl-LDL-mediated CaMKII oxidation in GPV myocytes (Figure 19A). This phenomenon could be due reduced I_{K1} density at membrane potential positive to resting membrane potential. As a consequence, APD at 90% of repolarization is prolonged as observed in HOCl-LDL-treated myocytes (Figure 5A). In addition to I_{K1} reduction, an increase in I_{NaL} (Figure 17) may contribute to APD prolongation (Figure 5A). In contrast, increased outward I_{SS} density at positive membrane potentials shortens APD. Experiments performed in the presence of Cd^{2+} but absence of K^+ suggest that I_{NS}

contributes to the observed increase in repolarizing outward current at positive membrane potentials in HOCl-LDL-treated myocytes. However, KN93 had no effect on HOCl-LDL-mediated alterations in I_{SS} at positive membrane potentials (Figure 14B) or I_{NS} (Figure 16B). Therefore, we may conclude that reversal of APD by KN93 in HOCl-LDL-treated cells is mainly due to KN93-induced I_{K1} density.

I_{K1} controls upstroke velocity of AP indirectly via maintenance of resting membrane potential. Reduced I_{K1} and therefore depolarization of resting membrane potential increases population of voltage-gated Na^+ channels NaV1.5 being inactivated. From previously published data on steady-state I_{Na} inactivation of GPV myocytes we may correlate a shift of resting membrane potential ranging from -70 to -65 mV by HOCl-LDL (Figure 15B, inset) with reduction of approx. 10% sodium channels being available for activation (Koidl et al., 1990). This fact may contribute to the observed reduction in upstroke velocity. Although HOCl-LDL treatment did not alter NaV1.5 expression directly, we may conclude that HOCl-LDL indirectly alters sodium channel function, probably via oxCaMKII as KN93 was able to reverse upstroke velocity (Figure 19B).

I_{NaL} is the residual current that flows through Na^+ channels which are not completely closed after the peak I_{Na}. Although I_{NaL} contributes approx. 0.5% of peak I_{Na} current, it is large enough to prolong APD and to generate EADs. Due to increase in I_{NaL}, Na^+ movement into the myocytes keeps the membrane potential positive for a longer time in the plateau phase of AP. Increased I_{NaL} has been observed during cardiac hypertrophy, HF, MI and diabetes (Makielski, 2015). CaMKII activation led to an increase in I_{Na} as well as I_{NaL} in rabbit and mouse ventricular myocytes (Wagner et al., 2006), whereby KN93-mediated CaMKII inhibition blocked I_{NaL}. In contrast, KN93 was unable to inhibit I_{NaL} induced by HOCl-LDL (Figure 17A/C). Therefore, we may conclude that elevation of I_{NaL} in the present study is independent of CaMKII oxidation. Ranolazine, an inhibitor of I_{NaL}, blocked HOCl-LDL-induced I_{NaL} in GVP myocytes (Figure 17B/C). In parallel, we also observed reversal of upstroke velocity and APD by Ranolazine (Figure 20A/B). These data confirm that along with reduced I_{K1}, increased I_{NaL} also contributes to HOCl-LDL-induced prolongation in APD. In case of upstroke velocity, some reports suggest a decrease of upstroke velocity by I_{NaL} inhibitors including Ranolazine (Belardinelli et al., 2013; Poulet et al., 2015). In contrast, we

did not observe any significant effect of Ranolazine treatment on upstroke velocity of GPV myocytes (Figure 21B).

I_{NaL} activation was correlated with EADs in rabbit cardiomyocytes in response to oxidative stress (Wagner et al., 2011). In a recent human ventricular model, I_{NaL} was found to play a crucial role in augmentation of EADs (Asakura et al., 2014). In the present study, HOCl-LDL induced EADs and DADs in GPV myocytes (Figure 4C). Acute treatment of myocytes with Ranolazine blocked HOCl-LDL-induced arrhythmic events completely (Figure 18). These observations conclude that I_{NaL} augmentation by HOCl-LDL is a major contributor for the observed arrhythmic events. In support of this conclusion, no arrhythmic event was observed in HOCl-LDL-incubated cells that were pre-treated with Ranolazine. In accordance to our data, GS967, a selective I_{NaL} blocker, was recently reported to suppress EADs, DADs and APD prolongation in rat ventricle (Pezhouman et al., 2014).

Our experimental data obtained from the cellular level underscore the underlying mechanism behind the effects of HOCl-LDL on cardiac tissue. Human RAA treated with HOCl-LDL showed arrhythmic events (Figure 2, 3B) that were reversed by Ranolazine and KN93 (Figure 22A). The protective effect of Ranolazine against arrhythmia is most likely due to the inhibition of increased I_{NaL}, while for KN93 it could be due to its protective effects against decreased I_{K1} and prolonged APD in response to HOCl-LDL. Moreover, we observed an increase of diastolic tension in trabeculae incubated with HOCl-LDL (Figure 2, 3C). This might be due to increased I_{NaL}, as it causes Na^+ overload that further activates NCX1 and leads to Ca^{2+} overload (Noble and Noble, 2006). However, we did not observe any effect of HOCl-LDL on diastolic calcium in GPV myocytes (Figure 13D). These might be due to i) trabeculae were incubated for 90 min and myocytes were incubated for 14 h with HOCl-LDL, ii) unlike GPV myocytes, trabeculae were stimulated with a frequency of 1 Hz during the whole experiment and iii) human cardiomyocytes have much higher expression of NCX1 compared to guinea pig cells and NCX1 expression was reduced in HOCl-LDL-treated GPV cells. Both, KN93 and Ranolazine, blocked contractile dysfunction of cardiac tissue in response to HOCl-LDL. Moreover, we observed diastolic arrhythmia in trabeculae

incubated with HOCl-LDL (Figure 2). This might be the consequence of HOCl-LDL-induced DADs in GPV myocytes.

Elevated levels of MPO in serum and myocardium have been reported to alter cardiac function in CVDs patients as well as animal models of CVDs. MPO-generated oxidants were found to contribute to LV dilation and worsen cardiac function post-MI (Vasilyev et al., 2005). LAD ligation in $MPO^{-/-}$ mice showed reduced leukocyte infiltration in myocardium, improved LV end diastolic diameter (LVEDD), preserved systolic function and reduced mortality (Askari et al., 2003). Higher MPO levels were correlated with reduced LVEF in MI patients (Mocatta et al., 2007), increased mortality in ST-elevation MI (Kaya et al., 2012) and HF in elderly patients (Tang et al., 2011). Our data confirm infiltration of neutrophils, elevation of MPO expression and evidence of LDL modification by HOCl in the LV of MI patients. In a recent clinical study, plasma MPO level but not genetic polymorphism of MPO was found as an independent risk factor to predict cardiovascular mortality (Scharnagl et al., 2014). During development of atrial fibrillation, MPO was found as a crucial requisite for myocardial remodelling (Rudolph et al., 2010). All these studies conclude that elevated MPO level in the myocardium is detrimental for cardiac function and leads to development and progression of various CVDs.

Our data may provide molecular mechanism and basis for the better understanding of the adverse effects of the MPO-H_2O_2-chloride system on cardiac function during CVDs.

5. References

Alfakry H, Sinisalo J, Paju S, Nieminen MS, Valtonen V, Tervahartiala T, Pussinen PJ, Sorsa T. The association of serum neutrophil markers and acute coronary syndrome. *Scandinavian journal of immunology*. 2012; 76(2):181-187.

Anderson ME, Braun AP, Wu Y, Lu T, Wu Y, Schulman H, Sung RJ. KN-93, an inhibitor of multifunctional Ca++/calmodulin-dependent protein kinase, decreases early afterdepolarizations in rabbit heart. *The Journal of pharmacology and experimental therapeutics*. 1998; 287(3):996-1006.

Antos CL, Frey N, Marx SO, Reiken S, Gaburjakova M, Richardson JA, Marks AR, Olson EN. Dilated cardiomyopathy and sudden death resulting from constitutive activation of protein kinase a. *Circulation research*. 2001; 89(11):997-1004.

Arita M, Surawicz B. Depolarization and action potential duration in cardiac Purkinje fibers. *Circulation research*. 1973; 33(1):39-47.

Arnhold J, Flemmig J. Human myeloperoxidase in innate and acquired immunity. *Archives of biochemistry and biophysics*. 2010; 500(1):92-106.

Arnold K, Arnhold J, Zschornig O, Wiegel D, Krumbiegel M. Characterization of chemical modifications of surface properties of low density lipoproteins. *Biomedica biochimica acta*. 1989; 48(10):735-742.

Asakura K, Cha CY, Yamaoka H, Horikawa Y, Memida H, Powell T, Amano A, Noma A. EAD and DAD mechanisms analyzed by developing a new human ventricular cell model. *Progress in biophysics and molecular biology*. 2014; 116(1):11-24.

Askari AT, Brennan ML, Zhou X, Drinko J, Morehead A, Thomas JD, Topol EJ, Hazen SL, Penn MS. Myeloperoxidase and plasminogen activator inhibitor 1 play a central role in ventricular remodeling after myocardial infarction. *The Journal of experimental medicine*. 2003; 197(5):615-624.

Baigent C, Keech A, Kearney PM, Blackwell L, Buck G, Pollicino C, Kirby A, Sourjina T, Peto R, Collins R, Simes R, Cholesterol Treatment Trialists C. Efficacy and safety of cholesterol-lowering treatment: prospective meta-analysis of data from 90,056 participants in 14 randomised trials of statins. *Lancet*. 2005; 366(9493):1267-1278.

Belardinelli L, Liu G, Smith-Maxwell C, Wang WQ, El-Bizri N, Hirakawa R, Karpinski S, Li CH, Hu L, Li XJ, Crumb W, Wu L, Koltun D, Zablocki J, Yao L, Dhalla AK, Rajamani S, Shryock JC. A novel, potent, and selective inhibitor of cardiac late sodium current suppresses experimental arrhythmias. *The Journal of pharmacology and experimental therapeutics*. 2013; 344(1):23-32.

Ben J, Zhu X, Zhang H, Chen Q. Class A1 scavenger receptors in cardiovascular diseases. *British journal of pharmacology*. 2015;

Bendall JK, Cave AC, Heymes C, Gall N, Shah AM. Pivotal role of a gp91(phox)-containing NADPH oxidase in angiotensin II-induced cardiac hypertrophy in mice. *Circulation*. 2002; 105(3):293-296.

Benitah JP, Gomez AM, Fauconnier J, Kerfant BG, Perrier E, Vassort G, Richard S. Voltage-gated Ca2+ currents in the human pathophysiologic heart: a review. *Basic research in cardiology*. 2002; 97 Suppl 1:I11-18.

Beuckelmann DJ, Nabauer M, Erdmann E. Alterations of K+ currents in isolated human ventricular myocytes from patients with terminal heart failure. *Circulation research*. 1993; 73(2):379-385.

Bhat T, Teli S, Rijal J, Bhat H, Raza M, Khoueiry G, Meghani M, Akhtar M, Costantino T. Neutrophil to lymphocyte ratio and cardiovascular diseases: a review. *Expert review of cardiovascular therapy*. 2013; 11(1):55-59.

Boekholdt SM, Arsenault BJ, Mora S, Pedersen TR, LaRosa JC, Nestel PJ, Simes RJ, Durrington P, Hitman GA, Welch KM, DeMicco DA, Zwinderman AH, Clearfield MB, Downs JR, Tonkin AM, Colhoun HM, Gotto AM, Jr., Ridker PM, Kastelein JJ. Association of LDL cholesterol, non-HDL cholesterol, and apolipoprotein B levels with risk of cardiovascular events among patients treated with statins: a meta-analysis. *Jama*. 2012; 307(12):1302-1309.

Boren J, Veniant MM, Young SG. Apo B100-containing lipoproteins are secreted by the heart. *The Journal of clinical investigation*. 1998; 101(6):1197-1202.

Bos A, Wever R, Roos D. Characterization and quantification of the peroxidase in human monocytes. *Biochimica et biophysica acta*. 1978; 525(1):37-44.

Brennan AM, Suh SW, Won SJ, Narasimhan P, Kauppinen TM, Lee H, Edling Y, Chan PH, Swanson RA. NADPH oxidase is the primary source of superoxide induced by NMDA receptor activation. *Nature neuroscience*. 2009; 12(7):857-863.

Brown KE, Brunt EM, Heinecke JW. Immunohistochemical detection of myeloperoxidase and its oxidation products in Kupffer cells of human liver. *The American journal of pathology*. 2001; 159(6):2081-2088.

Calay D, Rousseau A, Mattart L, Nuyens V, Delporte C, Van Antwerpen P, Moguilevsky N, Arnould T, Boudjeltia KZ, Raes M. Copper and Myeloperoxidase-Modified LDLs Activate Nrf2 Through Different Pathways of ROS Production in Macrophages. *Antioxid Redox Sign*. 2010; 13(10):1491-1502.

Carbone F, Nencioni A, Mach F, Vuilleumier N, Montecucco F. Pathophysiological role of neutrophils in acute myocardial infarction. *Thrombosis and haemostasis*. 2013; 110(3):501-514.

Carr AC, Myzak MC, Stocker R, McCall MR, Frei B. Myeloperoxidase binds to low-density lipoprotein: potential implications for atherosclerosis. *FEBS letters*. 2000; 487(2):176-180.

Cominacini L, Rigoni A, Pasini AF, Garbin U, Davoli A, Campagnola M, Pastorino AM, Lo Cascio V, Sawamura T. The binding of oxidized low density lipoprotein (ox-LDL) to ox-LDL receptor-1 reduces the intracellular concentration of nitric oxide in endothelial cells through an increased production of superoxide. *The Journal of biological chemistry*. 2001; 276(17):13750-13755.

Couchonnal LF, Anderson ME. The role of calmodulin kinase II in myocardial physiology and disease. *Physiology*. 2008; 23:151-159.

Daugherty A, Dunn JL, Rateri DL, Heinecke JW. Myeloperoxidase, a catalyst for lipoprotein oxidation, is expressed in human atherosclerotic lesions. *The Journal of clinical investigation*. 1994; 94(1):437-444.

De Backer D, Scolletta S. Clinical management of the cardiovascular failure in sepsis. *Current vascular pharmacology*. 2013; 11(2):222-242.

Delporte C, Boudjeltia KZ, Noyon C, Furtmuller PG, Nuyens V, Slomianny MC, Madhoun P, Desmet JM, Raynal P, Dufour D, Koyani CN, Reye F, Rousseau A, Vanhaeverbeek M, Ducobu J, Michalski JC, Neve J, Vanhamme L, Obinger C, Malle E, Van Antwerpen P. Impact of myeloperoxidase-LDL interactions on enzyme activity and subsequent posttranslational oxidative modifications of apoB-100. *Journal of lipid research*. 2014; 55(4):747-757.

Dhalla NS, Temsah RM, Netticadan T. Role of oxidative stress in cardiovascular diseases. *Journal of hypertension*. 2000; 18(6):655-673.

Dzhura I, Wu Y, Colbran RJ, Balser JR, Anderson ME. Calmodulin kinase determines calcium-dependent facilitation of L-type calcium channels. *Nature cell biology*. 2000; 2(3):173-177.

Ebrahim S, Taylor FC, Brindle P. Statins for the primary prevention of cardiovascular disease. *Bmj*. 2014; 348:g280.

Erickson JR, He BJ, Grumbach IM, Anderson ME. CaMKII in the cardiovascular system: sensing redox states. *Physiological reviews*. 2011; 91(3):889-915.

Erickson JR, Joiner ML, Guan X, Kutschke W, Yang J, Oddis CV, Bartlett RK, Lowe JS, O'Donnell SE, Aykin-Burns N, Zimmerman MC, Zimmerman K, Ham AJ, Weiss RM, Spitz DR, Shea MA, Colbran RJ, Mohler PJ, Anderson ME. A dynamic pathway for calcium-independent activation of CaMKII by methionine oxidation. *Cell*. 2008; 133(3):462-474.

Fearon IM, Faux SP. Oxidative stress and cardiovascular disease: novel tools give (free) radical insight. *Journal of molecular and cellular cardiology*. 2009; 47(3):372-381.

Fomenko DE, Novoselov SV, Natarajan SK, Lee BC, Koc A, Carlson BA, Lee TH, Kim HY, Hatfield DL, Gladyshev VN. MsrB1 (methionine-R-sulfoxide reductase 1) knock-out mice: roles of MsrB1 in redox regulation and identification of a novel selenoprotein form. *The Journal of biological chemistry*. 2009; 284(9):5986-5993.

Foteinou PT, Greenstein JL, Winslow RL. Mechanistic Investigation of the Arrhythmogenic Role of Oxidized CaMKII in the Heart. *Biophysical journal*. 2015; 109(4):838-849.

Gao L, Blair LA, Marshall J. CaMKII-independent effects of KN93 and its inactive analog KN92: reversible inhibition of L-type calcium channels. *Biochem Biophys Res Commun*. 2006; 345(4):1606-1610.

Giorgio M, Trinei M, Migliaccio E, Pelicci PG. Hydrogen peroxide: a metabolic by-product or a common mediator of ageing signals? *Nature reviews. Molecular cell biology*. 2007; 8(9):722-728.

Golia E, Limongelli G, Natale F, Fimiani F, Maddaloni V, Pariggiano I, Bianchi R, Crisci M, D'Acierno L, Giordano R, Di Palma G, Conte M, Golino P, Russo MG, Calabro R, Calabro P. Inflammation and cardiovascular disease: from pathogenesis to therapeutic target. *Current atherosclerosis reports*. 2014; 16(9):435.

Gray E, Thomas TL, Betmouni S, Scolding N, Love S. Elevated activity and microglial expression of myeloperoxidase in demyelinated cerebral cortex in multiple sclerosis. *Brain pathology*. 2008; 18(1):86-95.

Greenwalt DE, Scheck SH, Rhinehart-Jones T. Heart CD36 expression is increased in murine models of diabetes and in mice fed a high fat diet. *The Journal of clinical investigation*. 1995; 96(3):1382-1388.

Grueter CE, Abiria SA, Dzhura I, Wu Y, Ham AJ, Mohler PJ, Anderson ME, Colbran RJ. L-type Ca2+ channel facilitation mediated by phosphorylation of the beta subunit by CaMKII. *Molecular cell*. 2006; 23(5):641-650.

Hagemann D, Kuschel M, Kuramochi T, Zhu W, Cheng H, Xiao RP. Frequency-encoding Thr17 phospholamban phosphorylation is independent of Ser16 phosphorylation in cardiac myocytes. *The Journal of biological chemistry*. 2000; 275(29):22532-22536.

Hain J, Onoue H, Mayrleitner M, Fleischer S, Schindler H. Phosphorylation modulates the function of the calcium release channel of sarcoplasmic reticulum from cardiac muscle. *The Journal of biological chemistry*. 1995; 270(5):2074-2081.

Hammerschmidt S, Wahn H. The effect of the oxidant hypochlorous acid on the L-type calcium current in isolated ventricular cardiomyocytes. *Journal of molecular and cellular cardiology*. 1998; 30(9):1855-1867.

Haumer M, Amighi J, Exner M, Mlekusch W, Sabeti S, Schlager O, Schwarzinger I, Wagner O, Minar E, Schillinger M. Association of neutrophils and future cardiovascular events in patients with peripheral artery disease. *Journal of vascular surgery*. 2005; 41(4):610-617.

Hazell LJ, Arnold L, Flowers D, Waeg G, Malle E, Stocker R. Presence of hypochlorite-modified proteins in human atherosclerotic lesions. *The Journal of clinical investigation*. 1996; 97(6):1535-1544.

Hazell LJ, Stocker R. Oxidation of low-density lipoprotein with hypochlorite causes transformation of the lipoprotein into a high-uptake form for macrophages. *The Biochemical journal*. 1993; 290 (Pt 1):165-172.

Hazen SL, Heinecke JW. 3-Chlorotyrosine, a specific marker of myeloperoxidase-catalyzed oxidation, is markedly elevated in low density lipoprotein isolated from human atherosclerotic intima. *The Journal of clinical investigation*. 1997; 99(9):2075-2081.

Heneghan HM, Huang H, Kashyap SR, Gornik HL, McCullough AJ, Schauer PR, Brethauer SA, Kirwan JP, Kasumov T. Reduced cardiovascular risk after bariatric surgery is linked to plasma ceramides, apolipoprotein-B100, and ApoB100/A1 ratio. *Surgery for obesity and related diseases : official journal of the American Society for Bariatric Surgery*. 2013; 9(1):100-107.

Hill MF, Singal PK. Right and left myocardial antioxidant responses during heart failure subsequent to myocardial infarction. *Circulation*. 1997; 96(7):2414-2420.

Hirayama S, Miida T. Small dense LDL: An emerging risk factor for cardiovascular disease. *Clinica chimica acta; international journal of clinical chemistry*. 2012; 414:215-224.

Ho HT, Liu B, Snyder JS, Lou Q, Brundage EA, Velez-Cortes F, Wang H, Ziolo MT, Anderson ME, Sen CK, Wehrens XH, Fedorov VV, Biesiadecki BJ, Hund TJ, Gyorke S. Ryanodine receptor phosphorylation by oxidized CaMKII contributes to the cardiotoxic effects of cardiac glycosides. *Cardiovascular research*. 2014; 101(1):165-174.

Hoekstra M, Mummery CL, Wilde AA, Bezzina CR, Verkerk AO. Induced pluripotent stem cell derived cardiomyocytes as models for cardiac arrhythmias. *Frontiers in physiology*. 2012; 3:346.

Hoffmann J, Marsh LM, Pieper M, Stacher E, Ghanim B, Kovacs G, Konig P, Wilkens H, Haitchi HM, Hoefler G, Klepetko W, Olschewski H, Olschewski A, Kwapiszewska G. Compartment-specific expression of collagens and their processing enzymes in intrapulmonary arteries of IPAH patients. *American journal of physiology. Lung cellular and molecular physiology*. 2015; 308(10):L1002-1013.

Holvoet P, Mertens A, Verhamme P, Bogaerts K, Beyens G, Verhaeghe R, Collen D, Muls E, Van de Werf F. Circulating oxidized LDL is a useful marker for identifying patients with coronary artery disease. *Arteriosclerosis, thrombosis, and vascular biology*. 2001; 21(5):844-848.

Hu C, Chen J, Dandapat A, Fujita Y, Inoue N, Kawase Y, Jishage K, Suzuki H, Li D, Hermonat PL, Sawamura T, Mehta JL. LOX-1 abrogation reduces myocardial ischemia-reperfusion injury in mice. *Journal of molecular and cellular cardiology*. 2008; 44(1):76-83.

Hu Y, Zhang H, Lu Y, Bai H, Xu Y, Zhu X, Zhou R, Ben J, Xu Y, Chen Q. Class A scavenger receptor attenuates myocardial infarction-induced cardiomyocyte necrosis through suppressing M1 macrophage subset polarization. *Basic research in cardiology*. 2011; 106(6):1311-1328.

Huang Y, Cai X, Chen P, Mai W, Tang H, Huang Y, Hu Y. Associations of prediabetes with all-cause and cardiovascular mortality: a meta-analysis. *Annals of medicine*. 2014; 46(8):684-692.

Ipadeola A, Adeleye JO. THE metabolic syndrome and accurate cardiovascular risk prediction in persons with type 2 diabetes mellitus. *Diabetes & metabolic syndrome*. 2015;

Jordan JE, Zhao ZQ, Vinten-Johansen J. The role of neutrophils in myocardial ischemia-reperfusion injury. *Cardiovascular research*. 1999; 43(4):860-878.

Kalasz J, Pasztor ET, Fagyas M, Balogh A, Toth A, Csato V, Edes I, Papp Z, Borbely A. Myeloperoxidase impairs the contractile function in isolated human cardiomyocytes. *Free radical biology & medicine*. 2015; 84:116-127.

Kataoka K, Hasegawa K, Sawamura T, Fujita M, Yanazume T, Iwai-Kanai E, Kawamura T, Hirai T, Kita T, Nohara R. LOX-1 pathway affects the extent of myocardial ischemia-reperfusion injury. *Biochem Biophys Res Commun*. 2003; 300(3):656-660.

Kaya MG, Yalcin R, Okyay K, Poyraz F, Bayraktar N, Pasaoglu H, Boyaci B, Cengel A. Potential role of plasma myeloperoxidase level in predicting long-term outcome of acute myocardial infarction. *Texas Heart Institute journal / from the Texas Heart Institute of St. Luke's Episcopal Hospital, Texas Children's Hospital*. 2012; 39(4):500-506.

Kinugawa S, Tsutsui H, Hayashidani S, Ide T, Suematsu N, Satoh S, Utsumi H, Takeshita A. Treatment with dimethylthiourea prevents left ventricular remodeling and failure after experimental myocardial infarction in mice: role of oxidative stress. *Circulation research*. 2000; 87(5):392-398.

Kohlhaas M, Zhang T, Seidler T, Zibrova D, Dybkova N, Steen A, Wagner S, Chen L, Brown JH, Bers DM, Maier LS. Increased sarcoplasmic reticulum calcium leak but unaltered contractility by acute CaMKII overexpression in isolated rabbit cardiac myocytes. *Circulation research*. 2006; 98(2):235-244.

Koidl B, Schreibmayer W, Wolf P, Tritthart HA. Inhibition of the fast sodium inward current in ventricular cardiomyocytes of rats and guinea pigs by a novel potent sodium channel blocking agent. *Naunyn-Schmiedeberg's archives of pharmacology*. 1990; 342(5):582-591.

Kono Y, Nakamura K, Kimura H, Nishii N, Watanabe A, Banba K, Miura A, Nagase S, Sakuragi S, Kusano KF, Matsubara H, Ohe T. Elevated levels of oxidative DNA

damage in serum and myocardium of patients with heart failure. *Circulation journal : official journal of the Japanese Circulation Society*. 2006; 70(8):1001-1005.

Koyani CN, Windischhofer W, Rossmann C, Jin G, Kickmaier S, Heinzel FR, Groschner K, Alavian-Ghavanini A, Sattler W, Malle E. 15-deoxy-Delta(1)(2),(1)(4)-PGJ(2) promotes inflammation and apoptosis in cardiomyocytes via the DP2/MAPK/TNFalpha axis. *International journal of cardiology*. 2014; 173(3):472-480.

Kuroda J, Ago T, Matsushima S, Zhai P, Schneider MD, Sadoshima J. NADPH oxidase 4 (Nox4) is a major source of oxidative stress in the failing heart. *Proceedings of the National Academy of Sciences of the United States of America*. 2010; 107(35):15565-15570.

Levitan I, Volkov S, Subbaiah PV. Oxidized LDL: diversity, patterns of recognition, and pathophysiology. *Antioxid Redox Signal*. 2010; 13(1):39-75.

Li D, Williams V, Liu L, Chen H, Sawamura T, Antakli T, Mehta JL. LOX-1 inhibition in myocardial ischemia-reperfusion injury: modulation of MMP-1 and inflammation. *American journal of physiology. Heart and circulatory physiology*. 2002; 283(5):H1795-1801.

Li J, Marionneau C, Zhang R, Shah V, Hell JW, Nerbonne JM, Anderson ME. Calmodulin kinase II inhibition shortens action potential duration by upregulation of K+ currents. *Circulation research*. 2006; 99(10):1092-1099.

Loria V, Dato I, Graziani F, Biasucci LM. Myeloperoxidase: a new biomarker of inflammation in ischemic heart disease and acute coronary syndromes. *Mediators of inflammation*. 2008; 2008:135625.

Lu YM, Huang J, Shioda N, Fukunaga K, Shirasaki Y, Li XM, Han F. CaMKIIdeltaB mediates aberrant NCX1 expression and the imbalance of NCX1/SERCA in transverse aortic constriction-induced failing heart. *Plos One*. 2011; 6(9):e24724.

Luo M, Guan X, Luczak ED, Lang D, Kutschke W, Gao Z, Yang J, Glynn P, Sossalla S, Swaminathan PD, Weiss RM, Yang B, Rokita AG, Maier LS, Efimov IR, Hund TJ, Anderson ME. Diabetes increases mortality after myocardial infarction by oxidizing CaMKII. *The Journal of clinical investigation*. 2013; 123(3):1262-1274.

Maack C, Kartes T, Kilter H, Schafers HJ, Nickenig G, Bohm M, Laufs U. Oxygen free radical release in human failing myocardium is associated with increased activity of rac1-GTPase and represents a target for statin treatment. *Circulation*. 2003; 108(13):1567-1574.

Maier LS, Bers DM. Role of Ca2+/calmodulin-dependent protein kinase (CaMK) in excitation-contraction coupling in the heart. *Cardiovascular research*. 2007; 73(4):631-640.

Maier LS, Zhang T, Chen L, DeSantiago J, Brown JH, Bers DM. Transgenic CaMKIIdeltaC overexpression uniquely alters cardiac myocyte Ca2+ handling: reduced SR Ca2+ load and activated SR Ca2+ release. *Circulation research*. 2003; 92(8):904-911.

Makielski JC. Late sodium current: A mechanism for angina, heart failure, and arrhythmia. *Trends in cardiovascular medicine*. 2015;

Makielski JC, Valdivia CR. Ranolazine and late cardiac sodium current--a therapeutic target for angina, arrhythmia and more? *British journal of pharmacology*. 2006; 148(1):4-6.

Malle E, Buch T, Grone HJ. Myeloperoxidase in kidney disease. *Kidney international*. 2003; 64(6):1956-1967.

Malle E, Hazell L, Stocker R, Sattler W, Esterbauer H, Waeg G. Immunologic detection and measurement of hypochlorite-modified LDL with specific monoclonal antibodies. *Arteriosclerosis, thrombosis, and vascular biology*. 1995a; 15(7):982-989.

Malle E, Ibovnik A, Leis HJ, Kostner GM, Verhallen PF, Sattler W. Lysine modification of LDL or lipoprotein(a) by 4-hydroxynonenal or malondialdehyde decreases platelet serotonin secretion without affecting platelet aggregability and eicosanoid formation. *Arteriosclerosis, thrombosis, and vascular biology*. 1995b; 15(3):377-384.

Malle E, Marsche G, Arnhold J, Davies MJ. Modification of low-density lipoprotein by myeloperoxidase-derived oxidants and reagent hypochlorous acid. *Biochimica et biophysica acta*. 2006a; 1761(4):392-415.

Malle E, Marsche G, Panzenboeck U, Sattler W. Myeloperoxidase-mediated oxidation of high-density lipoproteins: fingerprints of newly recognized potential proatherogenic lipoproteins. *Archives of biochemistry and biophysics*. 2006b; 445(2):245-255.

Malle E, Waeg G, Schreiber R, Grone EF, Sattler W, Grone HJ. Immunohistochemical evidence for the myeloperoxidase/H2O2/halide system in human atherosclerotic lesions: colocalization of myeloperoxidase and

hypochlorite-modified proteins. *European journal of biochemistry / FEBS*. 2000; 267(14):4495-4503.

Marklund S. Spectrophotometric study of spontaneous disproportionation of superoxide anion radical and sensitive direct assay for superoxide dismutase. *The Journal of biological chemistry*. 1976; 251(23):7504-7507.

Marsche G, Zimmermann R, Horiuchi S, Tandon NN, Sattler W, Malle E. Class B scavenger receptors CD36 and SR-BI are receptors for hypochlorite-modified low density lipoprotein. *The Journal of biological chemistry*. 2003; 278(48):47562-47570.

Miake J, Marban E, Nuss HB. Biological pacemaker created by gene transfer. *Nature*. 2002; 419(6903):132-133.

Michowitz Y, Kisil S, Guzner-Gur H, Rubinstein A, Wexler D, Sheps D, Keren G, George J. Usefulness of serum myeloperoxidase in prediction of mortality in patients with severe heart failure. *The Israel Medical Association journal : IMAJ*. 2008; 10(12):884-888.

Mocatta TJ, Pilbrow AP, Cameron VA, Senthilmohan R, Frampton CM, Richards AM, Winterbourn CC. Plasma concentrations of myeloperoxidase predict mortality after myocardial infarction. *Journal of the American College of Cardiology*. 2007; 49(20):1993-2000.

Mollova MY, Katus HA, Backs J. Regulation of CaMKII signaling in cardiovascular disease. *Frontiers in pharmacology*. 2015; 6:178.

Morris JC. The Acid Ionization Constant of HOCl from 5 to 35°. *The Journal of Physical Chemistry*. 1966; 70(12):3798-3805.

Mullane KM, Kraemer R, Smith B. Myeloperoxidase activity as a quantitative assessment of neutrophil infiltration into ischemic myocardium. *Journal of pharmacological methods*. 1985; 14(3):157-167.

Munzel T, Harrison DG. Increased superoxide in heart failure: a biochemical baroreflex gone awry. *Circulation*. 1999; 100(3):216-218.

Nambi V. The use of myeloperoxidase as a risk marker for atherosclerosis. *Current atherosclerosis reports*. 2005; 7(2):127-131.

Neef S, Maier LS. Novel aspects of excitation-contraction coupling in heart failure. *Basic research in cardiology*. 2013; 108(4):360.

Nicholls SJ, Hazen SL. Myeloperoxidase and cardiovascular disease. *Arteriosclerosis, thrombosis, and vascular biology*. 2005; 25(6):1102-1111.

Nielsen LB, Veniant M, Boren J, Raabe M, Wong JS, Tam C, Flynn L, Vanni-Reyes T, Gunn MD, Goldberg IJ, Hamilton RL, Young SG. Genes for apolipoprotein B and microsomal triglyceride transfer protein are expressed in the heart: evidence that the heart has the capacity to synthesize and secrete lipoproteins. *Circulation*. 1998; 98(1):13-16.

Noble D, Noble PJ. Late sodium current in the pathophysiology of cardiovascular disease: consequences of sodium-calcium overload. *Heart*. 2006; 92 Suppl 4:iv1-iv5.

O'Keefe JH, Jr., Cordain L, Harris WH, Moe RM, Vogel R. Optimal low-density lipoprotein is 50 to 70 mg/dl: lower is better and physiologically normal. *Journal of the American College of Cardiology*. 2004; 43(11):2142-2146.

O Hartaigh B, Bosch JA, Carroll D, Hemming K, Pilz S, Loerbroks A, Kleber ME, Grammer TB, Fischer JE, Boehm BO, Marz W, Thomas GN. Evidence of a synergistic association between heart rate, inflammation, and cardiovascular mortality in patients undergoing coronary angiography. *European heart journal*. 2013; 34(12):932-941.

Pelzmann B, Schaffer P, Bernhart E, Lang P, Machler H, Rigler B, Koidl B. L-type calcium current in human ventricular myocytes at a physiological temperature from children with tetralogy of Fallot. *Cardiovascular research*. 1998; 38(2):424-432.

Pezhouman A, Madahian S, Stepanyan H, Ghukasyan H, Qu Z, Belardinelli L, Karagueuzian HS. Selective inhibition of late sodium current suppresses ventricular tachycardia and fibrillation in intact rat hearts. *Heart rhythm : the official journal of the Heart Rhythm Society*. 2014; 11(3):492-501.

Picht E, DeSantiago J, Huke S, Kaetzel MA, Dedman JR, Bers DM. CaMKII inhibition targeted to the sarcoplasmic reticulum inhibits frequency-dependent acceleration of relaxation and Ca2+ current facilitation. *Journal of molecular and cellular cardiology*. 2007; 42(1):196-205.

Pietka TA, Sulkin MS, Kuda O, Wang W, Zhou D, Yamada KA, Yang K, Su X, Gross RW, Nerbonne JM, Efimov IR, Abumrad NA. CD36 protein influences myocardial Ca2+ homeostasis and phospholipid metabolism: conduction

anomalies in CD36-deficient mice during fasting. *The Journal of biological chemistry*. 2012; 287(46):38901-38912.

Piper HM, Probst I, Schwartz P, Hutter FJ, Spieckermann PG. Culturing of calcium stable adult cardiac myocytes. *Journal of molecular and cellular cardiology*. 1982; 14(7):397-412.

Pogwizd SM, Schlotthauer K, Li L, Yuan W, Bers DM. Arrhythmogenesis and contractile dysfunction in heart failure: Roles of sodium-calcium exchange, inward rectifier potassium current, and residual beta-adrenergic responsiveness. *Circulation research*. 2001; 88(11):1159-1167.

Poteser M, Schleifer H, Lichtenegger M, Schernthaner M, Stockner T, Kappe CO, Glasnov TN, Romanin C, Groschner K. PKC-dependent coupling of calcium permeation through transient receptor potential canonical 3 (TRPC3) to calcineurin signaling in HL-1 myocytes. *Proceedings of the National Academy of Sciences of the United States of America*. 2011; 108(26):10556-10561.

Poulet C, Wettwer E, Grunnet M, Jespersen T, Fabritz L, Matschke K, Knaut M, Ravens U. Late Sodium Current in Human Atrial Cardiomyocytes from Patients in Sinus Rhythm and Atrial Fibrillation. *Plos One*. 2015; 10(6)

Prentice HM, Moench IA, Rickaway ZT, Dougherty CJ, Webster KA, Weissbach H. MsrA protects cardiac myocytes against hypoxia/reoxygenation induced cell death. *Biochem Biophys Res Commun*. 2008; 366(3):775-778.

Prutz WA. Hypochlorous acid interactions with thiols, nucleotides, DNA, and other biological substrates. *Archives of biochemistry and biophysics*. 1996; 332(1):110-120.

Rashidi F, Rashidi A, Golmohamadi A, Hoseinzadeh E, Mohammadi B, Mirzajani H, Kheiri M, Jamshidi P. Does absolute neutrophilia predict early congestive heart failure after acute myocardial infarction? A cross-sectional study. *Southern medical journal*. 2008; 101(1):19-23.

Ren D, Wang X, Ha T, Liu L, Kalbfleisch J, Gao X, Williams D, Li C. SR-A deficiency reduces myocardial ischemia/reperfusion injury; involvement of increased microRNA-125b expression in macrophages. *Biochimica et biophysica acta*. 2013; 1832(2):336-346.

Resch U, Semlitsch M, Hammer A, Susani-Etzerodt H, Walczak H, Sattler W, Malle E. Hypochlorite-modified low-density lipoprotein induces the apoptotic machinery in Jurkat T-cell lines. *Biochem Bioph Res Co*. 2011; 410(4):895-900.

Riahi S, Mohammadi MT, Sobhani V, Ababzadeh S. Chronic Aerobic Exercise Decreases Lectin-Like Low Density Lipoprotein (LOX-1) Receptor Expression in Heart of Diabetic Rat. *Iranian biomedical journal*. 2015;

Ringseis R, Wen G, Saal D, Eder K. Conjugated linoleic acid isomers reduce cholesterol accumulation in acetylated LDL-induced mouse RAW264.7 macrophage-derived foam cells. *Lipids*. 2008; 43(10):913-923.

Ronkainen JJ, Hanninen SL, Korhonen T, Koivumaki JT, Skoumal R, Rautio S, Ronkainen VP, Tavi P. Ca2+-calmodulin-dependent protein kinase II represses cardiac transcription of the L-type calcium channel alpha(1C)-subunit gene (Cacna1c) by DREAM translocation. *The Journal of physiology*. 2011; 589(Pt 11):2669-2686.

Rudolph V, Andrie RP, Rudolph TK, Friedrichs K, Klinke A, Hirsch-Hoffmann B, Schwoerer AP, Lau D, Fu X, Klingel K, Sydow K, Didie M, Seniuk A, von Leitner EC, Szoecs K, Schrickel JW, Treede H, Wenzel U, Lewalter T, Nickenig G, Zimmermann WH, Meinertz T, Boger RH, Reichenspurner H, Freeman BA, Eschenhagen T, Ehmke H, Hazen SL, Willems S, Baldus S. Myeloperoxidase acts as a profibrotic mediator of atrial fibrillation. *Nature medicine*. 2010; 16(4):470-474.

Saad M, Mahmoud A, Elgendy IY, Richard Conti C. Ranolazine in Cardiac Arrhythmia. *Clinical cardiology*. 2015;

Scharnagl H, Kleber ME, Genser B, Kickmaier S, Renner W, Weihrauch G, Grammer T, Rossmann C, Winkelmann BR, Boehm BO, Sattler W, Marz W, Malle E. Association of myeloperoxidase with total and cardiovascular mortality in individuals undergoing coronary angiography--the LURIC study. *International journal of cardiology*. 2014; 174(1):96-105.

Schindhelm RK, van der Zwan LP, Teerlink T, Scheffer PG. Myeloperoxidase: a useful biomarker for cardiovascular disease risk stratification? *Clinical chemistry*. 2009; 55(8):1462-1470.

Schofield ZV, Woodruff TM, Halai R, Wu MC, Cooper MA. Neutrophils--a key component of ischemia-reperfusion injury. *Shock*. 2013; 40(6):463-470.

Schultz J, Kaminker K. Myeloperoxidase of the leucocyte of normal human blood. I. Content and localization. *Archives of biochemistry and biophysics*. 1962; 96:465-467.

Shryock JC. Role of Late Sodium Channel Current in Arrhythmogenesis. *Cardiac Electrophysiology Clinics*. 2011; 3(1):125-140.

Siminiak T, Ozawa T. Neutrophil mediated myocardial injury. *The International journal of biochemistry*. 1993; 25(2):147-156.

Singh MV, Kapoun A, Higgins L, Kutschke W, Thurman JM, Zhang R, Singh M, Yang J, Guan X, Lowe JS, Weiss RM, Zimmermann K, Yull FE, Blackwell TS, Mohler PJ, Anderson ME. Ca2+/calmodulin-dependent kinase II triggers cell membrane injury by inducing complement factor B gene expression in the mouse heart. *The Journal of clinical investigation*. 2009; 119(4):986-996.

Slezak J, Tribulova N, Pristacova J, Uhrik B, Thomas T, Khaper N, Kaul N, Singal PK. Hydrogen-Peroxide Changes in Ischemic and Reperfused Heart - Cytochemistry and Biochemical and X-Ray-Microanalysis. *American Journal of Pathology*. 1995; 147(3):772-781.

Soehnlein O. Multiple roles for neutrophils in atherosclerosis. *Circulation research*. 2012; 110(6):875-888.

Sokolov AV, Chekanov AV, Kostevich VA, Aksenov DV, Vasilyev VB, Panasenko OM. Revealing binding sites for myeloperoxidase on the surface of human low density lipoproteins. *Chemistry and physics of lipids*. 2011; 164(1):49-53.

Song Y, Shryock JC, Belardinelli L. An increase of late sodium current induces delayed afterdepolarizations and sustained triggered activity in atrial myocytes. *American journal of physiology. Heart and circulatory physiology*. 2008; 294(5):H2031-2039.

Song Y, Shryock JC, Wu L, Belardinelli L. Antagonism by ranolazine of the pro-arrhythmic effects of increasing late INa in guinea pig ventricular myocytes. *Journal of cardiovascular pharmacology*. 2004; 44(2):192-199.

Stankovic S, Asanin M, Majkic-Singh N, Ignjatovic S, Mihailovic M, Nikolajevic I, Mrdovic I, Matic D, Savic L, Marinkovic J, Ostojic M, Vasiljevic Z. The usefulness of myeloperoxidase in prediction of in-hospital mortality in patients with ST-segment elevation myocardial infarction treated by primary percutaneous coronary intervention. *Clinical laboratory*. 2012; 58(1-2):125-131.

Steinberg D, Parthasarathy S, Carew TE, Khoo JC, Witztum JL. Beyond cholesterol. Modifications of low-density lipoprotein that increase its atherogenicity. *The New England journal of medicine*. 1989; 320(14):915-924.

Steinberg D, Witztum JL. Is the oxidative modification hypothesis relevant to human atherosclerosis? Do the antioxidant trials conducted to date refute the hypothesis? *Circulation*. 2002; 105(17):2107-2111.

Strack S, Barban MA, Wadzinski BE, Colbran RJ. Differential inactivation of postsynaptic density-associated and soluble Ca2+/calmodulin-dependent protein kinase II by protein phosphatases 1 and 2A. *Journal of neurochemistry*. 1997; 68(5):2119-2128.

Sugamura K, Keaney JF, Jr. Reactive oxygen species in cardiovascular disease. *Free radical biology & medicine*. 2011; 51(5):978-992.

Sun W, Liu D, Gong P, Shi X, Wang Y, Wang P, Gong W. Predicting cardiovascular mortality in chronic kidney disease (CKD) patients. *Annals of transplantation : quarterly of the Polish Transplantation Society*. 2014; 19:513-518.

Swaminathan PD, Purohit A, Soni S, Voigt N, Singh MV, Glukhov AV, Gao Z, He BJ, Luczak ED, Joiner ML, Kutschke W, Yang J, Donahue JK, Weiss RM, Grumbach IM, Ogawa M, Chen PS, Efimov I, Dobrev D, Mohler PJ, Hund TJ, Anderson ME. Oxidized CaMKII causes cardiac sinus node dysfunction in mice. *The Journal of clinical investigation*. 2011; 121(8):3277-3288.

Tang WH, Shrestha K, Troughton RW, Borowski AG, Klein AL. Integrating plasma high-sensitivity C-reactive protein and myeloperoxidase for risk prediction in chronic systolic heart failure. *Congestive heart failure*. 2011; 17(3):105-109.

Tavori H, Giunzioni I, Fazio S. PCSK9 inhibition to reduce cardiovascular disease risk: recent findings from the biology of PCSK9. *Current opinion in endocrinology, diabetes, and obesity*. 2015; 22(2):126-132.

Tay A, Tamam Y, Yokus B, Ustundag M, Orak M. Serum myeloperoxidase levels in predicting the severity of stroke and mortality in acute ischemic stroke patients. *European review for medical and pharmacological sciences*. 2015; 19(11):1983-1988.

Vasilyev N, Williams T, Brennan ML, Unzek S, Zhou X, Heinecke JW, Spitz DR, Topol EJ, Hazen SL, Penn MS. Myeloperoxidase-generated oxidants modulate left ventricular remodeling but not infarct size after myocardial infarction. *Circulation*. 2005; 112(18):2812-2820.

Verkerk AO, Wilders R, van Borren MM, Peters RJ, Broekhuis E, Lam K, Coronel R, de Bakker JM, Tan HL. Pacemaker current (I(f)) in the human sinoatrial node. *European heart journal*. 2007; 28(20):2472-2478.

Wagner S, Dybkova N, Rasenack EC, Jacobshagen C, Fabritz L, Kirchhof P, Maier SK, Zhang T, Hasenfuss G, Brown JH, Bers DM, Maier LS.

Ca2+/calmodulin-dependent protein kinase II regulates cardiac Na+ channels. *The Journal of clinical investigation*. 2006; 116(12):3127-3138.

Wagner S, Hacker E, Grandi E, Weber SL, Dybkova N, Sossalla S, Sowa T, Fabritz L, Kirchhof P, Bers DM, Maier LS. Ca/calmodulin kinase II differentially modulates potassium currents. *Circulation. Arrhythmia and electrophysiology*. 2009; 2(3):285-294.

Wagner S, Ruff HM, Weber SL, Bellmann S, Sowa T, Schulte T, Anderson ME, Grandi E, Bers DM, Backs J, Belardinelli L, Maier LS. Reactive oxygen species-activated Ca/calmodulin kinase IIdelta is required for late I(Na) augmentation leading to cellular Na and Ca overload. *Circulation research*. 2011; 108(5):555-565.

Wallner M, Kolesnik E, Ablasser K, Khafaga M, Wakula P, Ljubojevic S, Thon-Gutschi EM, Sourij H, Kapl M, Edmunds NJ, Brent Kuzmiski J, Griffith DA, Knez I, Pieske B, von Lewinski D. Exenatide exerts a PKA-dependent positive inotropic effect in human atrial myocardium: GLP-1R mediated effects in human myocardium. *Journal of molecular and cellular cardiology*. 2015;

Werner U, Szelenyi I. Measurement of MPO activity as model for detection of granulocyte infiltration in different tissues. *Agents and actions*. 1992; Spec No:C101-103.

WHO, 2015. WHO.

Williams BA, Dickenson DR, Beatch GN. Kinetics of rate-dependent shortening of action potential duration in guinea-pig ventricle; effects of IK1 and IKr blockade. *British journal of pharmacology*. 1999; 126(6):1426-1436.

Wood D, Joint European Societies Task F. Established and emerging cardiovascular risk factors. *American heart journal*. 2001; 141(2 Suppl):S49-57.

Xie LH, Chen F, Karagueuzian HS, Weiss JN. Oxidative-stress-induced afterdepolarizations and calmodulin kinase II signaling. *Circulation research*. 2009; 104(1):79-86.

Xu L, Lai D, Cheng J, Lim HJ, Keskanokwong T, Backs J, Olson EN, Wang Y. Alterations of L-type calcium current and cardiac function in CaMKII{delta} knockout mice. *Circulation research*. 2010; 107(3):398-407.

Yach D, Hawkes C, Gould CL, Hofman KJ. The global burden of chronic diseases: overcoming impediments to prevention and control. *Jama*. 2004; 291(21):2616-2622.

Yatsuya H, Li Y, Hilawe EH, Ota A, Wang C, Chiang C, Zhang Y, Uemura M, Osako A, Ozaki Y, Aoyama A. Global trend in overweight and obesity and its association with cardiovascular disease incidence. *Circulation journal : official journal of the Japanese Circulation Society*. 2014; 78(12):2807-2818.

Zhang QQ, Lu LG. Nonalcoholic Fatty Liver Disease: Dyslipidemia, Risk for Cardiovascular Complications, and Treatment Strategy. *Journal of clinical and translational hepatology*. 2015; 3(1):78-84.

Zorn-Pauly K, Schaffer P, Pelzmann B, Bernhart E, Lang P, Koidl B. L-type and T-type Ca2+ current in cultured ventricular guinea pig myocytes. *Physiological research / Academia Scientiarum Bohemoslovaca*. 2004; 53(4):369-377.

Zorn-Pauly K, Schaffer P, Pelzmann B, Bernhart E, Wei G, Lang P, Ledinski G, Greilberger J, Koidl B, Jurgens G. Oxidized LDL induces ventricular myocyte damage and abnormal electrical activity--role of lipid hydroperoxides. *Cardiovascular research*. 2005; 66(1):74-83.

6. Supplement

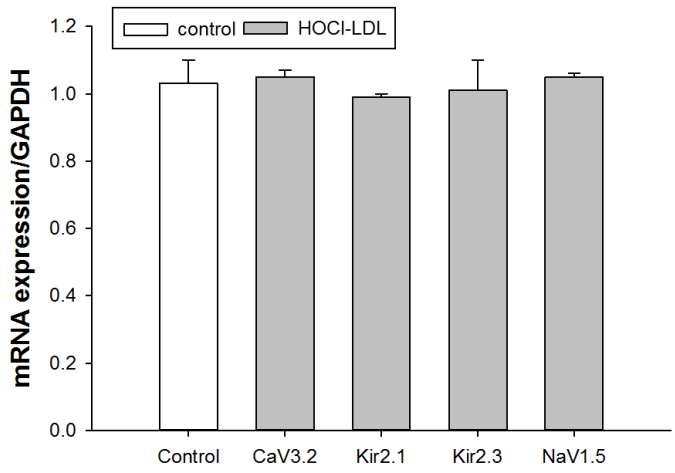

Supplement Figure I. Impact of HOCl-LDL on the ion channel expression

Expression pattern of the indicated ion channels in HL-1 cells in response to HOCl-LDL (200:1, 250 µg/ml, 12 h) treatment is shown. Cells were lysed, RNA was isolated and qPCR was performed to follow mRNA expression levels of the indicated ion channels. Values are expressed as mean±SEM (n=6).

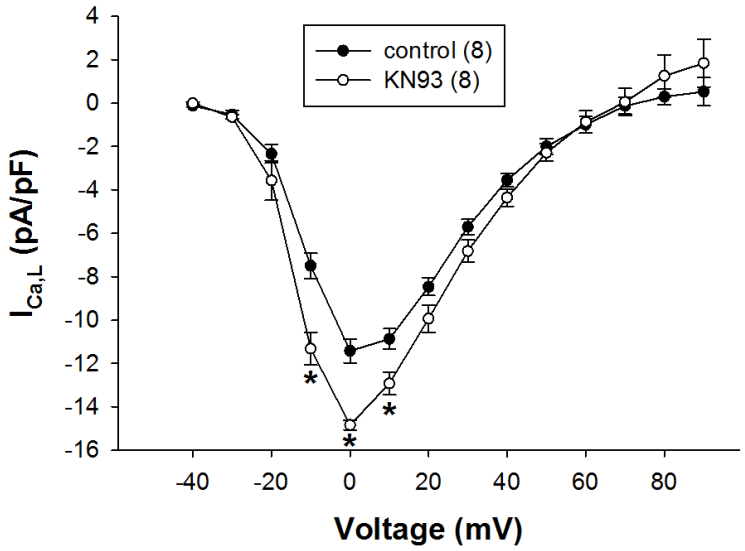

Supplement Figure II. KN93 increases L-type Ca^{2+} current ($I_{Ca,L}$) density

GPV cells were treated (12-16 h) with KN93 (5 μM) to follow $I_{Ca,L}$ density. Cardiomyocytes were patched using Cs-T and Cs-pip solutions. After inactivation of I_{Na} achieved by a prestep from -80 to -40 mV (50 ms), $I_{Ca,L}$ was elicited by voltage steps from -40 to +90 mV (10 mV increments, 400 ms). Values are expressed as mean±SEM; (n) represents number of cells. *p≤0.05 vs. control.

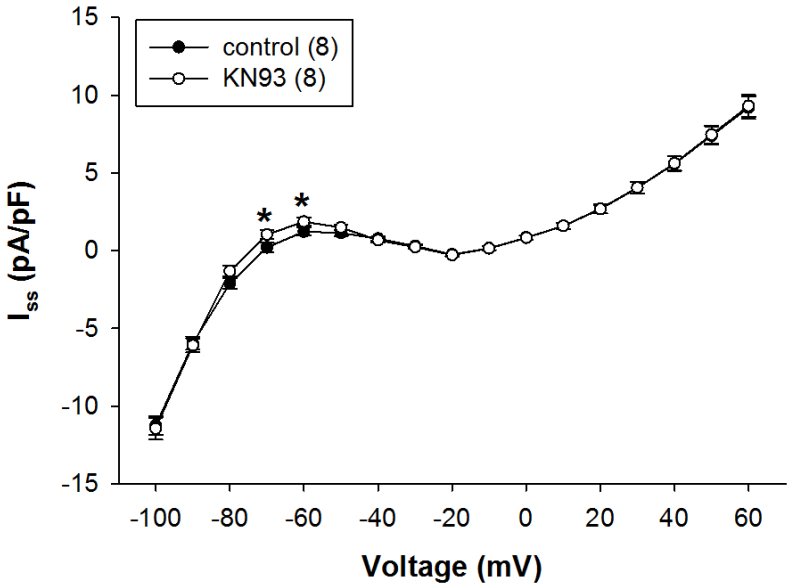

Supplement Figure III. Steady-state current (I_{ss})-voltage relationship in response to KN93

GPV cardiomyocytes were treated (12-16 h) with KN93 (5 μM). Cardiomyocytes were patched using NT and N-pip solutions. I_{ss} was elicited by voltage ramps (-100 to +60 mV, duration 20 s). Values are expressed as mean±SEM (each ramp current was discretized at 10 mV intervals by averaging 3 adjacent data points); (n) represents number of cells. *p≤0.05 vs. control.

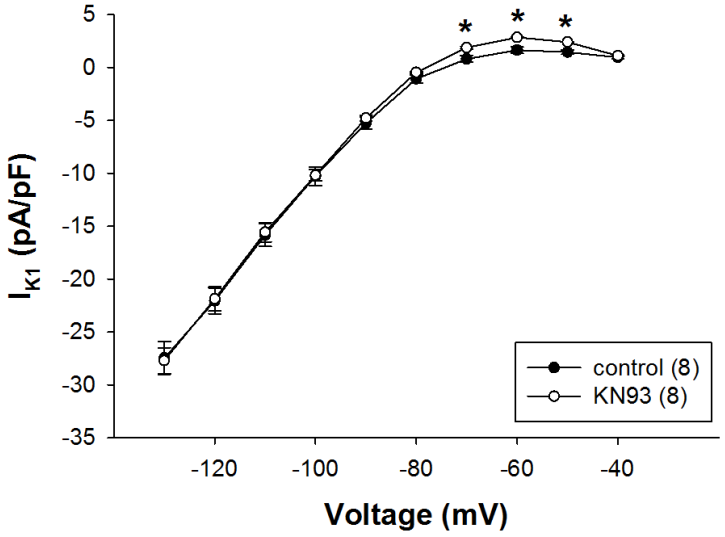

Supplement Figure IV. KN93 increased inward-rectifier potassium current (I_{K1})

Cells were treated (12-16 h) with KN93 (5 μM) and patched using N-pip and NT solutions (with and without 0.5 mM $BaCl_2$). I_{K1} was measured as the Ba^{2+}-sensitive current (obtained by digital subtraction) elicited by hyperpolarizing voltage steps (3 s) from -40 mV to -130 mV (10 mV increments, holding potential -40 mV). Values are expressed as mean±SEM; (n) represents number of cells. *p≤0.05 vs. control.

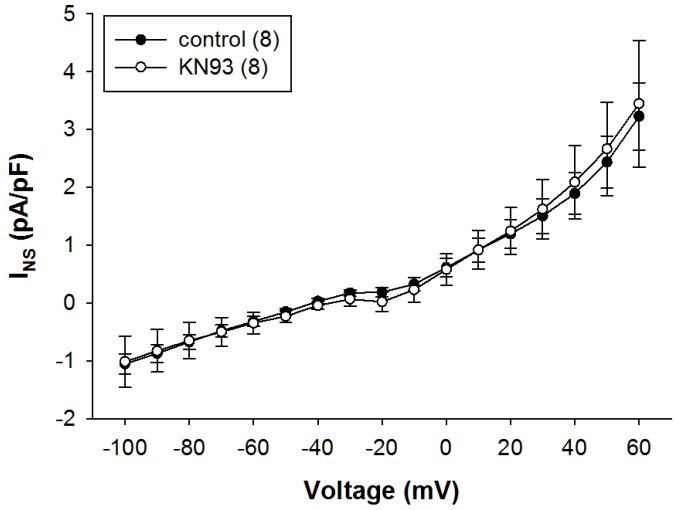

Supplement Figure V. Non-selective cation current (I_{NS}) in response to KN93
GPV cardiomyocytes were treated (12-16 h) KN93 (5 μM) and patched using Cs-pip and $CdCl_2$ (200 μM)-containing CsT solutions. I_{NS} was elicited by voltage ramps (-100 to +60 mV, duration 20 s). Values are expressed as mean±SEM (each ramp current was discretized at 10-mV intervals by averaging 3 adjacent data points); (n) represents number of patched cells.

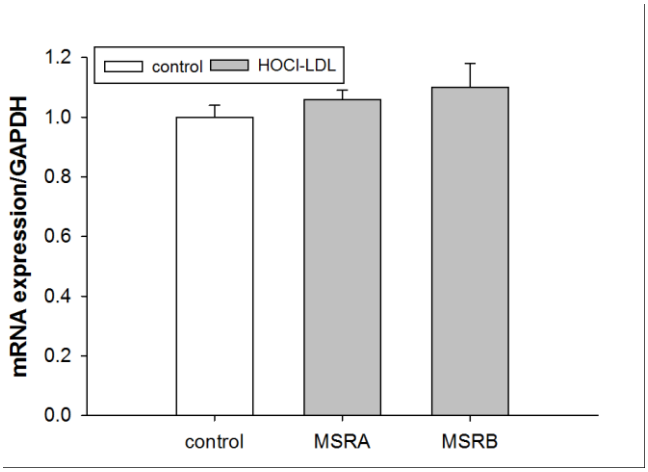

Supplement Figure VI. Impact of HOCl-LDL on the MSRA and MSRB expression

Expression pattern of the indicated enzymes in HL-1 cells in response to HOCl-LDL (200:1, 250 µg/ml, 12 h) treatment is shown. Cells were lysed, RNA was isolated and qPCR was performed to follow mRNA expression levels of the indicated ion channels. Values are expressed as mean±SEM (n=6).

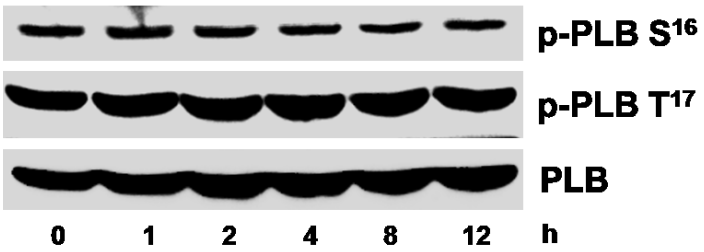

Supplement Figure VII. Effect of HOCl-LDL on phosphorylation of phospholamban

HL-1 cells were incubated with HOCl-LDL (200:1, 250 μg/ml) for indicated time periods to follow (**A**) pCaMKII (phospho-CaMKII) and (**B**) oxCaMKII (oxidized-CaMKII) expression using Western blot analysis. CaMKII was used as a loading control. One representative blot out of three is shown.

7. Articles published during PhD

7.1 List of publication

2015

- Jain P., Hassan A.M., **Koyani C.N.**, Mayerhofer R., Reichmann F., Farzi A., Schuligoi R., Malle E., Holzer P., 2015. Behavioral and molecular processing of visceral pain in the brain of mice: impact of colitis and psychological stress. Frontiers in behavioral neuroscience 9, 177. DOI: 10.3389/fnbeh.2015.00177.

- Alfakry H., Malle E., **Koyani C.N.**, Pussinen P.J., Sorsa T., 2015. Neutrophil proteolytic activation cascades: a possible mechanistic link between chronic periodontitis and coronary heart disease. Innate Immunity (accepted). DOI: 10.1177/1753425915617521.

- **Koyani C.N.**, Flemmig J., Malle E., Arnhold J., 2015. Myeloperoxidase scavenges peroxynitrite: A novel anti-inflammatory action of the heme enzyme. Archives of biochemistry and biophysics 571, 1-9. DOI: 10.1016/j.abb.2015.02.028.

2014

- Rossmann C., Hammer A., **Koyani C.N.**, Kovacevic A., Siwetz M., Desoye G., Poehlmann T.G., Markert U.R., Huppertz B., Sattler W., Malle E., 2014. Expression of serum amyloid A4 in human trophoblast-like choriocarcinoma cell lines and human first trimester/term trophoblast cells. Placenta 35, 661-664. DOI: 10.1016/j.placenta.2014.05.012.

- Scheruebel S., **Koyani C.N.**, Hallstrom S., Lang P., Platzer D., Machler H., Lohner K., Malle E., Zorn-Pauly K., Pelzmann B., 2014. I(f) blocking potency of ivabradine is preserved under elevated endotoxin levels in human atrial myocytes. Journal of molecular and cellular cardiology 72, 64-73. DOI: 10.1016/j.yjmcc.2014.02.010.

- Delporte C., Boudjeltia K.Z., Noyon C., Furtmuller P.G., Nuyens V., Slomianny M.C., Madhoun P., Desmet J.M., Raynal P., Dufour D., **Koyani C.N.**, Reye F., Rousseau A., Vanhaeverbeek M., Ducobu J., Michalski J.C., Neve J., Vanhamme L., Obinger C., Malle E., Van Antwerpen P., 2014. Impact of myeloperoxidase-LDL interactions on enzyme activity and subsequent posttranslational oxidative modifications of apoB-100. Journal of lipid research 55, 747-757. DOI: 10.1194/jlr.M047449.

- **Koyani C.N.**, Windischhofer W., Rossmann C., Jin G., Kickmaier S., Heinzel F.R., Groschner K., Alavian-Ghavanini A., Sattler W., Malle E., 2014b. 15-deoxy-Delta(1)(2),(1)(4)-PGJ(2) promotes inflammation and apoptosis in cardiomyocytes via the DP2/MAPK/TNFalpha axis. International journal of cardiology 173, 472-480. DOI: 10.1016/j.ijcard.2014.03.086.

- **Koyani C.N.**, Windischhofer W., Rossmann C., Heinzel F.R., Sattler W., Malle E., 2014. Response to letter by Tsikas et al. International journal of cardiology 177, 140-141. DOI: 10.1016/j.ijcard.2014.09.111.

- Bernkopf M., Webersinke G., Tongsook C., **Koyani C.N.**, Rafiq M.A., Ayaz M., Muller D., Enzinger C., Aslam M., Naeem F., Schmidt K., Gruber K., Speicher M.R., Malle E., Macheroux P., Ayub M., Vincent J.B., Windpassinger C., Duba H.C., 2014. Disruption of the methyltransferase-like 23 gene METTL23 causes mild autosomal recessive intellectual disability. Human molecular genetics 23, 4015-4023. DOI: 10.1093/hmg/ddu115.

7.2 Title page of all publications

frontiers in Behavioral Neuroscience

ORIGINAL RESEARCH
published: 10 July 2015
doi: 10.3389/fnbeh.2015.00177

Behavioral and molecular processing of visceral pain in the brain of mice: impact of colitis and psychological stress

Piyush Jain[1], *Ahmed M. Hassan*[1], *Chintan N. Koyani*[2], *Raphaela Mayerhofer*[1], *Florian Reichmann*[1], *Aitak Farzi*[1], *Rufina Schuligoi*[1], *Ernst Malle*[2] *and Peter Holzer*[1]*

[1] *Research Unit of Translational Neurogastroenterology, Institute of Experimental and Clinical Pharmacology, Medical University of Graz, Graz, Austria,* [2] *Institute of Molecular Biology and Biochemistry, Medical University of Graz, Graz, Austria*

OPEN ACCESS

Edited by:
James P. Herman,
University of Cincinnati, USA

Reviewed by:
Avishek Adhikari,
Columbia University, USA
Muriel Larauche,
University of California, Los Angeles, USA

***Correspondence:**
Peter Holzer,
Research Unit of Translational Neurogastroenterology, Institute of Experimental and Clinical Pharmacology, Medical University of Graz, Universitätsplatz 4, Graz A-8010, Austria
peter.holzer@medunigraz.at

Received: *05 March 2015*
Accepted: *22 June 2015*
Published: *10 July 2015*

Citation:
Jain P, Hassan AM, Koyani CN, Mayerhofer R, Reichmann F, Farzi A, Schuligoi R, Malle E and Holzer P (2015) Behavioral and molecular processing of visceral pain in the brain of mice: impact of colitis and psychological stress. Front. Behav. Neurosci. 9:177. doi: 10.3389/fnbeh.2015.00177

Gastrointestinal disorders with abdominal pain are associated with central sensitization and psychopathologies that are often exacerbated by stress. Here we investigated the impact of colitis induced by dextran sulfate sodium (DSS) and repeated water avoidance stress (WAS) on spontaneous and nociception-related behavior and molecular signaling in the mouse brain. DSS increased the mechanical pain sensitivity of the abdominal skin while both WAS and DSS enhanced the mechanical and thermal pain sensitivity of the plantar skin. These manifestations of central sensitization were associated with augmented c-Fos expression in spinal cord, thalamus, hypothalamus, amygdala and prefrontal cortex. While WAS stimulated phosphorylation of mitogen-activated protein kinase (MAPK) p42/44, DSS activated another signaling pathway, both of which converged on c-Fos. The DSS- and WAS-induced hyperalgesia in the abdominal and plantar skin and c-Fos expression in the brain disappeared when the mice were subjected to WAS+DSS treatment. Intrarectal allyl isothiocyanate (AITC) evoked aversive behavior (freezing, reduction of locomotion and exploration) in association with p42/44 MAPK and c-Fos activation in spinal cord and brain. These effects were inhibited by morphine, which attests to their relationship with nociception. DSS and WAS exerted opposite effects on AITC-evoked p42/44 MAPK and c-Fos activation, which indicates that these transduction pathways subserve different aspects of visceral pain processing in the brain. In summary, behavioral perturbations caused by colitis and psychological stress are associated with distinct alterations in cerebral signaling. These findings provide novel perspectives on central sensitization and the sensory and emotional processing of visceral pain stimuli in the brain.

Keywords: cellular signaling, central nervous system, cerebral pain processing, colonic inflammation, emotional pain responses, intestinal nociception, psychological stress, somatic hypersensitivity

Review

Innate Immunity

Innate Immunity
0(0) 1–15

DOI: 10.1177/1753425915617521
ini.sagepub.com

SAGE

Neutrophil proteolytic activation cascades: a possible mechanistic link between chronic periodontitis and coronary heart disease

Hatem Alfakry[1], Ernst Malle[2], Chintan N Koyani[2], Pirkko J Pussinen[1] and Timo Sorsa[1,3]

Abstract

Cardiovascular diseases are chronic inflammatory diseases that affect a large segment of society. Coronary heart disease (CHD), the most common cardiovascular disease, progresses over several years and affects millions of people worldwide. Chronic infections may contribute to the systemic inflammation and enhance the risk for CHD. Periodontitis is one of the most common chronic infections that affects up to 50% of the adult population. Under inflammatory conditions the activation of endogenous degradation pathways mediated by immune responses leads to the release of destructive cellular molecules from both resident and immigrant cells. Matrix metalloproteinases (MMPs) and their regulators can activate each other and play an important role in immune response via degrading extracellular matrix components and modulating cytokines and chemokines. The action of MMPs is required for immigrant cell recruitment at the site of inflammation. Stimulated neutrophils represent the major pathogen-fighting immune cells that upregulate expression of several proteinases and oxidative enzymes, which can degrade extracellular matrix components (e.g. MMP-8, MMP-9 and neutrophil elastase). The activity of MMPs is regulated by endogenous inhibitors and/or candidate MMPs (e.g. MMP-7). The balance between MMPs and their inhibitors is thought to mirror the proteolytic burden. Thus, neutrophil-derived biomarkers, including myeloperoxidase, may activate proteolytic destructive cascades that are involved in subsequent immune-pathological events associated with both periodontitis and CHD. Here, we review the existing studies on the contribution of MMPs and their regulators to the infection-related pathology. Also, we discuss the possible proteolytic involvement and role of neutrophil-derived enzymes as an etiological link between chronic periodontitis and CHD.

Keywords

Aggregatibacter actinomycetemcomitans, cardiovascular disease, coronary artery disease, gingival crevicular fluids, hypochlorous acid, lipopolysaccharide, matrix metalloproteinases, myeloperoxidase, neutrophils, oral infections, periodontal diseases, *Porphyromonas gingivalis*, tissue inhibitor of matrix metalloproteinases

Date received: 23 April 2015; revised: 14 June 2015; 30 September 2015; accepted: 13 October 2015

Introduction

Chronic periodontitis

Chronic periodontitis (CP), the most prevalent form of periodontitis, is defined as an inflammatory disease of the tooth-supporting structures. CP is caused by a complex interplay between host defense and biofilm dysbiosis indicated by growth of specific pathogens or complexes of pathogens colonizing the subgingival area. To challenge the microbial biofilm and its virulence factors (LPS, enzymes and toxins), an immune-inflammatory response develops. Resident tissue cells induce and

[1]Department of Oral and Maxillofacial Diseases, University of Helsinki and Helsinki University Hospital, Helsinki, Finland
[2]Institute of Molecular Biology and Biochemistry, Medical University of Graz, Graz, Austria
[3]Division of Periodontology, Department of Dental Medicine, Karolinska Institutet, Huddinge, Sweden

Corresponding author:
Pirkko J Pussinen, Oral and Maxillofacial Diseases, University of Helsinki, P.O. Box 63, Haartmaninkatu 8, FI-00014 Helsinki, Finland.
Email: pirkko.pussinen@helsinki.fi

Archives of Biochemistry and Biophysics 571 (2015) 1–9

Contents lists available at ScienceDirect

Archives of Biochemistry and Biophysics

journal homepage: www.elsevier.com/locate/yabbi

Myeloperoxidase scavenges peroxynitrite: A novel anti-inflammatory action of the heme enzyme

Chintan N. Koyani [a], Joerg Flemmig [b,c], Ernst Malle [a], Juergen Arnhold [b,c,*]

[a] Institute of Molecular Biology and Biochemistry, Medical University of Graz, Harrachgasse 21, 8010 Graz, Austria
[b] Translational Centre for Regenerative Medicine Leipzig, University of Leipzig, Philipp-Rosenthal-Straße 55, 04103 Leipzig, Germany
[c] Institute for Medical Physics and Biophysics, Medical Faculty, University of Leipzig, Haertelstraße 16-18, 04107 Leipzig, Germany

ARTICLE INFO

Article history:
Received 9 December 2014
and in revised form 20 February 2015
Available online 27 February 2015

Keywords:
APF
Flavonoids
Hypochlorite
MPO–H_2O_2–Cl^- system
Nitric oxide
Superoxide

ABSTRACT

Peroxynitrite, a potent pro-inflammatory and cytotoxic species, interacts with a variety of heme containing proteins. We addressed the question whether (i) the interaction of myeloperoxidase (MPO, an enzyme generating hypochlorous acid from hydrogen peroxide and chloride ions) with peroxynitrite affects the clearance of peroxynitrite, and (ii) if peroxynitrite could modulate the chlorinating activity of MPO. Our results show that this interaction promotes the decomposition of the highly reactive pro-inflammatory oxidant, whereby MPO Compound II (but not Compound I) is formed. The efficiency of MPO to remove peroxynitrite was enhanced by L-tyrosine, nitrite and (−)-epicatechin, substances known to reduce Compound II with high reaction rate. Next, peroxynitrite (added as reagent) diminished the chlorinating activity of MPO in the presence of hydrogen peroxide. Alternatively, SIN-1, a peroxynitrite donor, reduced hypochlorous acid formation by MPO, as measured by aminophenyl fluorescein oxidation (time kinetics) and taurine chloramine formation (end point measurement). At inflammatory loci, scavenging of peroxynitrite by MPO may overcome the uncontrolled peroxynitrite decomposition and formation of reactive species, which lead to cell/tissue damage.

Introduction

Peroxynitrite, a reactive oxidant with a short half-life (approx. 10–20 ms at physiological pH [1,2]), is generated by the diffusion-controlled reaction of nitric oxide (·NO) and superoxide anion ($O_2^{\cdot-}$) with a rate constant of 1×10^{10} M^{-1} s^{-1} at pH 7.0 [3,4]. ·NO is a relatively stable radical, while $O_2^{\cdot-}$ has much shorter half-life and undergoes spontaneous dismutation with a second-order rate constant of 2×10^5 M^{-1} s^{-1} at pH 7.4 [5].

Peroxynitrite is a potent pro-inflammatory and cytotoxic molecule [6–8], which exerts a variety of inflammatory effects such as inhibition of antioxidants [9] and ion channels [10,11], lipid peroxidation [12,13], thiol oxidation and tyrosine nitration of proteins [14] as well as modulation of cyclooxygenase activity [15,16]. Under inflammatory conditions, the excessive production of ·NO and $O_2^{\cdot-}$ favors elevated levels of peroxynitrite that trigger dysregulation of cellular signaling pathways, activation of inflammatory stress and cell/organ injury in further consequence [17–19]. Peroxynitrite interacts with a variety of redox-active heme proteins including hemoglobin [20], myoglobin [20], catalase [21,22], lactoperoxidase [23], cytochrome P450 [24], nitric oxide synthase [25], cyclooxygenase-2 [26], and myeloperoxidase (MPO)[1] [27,28], respectively.

In activated neutrophils, dimeric MPO contributes to the inactivation and killing of phagocytosed microorganisms [29,30]. Under inflammatory conditions, cationic MPO protein becomes attached to negatively charged proteins and membrane epitopes [30–33]. Most importantly, in the presence of hydrogen peroxide (H_2O_2), MPO catalyzes the oxidation of small molecules including tyrosine, tryptophan, nitrite, ·NO, sulfhydryls, phenol and indole derivatives, xenobiotics and others [34–39]. As reported for the other peroxidases, the heme moiety of MPO undergoes characteristic conversions from the ferric state to the oxo-ferryl states: Compound I (which has an additional porphyryl radical function) and Compound II [40]. A unique property of MPO is its ability to oxidize chloride ions (Cl^-) by the abstraction of two electrons to form hypochlorous acid (HOCl); during this reaction Compound I is reduced to the ferric state [41,42].

* Corresponding author at: Institute for Medical Physics and Biophysics, Medical Faculty, University of Leipzig, Haertelstraße 16-18, 04107 Leipzig, Germany. Fax: +49 341 9715709.
E-mail address: juergen.arnhold@medizin.uni-leipzig.de (J. Arnhold).

[1] *Abbreviations used:* MPO, myeloperoxidase; H_2O_2, hydrogen peroxide; Cl^-, chloride ions; HOCl, hypochlorous acid; APF, aminophenyl fluorescein; KCN, potassium cyanide; PBS, phosphate buffered saline.

http://dx.doi.org/10.1016/j.abb.2015.02.028
0003-9861/

Placenta 35 (2014) 661–664

Contents lists available at ScienceDirect

Placenta

journal homepage: www.elsevier.com/locate/placenta

Short communication

Expression of serum amyloid A4 in human trophoblast-like choriocarcinoma cell lines and human first trimester/term trophoblast cells

C. Rossmann [a], A. Hammer [b], C.N. Koyani [a], A. Kovacevic [a], M. Siwetz [b], G. Desoye [c], T.G. Poehlmann [d], U.R. Markert [d], B. Huppertz [b], W. Sattler [a], E. Malle [a, *]

[a] Medical University of Graz, Institute of Molecular Biology and Biochemistry, Graz A-8010, Austria
[b] Medical University of Graz, Institute of Cell Biology, Histology and Embryology, Graz, Austria
[c] Medical University of Graz, Department of Obstetrics and Gynecology, Graz, Austria
[d] Placenta-Laboratory, Department of Obstetrics, University Hospital Jena, Jena, Germany

ARTICLE INFO

Article history:
Accepted 29 May 2014

Keywords:
SAA4
Placenta
Invasion
Cytokine
Outgrowing extravillous trophoblast

ABSTRACT

Trophoblast invasion into uterine tissues represents a hallmark of first trimester placental development. As expression of serum amyloid A4 (SAA4) occurs in tumorigenic and invasive tissues we here investigated whether SAA4 is present in trophoblast-like human AC1-M59/Jeg-3 cells and trophoblast preparations of human first trimester and term placenta. SAA4 mRNA was expressed in non-stimulated and cytokine-treated AC1-M59/Jeg-3 cells. In purified trophoblast cells SAA4 mRNA expression was upregulated at weeks 10 and 12 of pregnancy. Western-blot and immunohistochemical staining of first trimester placental tissue revealed pronounced SAA4 expression in invasive trophoblast cells indicating a potential role of SAA4 during invasion.

1. Introduction

The serum amyloid A (SAA) family comprises lipoprotein-associated proteins, encoded by different genes with a high allelic variation [1,2]. In humans, the non-glycosylated SAA1/2 proteins, highly induced during the acute-phase response [3], are considered as important clinical markers of inflammation [4]. While human *SAA3* is a pseudogene, *SAA4* codes for glycosylated SAA4 protein that represents the predominant SAA isoform under physiological conditions. Although the liver is the major source for SAA4 assumed to be constitutively expressed [5–7], some studies reported abundant expression specifically in tumorigenic tissues [8–11].

Acute-phase SAA1/2 is expressed in human placenta, trophoblast cells and choriocarcinoma cell lines [12–14]. Therefore, the present study aimed at identifying SAA4 in (i) human Jeg-3 choriocarcinoma and AC1-M59 cells (hybrid of term trophoblast cells and AC-1 cells derived from Jeg-3), (ii) trophoblast cells of human first trimester and term placenta and (iii) outgrowing human first trimester extravillous trophoblast (EVT) cells.

2. Materials and methods

2.1. Cell culture experiments

Placental tissues were obtained from born placentas of healthy pregnancies and from clinically normal human pregnancies, which were interrupted for psychosocial reasons (approved by the Ethical Committee at the Medical University of Graz [23-203 ex 10/11] and the Friedrich-Schiller-University Jena [1503-03/05]). Mononucleated human first trimester and term trophoblast cells were isolated as described [15,16]. Outgrowing EVT cells were isolated from placental villi after terminations of pregnancy (7–10 weeks, $n = 5$) and were incubated in Petri dishes for two days at 5% CO_2 in DMEM/Ham's F12 with 10% (v/v) human serum. Then the villi were transferred into collagen-coated 24-well plates (two explants/well) and incubated at 2.5% O_2, 5% CO_2. After three days of culture the villi were removed from the plates and the already outgrown cells were cultured for another day at 5% CO_2. Human hepatocellular carcinoma (HUH-7) cells, human Jeg-3 and human AC1-M59 cells were cultured as described [12,17,18]. AC1-M59 and Jeg-3 cells were seeded into cell culture dishes and upon reaching 80% confluence, incubated for 24 h in medium containing 10 ng/ml IL-1α, IL-1β, IL-6, or TNFα (R&D Systems, Minneapolis, MN, USA).

2.2. RNA isolation, RT-PCR and real-time RT-PCR (qPCR) analysis

RNA was isolated from (i) AC1-M59, Jeg-3, EVT, HUH-7 (using RNeasy Mini Kit from QIAGEN, Hilden, Germany) and (ii) first trimester (week 6–12) and term trophoblast cells (week 35 and 40) using Trizol-reagent (Sigma–Aldrich, Saint-Louis, MO, USA), followed by DNase treatment, reverse transcription and PCR for SAA4 and GAPDH (used as a housekeeping gene, see Supplementary Table I) as described [19]. The qPCR protocol was performed using LightCycler 480 system (Roche Diagnostics, Vienna, Austria) [20]. Gene specific primers used for SAA4 and HPRT (used as a

* Corresponding author. Tel.: +43 316 380 4208; fax: +43 316 380 9615.
E-mail address: ernst.malle@medunigraz.at (E. Malle).

http://dx.doi.org/10.1016/j.placenta.2014.05.012

Journal of Molecular and Cellular Cardiology 72 (2014) 64–73

Contents lists available at ScienceDirect

Journal of Molecular and Cellular Cardiology

journal homepage: www.elsevier.com/locate/yjmcc

Original article

I_f blocking potency of ivabradine is preserved under elevated endotoxin levels in human atrial myocytes

Susanne Scheruebel [a], Chintan N. Koyani [b], Seth Hallström [c], Petra Lang [a], Dieter Platzer [a], Heinrich Mächler [d], Karl Lohner [e], Ernst Malle [b], Klaus Zorn-Pauly [a,*], Brigitte Pelzmann [a,*]

[a] Institute of Biophysics, Medical University of Graz, Harrachgasse 21, A-8010 Graz, Austria
[b] Institute of Molecular Biology and Biochemistry, Medical University of Graz, Harrachgasse 21, A-8010 Graz, Austria
[c] Institute of Physiological Chemistry, Medical University of Graz, Harrachgasse 21, A-8010 Graz, Austria
[d] Division of Cardiac Surgery, Medical University of Graz, Auenbruggerplatz, A-8010 Graz, Austria
[e] Institute of Molecular Biosciences, Biophysics Division, University of Graz, Schmiedlstrasse 6, A-8042 Graz, Austria

ARTICLE INFO

Article history:
Received 12 December 2013
Received in revised form 23 January 2014
Accepted 14 February 2014
Available online 25 February 2014

Keywords:
Human pacemaker current
HCN channel
Ivabradine
Lipopolysaccharide
Patch clamp
Sinoatrial cell model

ABSTRACT

Lower heart rate is associated with better survival in patients with multiple organ dysfunction syndrome (MODS), a disease mostly caused by sepsis. The benefits of heart rate reduction by ivabradine during MODS are currently being investigated in the MODI_fY clinical trial. Ivabradine is a selective inhibitor of the pacemaker current I_f and since I_f is impaired by lipopolysaccharide (LPS, endotoxin), a trigger of sepsis, we aimed to explore I_f blocking potency of ivabradine under elevated endotoxin levels in human atrial cardiomyocytes. Treatment of myocytes with S-LPS (containing the lipid A moiety, a core oligosaccharide and an O-polysaccharide chain) but not R595 (an O-chain lacking LPS-form) caused I_f inhibition under acute and chronic septic conditions. The specific interaction of S-LPS but not R595 to pacemaker channels HCN2 and HCN4 proves the necessity of O-chain for S-LPS–HCN interaction. The efficacy of ivabradine to block I_f was reduced under septic conditions, an observation that correlated with lower intracellular ivabradine concentrations in S-LPS- but not R595-treated cardiomyocytes. Computational analysis using a sinoatrial pacemaker cell model revealed that despite a reduction of I_f under septic conditions, ivabradine further decelerated pacemaking activity. This novel finding, i.e. I_f inhibition by ivabradine under elevated endotoxin levels in vitro, may provide a molecular understanding for the efficacy of this drug on heart rate reduction under septic conditions in vivo, e.g. the MODI_fY clinical trial.

1. Introduction

Sepsis, a microbial induced inflammatory response, encompasses a spectrum of illness that ranges from systemic infection to multiple organ dysfunction syndrome (MODS) [1]. Mortality due to septic cardiac dysfunction has been encountered in critically ill patients [2] where an increased heart rate may act as an independent risk factor [3]. Patients with lower heart rate in the early phase of MODS have better survival rates than those with higher heart rate [3].

Sepsis is induced by lipopolysaccharide (LPS, endotoxin), a major component of the outer cell wall of gram-negative bacteria. Notably, LPS from wild type bacteria usually is a mix of S-form LPS and varying proportions of so-called R-form LPS [4]. S-form LPS consists of three entities: the lipid A moiety, that harbours the endotoxic activity of the entire molecule, the core oligosaccharide and the O-polysaccharide chain, that is absent in R-form LPS [5,6]. Irrespective of their structural components, both LPS forms are capable to initiate sepsis by triggering the inflammatory response [7]. Besides initiating the inflammatory response, S-form LPS directly affects ionic channels of immune, neuronal and cardiovascular cells [8–10], the latter include channels conducting the pacemaker current I_f. This current is a mixed Na^+/K^+ inward current carried by pacemaker channels comprising four different homo- or heteromeric isoforms of hyperpolarization-activated cyclic nucleotide-gated (HCN 1–4) channels [11]. I_f plays an important role in the regulation of heart rate [12] by contributing to the slow diastolic depolarization phase that determines the firing rate of spontaneous action potentials of sinoatrial node cells [13]. Moreover, in response to autonomic transmitters, I_f contributes to the chronotropic regulation of heart rate [13]. Previously, we reported I_f loss-of-function in human atrial myocytes after chronic S-LPS treatment, an observation that in turn might be responsible for reduction of heart rate variability during sepsis [14,15]. Meanwhile it was shown that S-form LPS also acutely impairs I_f [16,17] and that the polysaccharide part (O-chain) of the LPS molecule [16] is necessary for reduction of pacemaker channel activity.

Beta-blocker administration has been shown to reduce mortality in MODS [18,19]. However, negative inotropic effects of beta-blockers

* Corresponding authors. Tel.: +43 316 380 4145; fax: +43 316 380 9660.
E-mail addresses: klaus.zornpauly@medunigraz.at (K. Zorn-Pauly), brigitte.pelzmann@medunigraz.at (B. Pelzmann).

http://dx.doi.org/10.1016/j.yjmcc.2014.02.010
0022-2828

JOURNAL OF LIPID RESEARCH ASBMB

Impact of myeloperoxidase-LDL interactions on enzyme activity and subsequent posttranslational oxidative modifications of apoB-100

Cédric Delporte,[1,*,†] Karim Zouaoui Boudjeltia,[§] Caroline Noyon,[*] Paul G. Furtmüller,[**] Vincent Nuyens,[§] Marie-Christine Slomianny,[††] Philippe Madhoun,[§§] Jean-Marc Desmet,[§§] Pierre Raynal,[***] Damien Dufour,[*] Chintan N. Koyani,[†††] Florence Reyé,[*] Alexandre Rousseau,[§] Michel Vanhaeverbeek,[†] Jean Ducobu,[§] Jean-Claude Michalski,[††] Jean Nève,[*] Luc Vanhamme,[§§§] Christian Obinger,[**] Ernst Malle,[†††] and Pierre Van Antwerpen[*,†]

Laboratory of Pharmaceutical Chemistry[*] and Analytical Platform of the Faculty of Pharmacy,[†] Faculty of Pharmacy, Université Libre de Bruxelles, Brussels, Belgium; Laboratory of Experimental Medicine (ULB 222 Unit)[§] and Unit of Dialysis,[§§]CHU de Charleroi, A. Vésale Hospital, Université Libre de Bruxelles, Montigny-le-Tilleul, Belgium; Department of Chemistry, Division of Biochemistry,[**] Vienna Institute of BioTechnology, BOKU - University of Natural Resources and Life Sciences, Vienna, Austria; Unité Mixte de Recherche CNRS/USTL 8576,[††] Glycobiologie Structurale et Fonctionnelle, Université des Sciences et Technologies de Lille 1, Villeneuve d'Ascq, France; Service de Chirurgie Vasculaire,[***] ISPPC, CHU de Charleroi, Charleroi, Belgium; Medical University of Graz,[†††] Center for Molecular Medicine, Institute of Molecular Biology and Biochemistry, Graz, Austria; and Laboratory of Molecular Parasitology,[§§§] IBMM, Faculty of Sciences, Université Libre de Bruxelles, Gosselies, Belgium

Abstract Oxidation of LDL by the myeloperoxidase (MPO)-H_2O_2-chloride system is a key event in the development of atherosclerosis. The present study aimed at investigating the interaction of MPO with native and modified LDL and at revealing posttranslational modifications on apoB-100 (the unique apolipoprotein of LDL) in vitro and in vivo. Using amperometry, we demonstrate that MPO activity increases up to 90% when it is adsorbed at the surface of LDL. This phenomenon is apparently reflected by local structural changes in MPO observed by circular dichroism. Using MS, we further analyzed in vitro modifications of apoB-100 by hypochlorous acid (HOCl) generated by the MPO-H_2O_2-chloride system or added as a reagent. A total of 97 peptides containing modified residues could be identified. Furthermore, differences were observed between LDL oxidized by reagent HOCl or HOCl generated by the MPO-H_2O_2-chloride system. Finally, LDL was isolated from patients with high cardiovascular risk to confirm that our in vitro findings are also relevant in vivo. We show that several HOCl-mediated modifications of apoB-100 identified in vitro were also present on LDL isolated from patients who have increased levels of plasma MPO and MPO-modified LDL. In conclusion, these data emphasize the specificity of MPO to oxidize LDL.—Delporte, C., K. Z. Boudjeltia, C. Noyon, P. G. Furtmüller, V. Nuyens, M-C. Slomianny, P. Madhoun, J-M. Desmet, P. Raynal, D. Dufour, C. N. Koyani, F. Reyé, A. Rousseau, M. Vanhaeverbeek, J. Ducobu, J-C. Michalski, J. Nève, L. Vanhamme, C. Obinger, E. Malle, and P. Van Antwerpen. **Impact of myeloperoxidase-LDL interactions on enzyme activity and subsequent posttranslational oxidative modifications of apoB-100.** ***J. Lipid Res.*** **2014.** 55: **747–757.**

Supplementary key words inflammation • myeloperoxidase activity • hypochlorous acid • 3-chlorotyrosine • epitope mapping • low density lipoprotein • apolipoprotein B-100

Over the past several years, considerable evidence has been obtained in support of the hypothesis that oxidants generated by the heme enzyme myeloperoxidase (MPO, EC1.11.2.2) play a key role in oxidation reaction of the artery wall. The enzyme, abundantly present in neutrophils and, to a lesser extent, in monocytes, is released during inflammatory activation of immune cells. MPO produces hypochlorous acid (HOCl) by the reaction of hydrogen

This study was supported by the Belgian Fund for Scientific Research (FRS-FNRS) Grant 34553.08, a grant from the FER 2007 (Université Libre de Bruxelles), and the Austrian Science Fund Grants FWF F3007 and W1226-B18. C. Delporte is a postdoctoral researcher funded by the FRS-FNRS, C. Noyon is a research fellow of the FRS-FNRS, and L. Vanhamme is Research Director of the FRS-FNRS.

Manuscript received 22 January 2014.

Published, JLR Papers in Press, February 17, 2014
DOI 10.1194/jlr.M047449

Abbreviations: CD, circular dichroism; Cl-Tyr, 3-chlorotyrosine; di-OxTrp, dioxidized tryptophan; FA, formic acid; HOCl-LDL, HOCl-modified LDL; HOCl, hypochlorous acid; HO-Tyr, 3-hydroxytyrosine; MPO, myeloperoxidase; MPO-LDL, LDL modified by the MPO-H_2O_2-chloride system; O-Met, methionine sulfoxide; OxTrp, oxidized tryptophan; PTM, posttranslational modification; QTOF, quadrupole TOF; RRLC, rapid resolution LC; SPI, score peak intensity.

[1]To whom correspondence should be addressed.
e-mail: cedric.delporte@ulb.ac.be

International Journal of Cardiology 173 (2014) 472–480

Contents lists available at ScienceDirect

International Journal of Cardiology

journal homepage: www.elsevier.com/locate/ijcard

15-deoxy-$\Delta^{12,14}$-PGJ_2 promotes inflammation and apoptosis in cardiomyocytes via the DP2/MAPK/TNFα axis

Chintan N. Koyani [a], Werner Windischhofer [b], Christine Rossmann [a], Ge Jin [c,d], Sandra Kickmaier [a], Frank R. Heinzel [c], Klaus Groschner [e], Ali Alavian-Ghavanini [a], Wolfgang Sattler [a], Ernst Malle [a,*]

[a] Institute of Molecular Biology and Biochemistry, Medical University of Graz, Austria
[b] Department of Pediatrics and Adolescence Medicine, Research Unit of Osteological Research and Analytical Mass Spectrometry, Medical University of Graz, Austria
[c] Department of Internal Medicine, Division of Cardiology, Medical University of Graz, Austria
[d] Cardiology Department, Medical University of Wenzhou, Wenzhou, China
[e] Institute of Biophysics, Medical University of Graz, Austria

ARTICLE INFO

Article history:
Received 11 December 2013
Received in revised form 14 February 2014
Accepted 12 March 2014
Available online 20 March 2014

Keywords:
Cardiomyocytes
TNFα
15d-PGJ_2
Apoptosis
PGD_2 receptor

ABSTRACT

Background: Prostaglandins (PGs), lipid autacoids derived from arachidonic acid, play a pivotal role during inflammation. PGD_2 synthase is abundantly expressed in heart tissue and PGD_2 has recently been found to induce cardiomyocyte apoptosis. PGD_2 is an unstable prostanoid metabolite; therefore the objective of the present study was to elucidate whether its final dehydration product, 15-deoxy-$\Delta^{12,14}$-PGJ_2 (15d-PGJ_2, present at high levels in ischemic myocardium) might cause cardiomyocyte damage.

Methods and results: Using specific (ant)agonists we show that 15d-PGJ_2 induced formation of intracellular reactive oxygen species (ROS) and phosphorylation of p38 and p42/44 MAPKs via the PGD_2 receptor DP2 (but not DP1 or PPARγ) in the murine atrial cardiomyocyte HL-1 cell line. Activation of the DP2-ROS-MAPK axis by 15d-PGJ_2 enhanced transcription and translation of TNFα and induced apoptosis in HL-1 cardiomyocytes. Silencing of TNFα significantly attenuated the extrinsic (caspase-8) and intrinsic apoptotic pathways (bax and caspase-9), caspase-3 activation and downstream PARP cleavage and γH2AX activation. The apoptotic machinery was unaffected by intracellular calcium, transcription factor NF-κB and its downstream target p53. Of note, 9,10-dihydro-15d-PGJ_2 (lacking the electrophilic carbon atom in the cyclopentenone ring) did not activate cellular responses. Selected experiments performed in primary murine cardiomyocytes confirmed data obtained in HL-1 cells namely that the intrinsic and extrinsic apoptotic cascades are activated via DP2/MAPK/TNFα signaling.

Conclusions: We conclude that the reactive α,β-unsaturated carbonyl group of 15d-PGJ_2 is responsible for the pronounced upregulation of TNFα promoting cardiomyocyte apoptosis. We propose that inhibition of DP2 receptors could provide a possibility to modulate 15d-PGJ_2-induced myocardial injury.

1. Introduction

Cardiovascular diseases are more prevalent worldwide compared to other diseases, amongst which myocardial ischemia caused by coronary blockage is by far the most frequent cause of mortality [1,2]. Imbalanced oxygen demand and supply to cardiomyocytes during coronary artery disease (CAD) activates cell death cascades and promotes myocardial infarction (MI) [3]. Advances in treatment based on currently available targets have failed to change the status of CAD/MI and therefore we await novel strides in fundamental understanding through which we might be able to manipulate progression of CAD and MI.

Changes in fatty acid compositions of myocardial lipids were found to be associated with CAD and MI [2]. Elevated phospholipase A_2 (PLA_2) mass and activity, as reported in patients with myocardial ischemia [4], lead to accumulation of unesterified arachidonic acid (AA) from phospholipids in the heart [5]. As a consequence, increased tissue levels of prostaglandins (PGs) e.g., PGI_2, PGE_2, and its isomer PGD_2, generated via cyclooxygenase (COX)-mediated conversion of AA have been observed in the ischemic myocardium [6]. However, PGD_2 is degraded in vitro and in vivo to a variety of metabolites, the majority of which were thought, until recently, to be physiologically inactive [7]. PGD_2 is either metabolized enzymatically to 13,14-dihydro-15-keto PGD_2 [7] (for chemical structures, see Supplement Fig. I) or readily dehydrated into J series prostanoids characterized by the presence of an α,β-unsaturated ketone in the cyclopentenone ring. Particularly 15-deoxy-$\Delta^{12,14}$-PGJ_2 (15d-PGJ_2, Supplement Fig. I), the final dehydration product of PGD_2 has been shown to have broad effects on various

* Corresponding author at: Medical University of Graz, Institute of Molecular Biology and Biochemistry, Harrachgasse 21, A-8010 Graz, Austria. Tel.: +43 316 380 4208; fax: +43 316 380 9615.
E-mail address: ernst.malle@medunigraz.at (E. Malle).

http://dx.doi.org/10.1016/j.ijcard.2014.03.086

International Journal of Cardiology 177 (2014) 140–141

Contents lists available at ScienceDirect

International Journal of Cardiology

journal homepage: www.elsevier.com/locate/ijcard

Letter to the Editor

Response to letter by Tsikas et al.

Chintan N. Koyani [a], Werner Windischhofer [b], Christine Rossmann [a], Frank R. Heinzel [c], Wolfgang Sattler [a], Ernst Malle [a,*]

[a] Institute of Molecular Biology and Biochemistry, Medical University of Graz, Austria
[b] Department of Pediatrics and Adolescence Medicine, Research Unit of Osteological Research and Analytical Mass Spectrometry, Medical University of Graz, Austria
[c] Department of Internal Medicine, Division of Cardiology, Medical University of Graz, Austria

ARTICLE INFO

Article history:
Received 6 September 2014
Accepted 20 September 2014
Available online 28 September 2014

Keywords:
Cardiomyocytes
15d-PGJ_2
PGD_2 receptor
DP2
Reactive oxygen species
Therapeutic target

Dear Editor,

We appreciate the interest of Tsikas et al. [1] in our manuscript [2] and the opportunity to clarify theoretical and experimental aspects describing the effects of 15-deoxy-$\Delta^{12,14}$-PGJ_2 (15d-PGJ_2) on cardiomyocyte function.

We agree that concentrations of 15d-PGJ_2 (a degradation product of prostaglandin D_2 [PGD_2]) used in most in vitro studies [3–5] including ours (Figs. 1–6 [2]) are higher than occurring in vivo. In our study, HL-1 cells (an immortalized cardiomyocyte cell line [6]) required such a high 15d-PGJ_2 concentration (15 μM, Figs. 1–6 [2]) while in primary murine cardiomyocytes downstream signaling and induction of apoptosis were observed at much lower 15d-PGJ_2 concentrations (10–50 nM; Fig. 7B–C [2]). These data suggest that primary cardiomyocytes respond to 15d-PGJ_2 treatment at more physiologically relevant concentrations. Another point worth mentioning is avid binding of 15d-PGJ_2 to cardiomyocyte or hepatic stellate cell culture medium constituents [7–9], which significantly reduces bioavailability of the active 15d-PGJ_2 compound.

As the authors [1] correctly point out, the use of N-acetyl-L-cysteine (NAC) as reactive oxygen species (ROS) scavenger is questionable due to the formation of thioethers between NAC and 15d-PGJ_2. To overcome this problem we have used pyrrolidine dithiocarbamate and Tempol (Fig. 1E [2]), two compounds that reduced DCF fluorescence (an indicator of ROS formation) more efficiently than NAC.

Cyclopentenone PGs, such as 15d-PGJ_2, are characterized by a highly reactive electrophilic carbonyl group in the prostane ring, which can readily adduct thiol-containing compounds including reduced glutathione (GSH) or cysteine [10]. Thioether formation between 15d-PGJ_2 and GSH or cysteine reaches steady state levels after 2–3 h under in vitro conditions [11,12]. In contrast, most PGs exert their effects within few minutes [3]. In line, we report that 15d-PGJ_2-mediated cellular signaling cascades are activated 2.5 min post treatment (Fig. 1D [2]). This difference in kinetics suggests that the effects we observed are independent of thiolation reactions.

Using GC–MS/MS technology, Tsikas et al. [1,13] determined 15d-PGJ_2 levels in urine of healthy donors in the pM range. It remains to be evaluated whether these findings can be extrapolated to 15d-PGJ_2 levels in serum/plasma or organs/tissues. In light of local macrophage inflammasome activation that can result in an 'eicosanoid storm' [14] (including PGD_2, the parent eicosanoid of 15d-PGJ_2), it is conceivable that such an event could generate a rapid local increase of PG concentrations.

15d-PGJ_2 can exert its biological effects via receptor-independent or -dependent pathways. The latter include peroxisome proliferator-activated-receptor γ (PPARγ) [10] and PGD_2 receptors (DP1 and DP2) [7,15]. The Powell group [15] has unambiguously shown that PPARγ-mediated activation requires high 15d-PGJ_2 concentrations while DP2 receptor-mediated activation in eosinophils is favored at low (1–10 nM) concentrations. In line, our results demonstrate that low 15d-PGJ_2 concentrations (10–50 nM) activated DP2-dependent but PPARγ-independent signaling cascades in primary cardiomyocytes (Fig. 7 [2]). In HL-1 cells, 15d-PGJ_2 failed to activate PPARγ-dependent signaling even at high concentrations (10–30 μM, Figs. 1 and 4 [2]). The low 15d-PGJ_2 concentrations used in our study are in line with the assumption that low levels of this compound would be pro- rather than anti-inflammatory [16].

It is currently not clear whether the urinary 15(S)-8-iso-PGF/15d-PGJ_2 ratio, as mentioned by Tsikas et al. [1], might be considered a surrogate marker for the generation of 15d-PGJ_2-mediated oxidative stress. However, a series of published articles revealed an association of 15d-

* Corresponding author at: Medical University of Graz, Institute of Molecular Biology and Biochemistry, Harrachgasse 21, A-8010 Graz, Austria. Tel.: +43 316 380 4208; fax: +43 316 380 9615.
E-mail address: ernst.malle@medunigraz.at (E. Malle).

http://dx.doi.org/10.1016/j.ijcard.2014.09.111
0167-5273/

Human Molecular Genetics, 2014, Vol. 23, No. 15 **4015–4023**
doi:10.1093/hmg/ddu115
Advance Access published on March 13, 2014

Disruption of the methyltransferase-like 23 gene *METTL23* causes mild autosomal recessive intellectual disability

Marie Bernkopf[1,†], Gerald Webersinke[1,†], Chanakan Tongsook[2], Chintan N. Koyani[3], Muhammad A. Rafiq[4], Muhammad Ayaz[5], Doris Müller[6], Christian Enzinger[7], Muhammad Aslam[5], Farooq Naeem[5,9], Kurt Schmidt[10], Karl Gruber[11], Michael R. Speicher[8], Ernst Malle[3], Peter Macheroux[2], Muhammad Ayub[5,9], John B. Vincent[4,12,13], Christian Windpassinger[8,*] and Hans-Christoph Duba[6]

[1]Laboratory of Molecular Biology and Tumorcytogenetics, Department of Internal Medicine, Krankenhaus der Barmherzigen Schwestern, Linz, Austria, [2]Institute of Biochemistry, Graz University of Technology, Graz, Austria, [3]Institute of Molecular Biology and Biochemistry, Medical University of Graz, Graz, Austria, [4]Molecular Neuropsychiatry and Development (MiND) Lab, The Campbell Family Brain Research Institute, The Centre for Addiction & Mental Health (CAMH), Toronto, ON, Canada, [5]Lahore Institute of Research and Development, Lahore, Punjab Province, Pakistan, [6]Department of Human Genetics, Landes-Frauen und Kinderklinik, Linz, Austria, [7]Department of Neurology and [8]Institute of Human Genetics, Medical University of Graz, Graz, Austria, [9]Division of Developmental Disabilities, Department of Psychiatry, Queen's University, Kingston, ON, Canada, [10]Department of Pharmacology and Toxicology, Karl-Franzens University Graz, Graz, Austria, [11]Institute of Molecular Biosciences, University of Graz, Graz, Austria and [12]Department of Psychiatry and [13]Institute of Medical Science, University of Toronto, Toronto, ON, Canada

Received February 12, 2014; Revised February 12, 2014; Accepted March 10, 2014

We describe the characterization of a gene for mild nonsyndromic autosomal recessive intellectual disability (ID) in two unrelated families, one from Austria, the other from Pakistan. Genome-wide single nucleotide polymorphism microarray analysis enabled us to define a region of homozygosity by descent on chromosome 17q25. Whole-exome sequencing and analysis of this region in an affected individual from the Austrian family identified a 5 bp frameshifting deletion in the *METTL23* gene. By means of Sanger sequencing of *METTL23*, a nonsense mutation was detected in a consanguineous ID family from Pakistan for which homozygosity-by-descent mapping had identified a region on 17q25. Both changes lead to truncation of the putative METTL23 protein, which disrupts the predicted catalytic domain and alters the cellular localization. 3D-modelling of the protein indicates that METTL23 is strongly predicted to function as an *S*-adenosyl-methionine (SAM)-dependent methyltransferase. Expression analysis of METTL23 indicated a strong association with heat shock proteins, which suggests that these may act as a putative substrate for methylation by METTL23. A number of methyltransferases have been described recently in association with ID. Disruption of METTL23 presented here supports the importance of methylation processes for intact neuronal function and brain development.

*To whom correspondence should be addressed at:Institute of Human Genetics, Medical University of Graz, Harrachgasse 21/III, 8010 Graz, Austria. Tel: +43 (0) 3163804114; Email: christian.windpassinger@medunigraz.at
†These authors contributed equally.